Biophysical investigations of the LAH4 family peptides : enhancer of gene delivery, from peptide-peptide interactions to peptide-membrane interactions

Justine Wolf

UNIVERSITÉ DE STRASBOURG

ÉCOLE DOCTORALE DES SCIENCES CHIMIQUES

Institut de Chimie de Strasbourg, UMR 7177

THÈSE présentée par :

Justine WOLF

soutenue le : **20 septembre 2018**

pour obtenir le grade de : **Docteur de l'université de Strasbourg**

Discipline/ Spécialité : Chimie-Biologie/ Biophysique

Biophysical investigations of the LAH₄ family of peptides

enhancer of gene delivery, from peptide-peptide interactions to peptide-membrane interactions

THÈSE dirigée par :
  M. BECHINGER Burkhard   Professeur, Université de Strasbourg

THÈSE co-dirigée par :
  Mme. SÜSS Regine   Professeur, Albert-Ludwigs-Universität Freiburg

RAPPORTEURS :
  Mme. SIZUN Christina   HDR, CNRS
  M. LAKEY Jeremy   Professeur, Newcastle University

AUTRES MEMBRES DU JURY :
  M. KICHLER Antoine   Chargé de recherche, CNRS

Etude biophysique de peptides de la famille du LAH$_4$

- un amplificateur de systèmes de transport de gènes - de l'interaction peptide-peptide à l'interaction peptide-membrane.

Biophysical investigations of the LAH$_4$ family of peptides

- enhancer of gene delivery - from peptide-peptide interactions to peptide-membrane interactions.

Justine Wolf

Université de Strasbourg,
Institut de Chimie de Strasbourg, UMR 7177,
Laboratoire de RMN et biophysique des membranes

Ph.D. Thesis

September 2018

The work presented in this thesis took place from October 1st 2015 to September 28th 2018 and was carried out at the Université de Strasbourg, in the Institut de Chimie de Strasbourg in the laboratory of Membrane Biophysics and NMR (UMR7177).

The project in which this work has been enterded is "Membrane active polypeptides and liposomal complexes for nucleic acid delivery". It has been co-written by Pr. Regine Süss, University of Freiburg and Pr. Burkhard Bechinger, Université de Strasbourg, and it was supported by the University of Strasbourg (IDEX), to the International Research Traning Group (IRTG) Soft Matter Science (SoMaS).

Contents

CONTENTS

List of Abbreviations

AAV	Adeno-Associated Virus
AFM	Atomic Force Microscopy
AMP	AntiMicrobial Peptide
BMP	Bis(Monoacylglycero)Phosphate
CD	Circular Dichroism
CP	Cross Polarization
CPP	Cell Penetrating Peptide
CSA	Chemical shift anisotropy
DARR	Dipolar Assisted Rotational Resonance
DLS	Dynamic Light Scattering
DMEM	Dulbecco Modified Eagle Medium
DMPC	1,2-dimyristoyl-*sn*-glycero-3-phosphocholine
DPC	DodecylPhosphoCholine
HPLC	High performance liquid chromatography
HR-MAS	High Resolution-MAS
IP	In Planar
ITC	Isothermal Titration Calorimetry
LV	LentiVirus
MALDI-TOF	Matrix Assisted Laser Desorption Ionisation - Time of Flight
MAS	Magic angle spinning
MLV	Multi-Lamellar Vesicles
NMR	Nuclear Magnetic Resonance
PAGE	Polyacrylamide Gel Electrophoresis
POPC	1-palmitoyl-2-oleoyl-*sn*-glycero-3-phosphocholine
POPG	1-palmitoyl-2-oleoyl-*sn*-glycero-3-phospho-(1'*rac*-glycerol)
POPS	1-palmitoyl-2-oleoyl-*sn*-glycero-3-phospho-L-serine
SDS	Sodium Dodecyl Sulphate
SM	Sphingomyelin
TEM	Transmission Electron Microscopy
TFE	Trifluoroethanol
ThT	Thioflavin T
TM	Transmembrane

CONTENTS

1

Introduction:

In this manuscript, biophysical investigations of peptides of the LAH_4 family will be presented with the perspective to develop gene delivery systems. As cell penetrating peptides (CPP), LAH_4 peptides have shown efficiency to enhance cellular uptake for a wide variety of cargos. Differences of capability from one peptide to another, combined with a specific cargo, are still unclear. Supplementary knowledge on molecular interactions between the different components of the delivery system and the underlying mechanism occurring throughout the cellular uptake would help to improve these systems.

Gene delivery systems have been developed with the purpose of introducing foreign materials into cells, in order to modify a specific target. These systems are mixtures composed of a cargo (or vector): the active component which is used to modify the target; and a delivery systems: helper molecules used to lead the cargo to its target[1, 2]. Structural varieties of gene delivery systems are various, hence, it can be used for a wide range of diseases from cancer to genetic diseases[3].

Vectors are separated in two main classes: the viral and non-viral one[4]. The process to introduce a nucleic acid into a foreign eukaryotic cells is called transfection. When this process is done with a virus it is called transduction.

Viral vectors, has the advantage to use the natural propensity of viruses to modify the gene expression. Modification of their genomes ensures the safety of the systems. Nevertheless the immunogenicity susceptibility is problematic and these systems are often expensive[3]. Non-viral systems are used to deliver nucleic acids as effectors (DNA, mRNA, siRNA or miRNA) e.g. for gene delivery[5]. They have other disadvantages such as a poor stability, a rapid

3

degradation and a low specificity[6]. However, they have also many advantages like cost-effectiveness, availability and reduced induction of the immune response[3].

Key limitation steps like extracellular targeting, intracellular delivery and reduction of the toxicity can be reduced by the addition of other components, for both viral and non-viral systems[4]. Enhancers of gene delivery like CPPs can be used in a non-covalent manner, allowing to have a versatile system. Biological efficiency of these combined systems are then dependent on the carrier-cargo affinity, particle size and homogeneity[6]. CPPs such as LAH_4 peptides are mainly used to allow cellular uptake and thereafter, intracellular delivery (figure 1.1).
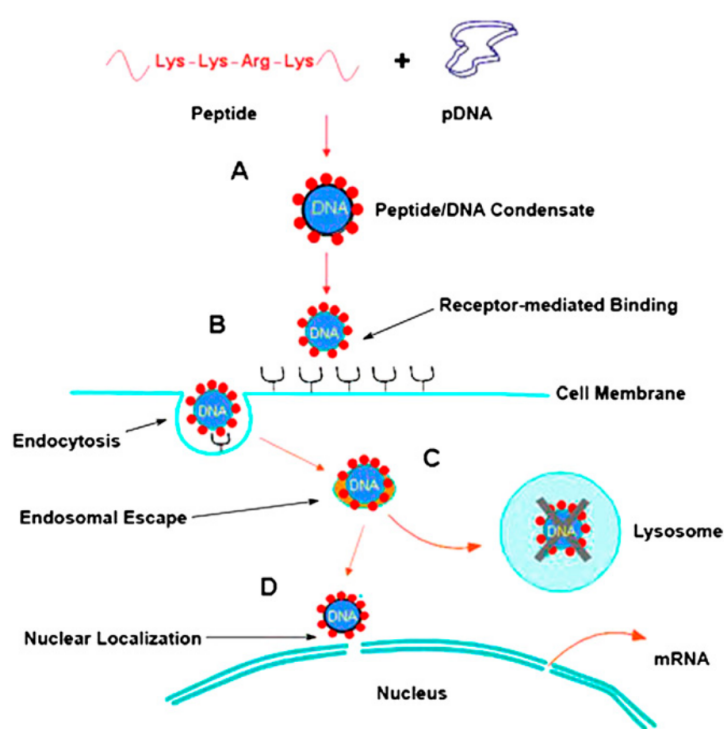
Figure 1.1: Schematic representation of peptide-guided gene delivery: example of peptide with plasmidic DNA. The main steps are indicated: A: condensation of the nucleic acid, B: specific cell recognition and uptake, C: endosomal escape before lysosomal degradation and D: nuclear interaction (extracted from [7]).

For gene delivery systems in particular, the non-crossing of the plasma membrane is detrimental for efficiency. Indeed, the failure of endosomal escape results in the degradation of the cargo by the lysosomes. Membrane active peptides such as CPPs use endocytosis or direct translocation to pass

through the membranes[8]. Their ability to specifically destabilize the membrane is particularly useful in the field of gene delivery systems[9, 10]. Other membrane active peptides like the cationic Tat-derived peptides or the amphiphilic GALA peptides are, like the LAH$_4$ peptide family, specifically used for this purpose[9, 10].

1.1   The LAH$_4$ peptide

The original LAH$_4$ was first designed as a model peptide in order to study peptide-lipid interactions[11]. This amphipathic peptide is composed of 4 types of amino acids. At each terminus, 2 lysines each allow the good water solubility of the peptide. The 4 histidines give an amphiphilic character to the peptide when folded to an α-helix and allow a pH-dependent behaviour. Finally, hydrophobic residues - alanines and leucines - were added to complete the sequence, for a total of 26 amino acids. In solution, the peptide is mainly in a random coil conformation at low pH, and less than half of it is in α-helical conformation at high pH (α-helical content of 13% at pH 4.5 or 43% at pH 8.5)[12]. In parallel, determination of the hydrodynamic radius indicates that at low pH the peptide is mainly in a monomeric state, when at neutral pH, the peptide is aggregated in particles bigger by two orders of magnitude compared to the monomers[13]. In presence of membranes, the α-helical conformation is more pronounced. Because of the cationic profile of the peptide, associations with membranes containing anionic lipids are stronger than interactions with zwitterionic lipids[12]. In presence of anionic lipids, LAH$_4$ induces a bigger permeabilization of membranes. Nevertheless, the pH induces a substantial difference. LAH$_4$ is more active at low pH than at neutral conditions[12]. In micelles composed of zwitterionic lipids at neutral pH 7.8, LAH$_4$ is structured as an α-helix from L4 to L21 (figure 1.2).

Just above the pKa of the histidines at pH 6.1 (pK values of 5.8, 5.4, 5.7 and 6.0 for H10, H11, H14 and H18 respectively) a break in the α-helix appeared and helix is present from A3 to L9, and from H14 to K24[14]. Orientation of the peptide in membranes is dependent on the protonation state of the histidines. At pH 5, when the histidines are protonated, LAH$_4$ adopts an in planar orientation. A switch of the peptide orientation in membranes happens at pH 6.1 ± 0.2[15]. Indeed, at neutral pH, deprotonation of histidines increases

1. INTRODUCTION:
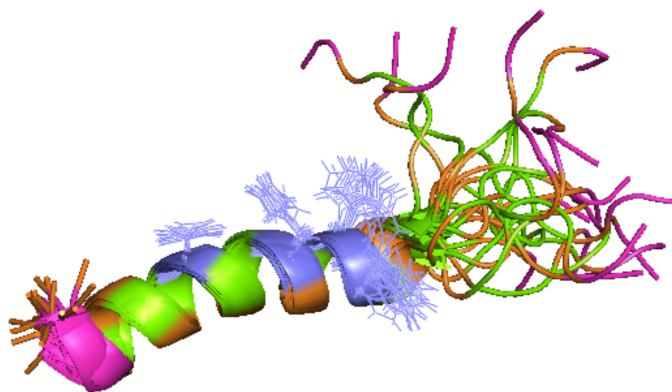
Figure 1.2: Structure of the LAH$_4$ in DPC micelles at pH 4.1: structure determined by liquid-state NMR. The different amino acids have been coloured in pink, orange, green and blue for lysines, alanines, leucines and histidines respectively (PDB reference: 2KJN [14]).

the hydrophobic propensity of the peptide, and a transmembrane orientation can be adopted [11].
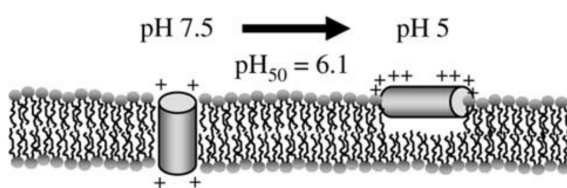
Figure 1.3: Schematic representation of LAH$_4$ orientation in membranes depending on the pH (extracted from [16]).

This propensity to interact and disturb membranes was studied for antimicrobial applications. LAH$_4$ has been shown to present antimicrobial activities by reducing the growth rate of the Gram negative bacteria *E. coli* or by inhibiting growth of the Gram positive *B. subtilis* [12]. Thereafter, as for numerous cationic amphiphilic peptides, the capability to transfect DNA was demonstrated for the LAH$_4$ [17]. Indeed, electrostatic interactions prompted the interaction between DNA and LAH$_4$ and then induce the condensation of the DNA [18]. It has been established that the complex was going through the interaction of lysine side chains of LAH$_4$ and the phosphate groups of DNA [19]. In cells, passage of the complex through the endosomal pathway, involving a decrease of the pH, allowed to shuffle the composition of the DNA:LAH$_4$ complex. Quantitative analyses of the interactions between LAH$_4$ and DNA demonstrated that when lowering the pH from neutral to 5.5, only half of the amount of peptides was required to form the DNA:LAH$_4$ complex [20]. The

release of the peptide allowed to interact and disturb the membrane, and to deliver DNA[21].

1.2 LAH$_4$ peptide derivates

Since the original peptide, a myriad of LAH$_4$ derivatives has been synthetized in order to improve potential applications (antimicrobial activity, transfection or transduction) or to determine the driving forces of the peptide interactions. Modifications are mainly changes of the hydrophobic angle (in an Edmundson helical wheel diagram) or insertion or substitution of amino acids to modify the α-helical properties of the peptide. In Figure 1.4 are represented the main peptides monitored in this thesis.
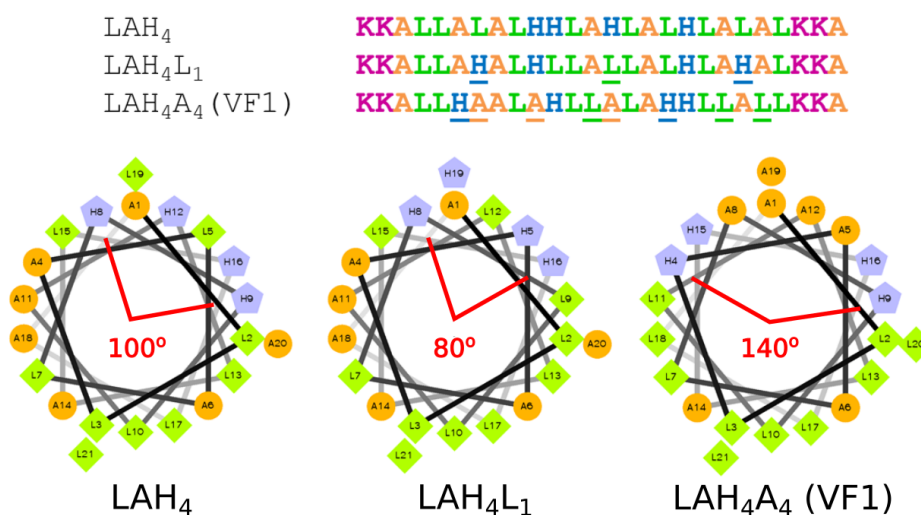
Figure 1.4: Sequences of LAH$_4$, LAH$_4$L$_1$ and VF1 and their wheel representation: The different amino acids have been coloured in pink, orange, green and blue for lysines, alanines, leucines and histidines respectively. Variant amino acids compared to the LAH$_4$ were underlined. Angles subtended by two pairs of histidines have been indicated in red. Helical Wheel Projections were done from http://rzlab.ucr.edu/scripts/wheel/wheel.cgi

1.2.1 Antimicrobial properties

Synthesis of LAH$_4$ isomers with various hydrophobic angles (from 60° to 180°) demonstrated that intermediate angles between 80° and 100° generated bigger membranes disruption[22]. An increase in the hydrophobic angle was achieved

1. INTRODUCTION:

by moving the histidine positions and intercalating leucines. ^{2}H solid-state NMR of chain deuterated phospholipid established that at pH 7.5, peptides did not affect significantly the lipid chains. On the contrary, at pH 5 LAH$_4$, isomers caused perturbations of lipid chains. The perturbations disturbed specifically the part close to the headgroup of the lipid chains. In addition, the isomers LAH$_4$L$_1$ and LAH$_4$L$_2$ (hydrophobic angle: 80° and 100° respectively) induced disordering at the lower part of the aliphatic lipids chain, in the hydrophobic core, of anionic lipids[16]. The derivate LAH$_4$A$_4$ presents a hydrophilic angle of 140°, and was not able to affect bacterial growth[23].

Utilization of these isomers allowed to determine that the antimicrobial activity of these peptides was bactericidal instead of bacteriostatic[22]. The bactericidal properties were present at low and neutral pH, but lower efficiency at neutral pH indicated that the mechanism of action was depending on the pH. Other peptide modifications, such as an increase of the number of histidines improved the activity at neutral pH, whereas addition of phenylalanine residues reduced the activity. Modifications of peptide properties by addition of hydrophobic ornithine residues, D-amino acids or insertion of a proline at the center modulate the toxicity for human cells or parasites[24]. The high propensity to disrupt anionic lipid model membranes has been shown for many LAH$_4$ derivatives. Although the tuning of peptide properties was possible, the precise mechanism has not been determined. A strong interaction between LAH$_4$ and anionic lipids allowed a good propensity to disturbe model membranes[16]. Nevertheless, antibiotic efficiencies of the different peptides were highly dependent on the bacterial strain[22].

In the table below are summarized the peptides cited in the section. *D*-amino acids are indicated in italic and O correspond to the ornithine residues.

8

	Peptide sequence	Hydrophobic angle	References
LAH$_4$	KKALLALALHHLAHLALHLALALKKA	100°	16
LAH$_4$L$_1$	KKALLAHALHLLALLALHLAHALKKA	80°	16,22
VF1 (LAH$_4$A$_4$)	KKALLHAALAHLLALAHHLLALLKKA	140°	23
LAH4-L0	KKALLAHALAHLALLALHLALHLKKA	60°	16,22
LAH4-L2	KKALLALALHHLALLALHLAHALKKA	100°	16,22
LAH4-AL6	KKALLHLALALLALHAHALALHLKKA	180°	16,22
LAH4-L1-F4	KKALLAHFFHLLALLALHFFHALKKA	80°	22
LAH6-L1	KKALLAHALHHLALLAHHLAHALKKA		22
HALO	KKALLOHALHOLALLAOHLAHOLKKA		24
HALO-P8	KKALLOHPLHOLALLAOHLAHOLKKA		24
D-HALO-rev	*AKKLOHALHOALLALOHLAHOLLAKK*		24

1.2.2   Applications in transfection

Design of new LAH$_4$ derivates allowed to specify the parameters needed for a better transfection efficiency. Modifications like hydrophobic angle and hydrophobicity, length, inclusion of amino acids in the central part of the sequence and modification of the termini were investigated.

Hydrophobic angle and hydrophobicity: Optimal DNA transfection was obtained with high hydrophobic angles. Addition of a histidine (in position 15), in order to increase the size of the hydrophilic face, resulted in the reduction of the transfection efficiency[18]. Nevertheless, extreme angles resulted in inefficient carrying[17]. Modification of the position of a number of histidines has a direct impact on hydrophobicity parameters. Removing all histidines was demonstrated to induce abolishment of transfection activity[23]. Reducing the number of histidines induced a diminution of DNA delivery. Nevertheless, depending of the position of the switched histidines, the decrease of activity was more or less significant[23]. The optimal number of histidines to preserve activity seemed to be between four and six[17, 25].

Minor modifications are possible and can result in significant changes in the capacity of nucleic acid delivery. Hydrophobic angle is one of the parameters responsible for the adjustment of the interaction strength of the peptide with nucleic acids. However, a simple correlation between the amount of transfected DNA and the level of DNA expression is not possible[17]. For broader application depending on the cargo to transfect - DNA or siRNA (deliverable into the nucleus or the cytoplasm, respectively) - the interaction needs to be

1. INTRODUCTION:

modulated to reach a balance between safe transport and delivery[26].

In the table below are summarized the peptides cited in the section.

	Peptide sequence	References
LAH$_4$	KKALLALALHHLAHLALHLALALKKA	17,18
LAH$_4$L$_1$	KKALLAHALHLLALLALHLAHALKKA	18,25
VF1(LAH$_4$A$_4$)	KKALLHAALAHLLALAHHLLALLKKA	23
LAH4-H15	KKALLALALHHLAHHLALHLALALKKA	18
LAH4-L3	KKALLALALHHLALLAHHLALALKKA	17
LAH4-L4	KKALLALALHHLALLAHLLALHLKKA	17
LAH4-A6	KKKKALAHLHALAAHLHALAAAALKKK	17
LAH4-L6	KKKKALLHLHLLALHLHLLALLALKKK	17
LAH4-G6	KKKKALGHLHGLAGHLHGLAGGALKK	17
K2-L10-A12-K2	KKALLAAALAALLALAAALLALLKKA	23
LAH2-A6	KKALLHAALAHLLALAAALLALLKKA	23
LAH2-A4	KKALLAAALAALLALAHHLLALLKKA	23
LAH1	KKLALALALALHALALALALKKA	17
LAH2	KKLAHLALALALGLALAHLAKKA	17
LAH3	KKALALGLHLAHLALHLALALKKA	17
LAH5	KKALLALALHHLAHLAHHLALALKKA	17
LAH6-L1	KKALLAHALHHLALLAHHLAHALKKA	25

Peptide length: The optimal size of the peptide has also been investigated. Reduction of the length to less than 26 amino acids did not appear possible without loosing transfection activity. Removing two and three uncharged residues close to the N-terminus or C-terminus did not alter the capacity to complex DNA, unlike the transfection activity[18]. Addition of amino acids was possible with, for example, the LAH$_6$L$_1$-80 peptide. This peptide was elongated through the addition of 2 histidines and the design was done in order to conserve the 80° angle between the histidines[25]. Analyses by solid-state ^{2}H NMR revealed that longer peptides induced an increase of the order of aliphatic chains of anionic lipids at pH 7.5[25].

In the table below are summarized the peptides cited in the section.

	Peptide sequence	Peptide length	References
LAH$_4$	KKALLALALHHLAHLALHLALALKKA	26	18
LAH$_4$L$_1$	KKALLAHALHLLALLALHLAHALKKA	26	18,25
LAH4-ΔN	KK-LALALHHLAHLALHLALALKKA	24	18
LAH4-ΔC	KKALLALALHHLAHLALHLAL-KK-	23	18
LAH6-L1-80	KKHLLAHALHLLALLALHLAHALAHLKKA	29	25
LAH4-L1-30	KKALLAAHLAHLLAALLAHLLHALLALKKA	30	25

10

Modifications in the central part of the sequence: In many cases, perturbation of the middle of the α-helix led to a decrease of the efficiency. Breaking the α-helix by substitution of a residue by a proline (position 15) resulted in nullifying the transfection activity of LAH$_4$[18]. Switching two leucines by α-aminobutyric acid (Aib) resulted also in the abolishment of cellular activities[27]. Inversion of the histidines by lysines presented poor transfection activities, despite a conservation of the interaction with DNA[17]. However, smaller modifications like exchanging alanines and/or leucines with phenylalanines induced only a small decrease on the transfection activities[27].

Utilization of D-amino acids instead of the L-enantiomers could be used in order to better resist enzymatic degradation[18]. Nevertheless, partial or full D-LAH$_4$ peptide derivatives did not present specific improvements of DNA delivery efficiency. ^{2}H solid-state NMR analysis did not indicate a specific decrease of the disturbance of the lipid chains[25]. No noticeable reduction in DNA binding was observed, despite a decrease of the transfection efficiency[18, 25]. A stronger interaction of the D-enantiomer peptides with DNA could explain the decrease of efficiency[27].

In the table below are summarized the peptides cited in the section. *D*-amino acids are indicated in italic and X correspond to the α-aminobutyric acid (Aib) residues.

	Peptide sequence	References
LAH$_4$	KKALLALALHHLAHLALHLALALKKA	17,18,27
LAH$_4$L$_1$	KKALLAHALHLLALLALHLAHALKKA	18,25,27
LAH4-P15	KKALLALALHHLAHPLALHLALALKKA	18,27
LAH4X2	KKALLALAXHHLAHLALHXALALKKA	27
LAH5X2	KKALLALAXHHLAHLAHHXALALKKA	27
LAK4	KKLAKALAKALAKALKLALALAKK	17
LAH4-L1-F4	KKALLAHFFHLLALLALHFFHALKKA	27
LAH4-L1-F2d	KKALLAHFLHLLALLALHLFHALKKA	27
LAH4-L1-Opt	KKLALAHALHLALLLALHLAHALKKA	27
LAH4 inv-AL	KKALLALALHHALHLALHLALALKKA	2
D-LAH4	*KKALLALALHHLAHLALHLALALKKA*	18,25,27
LAH4-*D*	*KK*ALLALALHHLAHLALHLALAL*KKA*	25

Modifications of the termini: Modification at the termini of peptides seemed to be more modular. Replacing the C-terminal amidation by a carboxyl group did not change the transfection activity[18]. Substitution of the lysines by identically charged arginine residues did not significantly modify

1. INTRODUCTION:

the efficiency of transfection[26]. However, modification of both termini by addition of charged residues at each terminus (2 and 2 lysines) caused a decrease of the cell viability[18].

Extension at the N-terminus is possible, but seemed to be limited by the size or the composition of the sequence inserted. Addition of 2 phenylalanines did not significantly modify the efficiency of transfection[26]. A recent study tested the extended N-termini with different nuclear localization signals (NLS)[28]. A GCG was added as linker between the NLS sequence and the LAH_4L_1 sequence. The extensions tested ranged from 7 amino acids to more than 30. The different constructs were still able to complex DNA but affinity of the two components was modified. Polydispersity of the complexes was similar and acceptable (0.20 to 0.27), nevertheless the longer construct formed the largest DNA complexes and failed to transfect the complexes. The three other peptides were more efficient than the LAH_4L_1 for cellular uptake and nuclear import of the complex. Live cell confocal imaging was then used to compare localization of the complex of one of the constructs and LAH_4L_1. The DNA was present in the nucleus and was absent from the lysozyme with the modified peptides, unlike for the original peptide, where the DNA was localized in the lysozyme and not the nucleus.

In the table below are summarized the peptides cited in the section.

	Peptide sequence	References
LAH4_COOH	KKALLALALHHLAHLALHLALALKKA_COOH	18
LAH4-L1-R	RRALLAHALHLLALLALHLAHALRRA	26
K2-LAH4-K2	KKKKALLALALHHLAHLALHLALALKKKK	18
LAH4-L1-F	FFKKLAHALHLLALLALHLAHALKKA	26
PK1-LAH4-L1	PKKKRKVGCG-LAH_4L_1	28
PK2-LAH4-L1	VKRKKKPGCG-LAH_4L_1	28
KR-LAH4-L1	VKRKKKPGCG-LAH_4L_1	28
NQ-LAH4-L1	NQSSNFGPMKGGNFGGRSSGPYGGGGQYFAK PRNQGGYGCG-LAH_4L_1	28

1.2.3   Applications in transduction

The efficiency of transduction was less studied, because utilization of the LAH_4 peptides for this purpose is more recent[29,30,31]. Peptide derivates from LAH_4A_4 (also called Vectofusin-1, VF1) were investigated for the enhancement of lentiviral (LV) gene transfer[30,23]. Two series were created LAH_4-Lx

and LAH$_4$-Ax. The LAH$_4$-Ax series presented a stronger degree of amphipathicity when compared to the Lx series. A high degree of amphipathicity (≥ 0.3) and a hydrophilic angle of 140° seemed to allow good transduction efficiencies. As it was observed for transfection applications, removing Lys induced a decrease of the efficiency[18]. Deletion of Lys from the C-terminus resulted in only a slight decrease of the activity while suppression of the N-terminal Lys abolished transfection because of toxicity. Modification of the number of N-terminus lysine at 1 and 3 only slightly decreased and did not change the activity, respectively. Similarly to transfection assays a reduction of the size of the peptide was damaging for LV transduction[18,23]. The original LAH$_4$ was unable to enhance transduction of LV under the conditions tested[23]. Otherwise, self-assembly of the peptide could improve the efficiency of delivery of the LV. Indeed, it has been observed that VF1 was able to form α-helical fibrils. Association of this peptide allowed facilitation of concentration of viruses, leading to an increase of cellular up-take and thereby, an increase of virus delivery[32].

The transduction of naked viruses has not been tested. Only the transduction of adeno-associated viruses (AAV) by the LAH$_4$ peptide has been reported[31].

1. INTRODUCTION:

In the table below are summarized the peptides tested in the paper of Majdoul et al.[23].

	Peptide sequence	μH	Hydrophobic angle
LAH$_4$	KKALLALALHHLAHLALHLALALKKA		
LAH$_4$L$_1$	KKALLAHALHLLALLALHLAHALKKA	0.191	80°
VF1 (LAH$_4$A$_4$)	KKALLHAALAHLLALAHHLLALLKKA	0.342	140°
LAH4-A1	KKALLAHALHLLAALALHLAHLLKKA	0.287	80°
LAH4-A2	KKALLLAALHHLAALALHLAHLLKKA	0.248	100°
LAH4-A3	KKALLLAALHHLLALAHHLAALLKKA	0.295	120°
LAH4-A5	KKALLHALLAHLAALLHALLAHLKKA	0.451	160°
LAH4-A6iso	KKALLHALLAALLAHLHALLAHLKKA	0.445	180°
LAH4-L0	KKALLAHALAHLALLALHLALHLKKA	0.118	60°
LAH4-L2	KKALLALALHHLALLALHLAHALKKA	0.135	100°
LAH4-L3	KKALLALALHHLALLAHHLALALKKA	0.133	120°
LAH4-L4iso	KKALLHLALLHAALLAHHLALALKKA	0.061	140°
LAH4-L5	KKALLHLALLHAALLAHLAALHLKKA	0.179	160°
LAH4-A6iso	KKALLHLALLLAALHAHLAALHLKKA	0.237	180°
LAH4-A4-dKn	ALLHAALAHLLALAHHLLALLKKA		
LAH4-A4-K1n	KALLHAALAHLLALAHHLLALLKKA		
LAH4-A4-K3n	KKKLLHAALAHLLALAHHLLALLKKA		
LAH4-A4-dKc	KKALLHAALAHLLALAHHLLALLA		
LAH-A4-d1aa	KKALLHAALAHLLALAHHLLALLKK		
LAH-A4-d2aa	KK LLHAALAHLLALAHHLLALLKK		
LAH-A4-d2Caa	KKALLHAALAHLLALAHHLLAL KK		
LAH-A4-d3aa	KK LHAALAHLLALAHHLLALLKK		
LAH-A4-d5aa	KK LHAALAHLLALAHHLLA KK		

For this transduction application, it could be convenient to distinguish between two kinds of viruses. Indeed, viruses can be subdivided in two classes: naked and enveloped. During the endosomal escape, two mechanisms can be distinguished. Pore formation or membrane disruption is necessary for naked viruses, like for nucleic acids. In contrast, for enveloped viruses, a membrane fusion between endosomal and viral membranes is sufficient (figure 1.5).
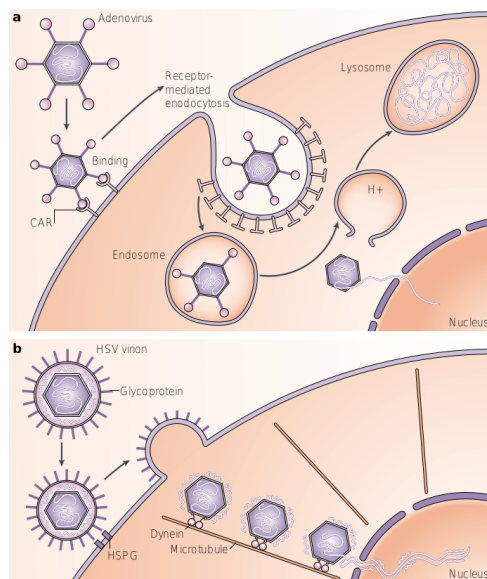
Figure 1.5: Schematic representation of different mechanism of virus entry into cells: a, endocytosis of the naked viral particles and endosomal escape. b, membrane fusion allowing the release of the viral particle into the cell (extracted from [33]).

1. INTRODUCTION:

1.2.4   Design of LAH$_4$ peptide derivates

The design of LAH$_4$ derivative peptides ensured significant improvement of delivery. Two peptides have proved better efficiency; LAH$_4$L$_1$ and VF1 (LAH$_4$A$_4$)[16, 30] (figure 1.6).
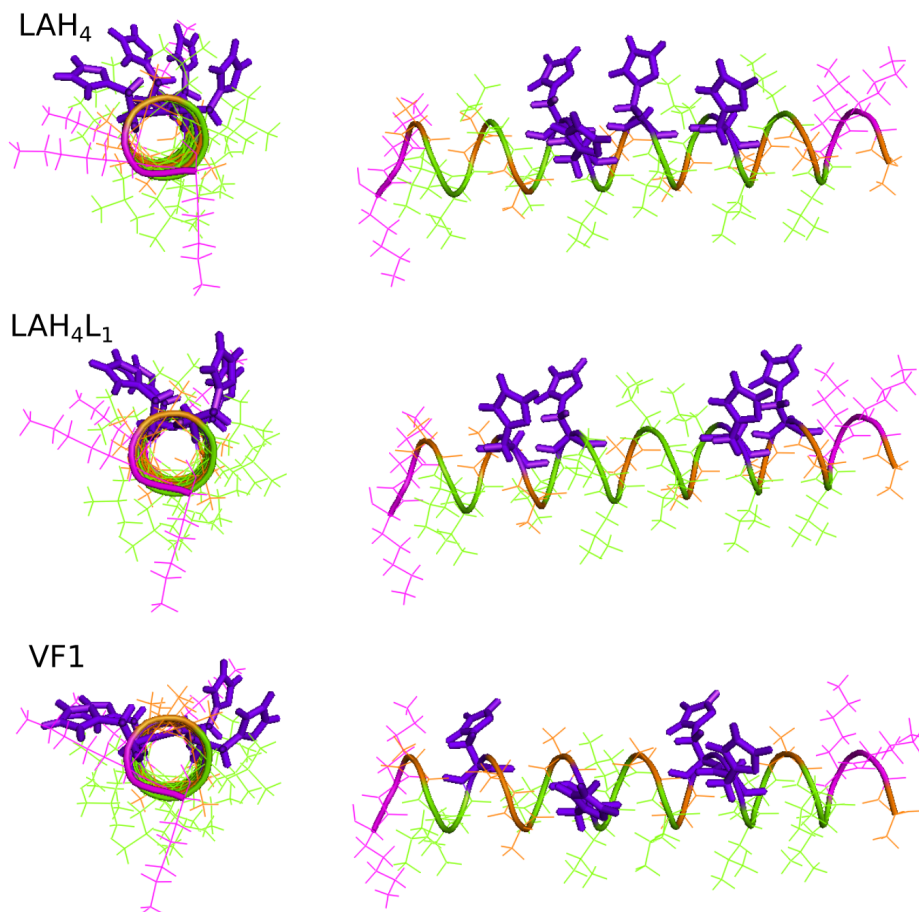
Figure 1.6: Representation of perfect helix of the LAH$_4$, LAH$_4$L$_1$ and VF1 peptides: The different amino acids have been coloured in pink, orange, green and purple for lysines, alanines, leucines and histidines respectively.

The sequence of LAH$_4$L$_1$ is close to the one of the LAH$_4$. On an α-helical wheel representation, the histidines cover an angle of 80° for LAH$_4$L$_1$ (100° for LAH$_4$, figure 1.4). Histidines are paired 2 by 2, and spaced by the same number of amino acids, giving an alignment of histidines 2 by 2 along the helix. Pairs of histidines are well spaced, as compared to the LAH$_4$ peptide, increasing the hydrophobic moment (represent the amphipathicity of an α-helix). For VF1, pairs of histidines are positioned to form an angle of 140°

and well spaced as for the LAH$_4$L$_1$. The hydrophobic moment is considerably higher because of the presence of alanine in the hydrophilic phase (hydrophobic moment of 0.191 and 0.342 for LAH$_4$L$_1$ and VF1 respectively)[23]. Alanines and leucines are also distributed more orderly along the helix.

LAH$_4$L$_1$ presents a broad range of applications. It has been shown to be an antimicrobial peptide, and was able to act as a carrier system like for DNA, siRNA or lentivirus (LV)[16, 25, 34, 29]. Interestingly, the LAH$_4$L$_1$ recently demonstrated its efficiency by allowing the delivery of a DNA transposon in specific cells, known to be difficult to transfect[35]. Also efficient for transfection activity, the VF1 peptide was much more efficient for transduction of LV[23]. Nevertheless, it did not present antimicrobial activities[23]. The angle of 140° present between the histidines could be responsible of a too small membranes disturbance, because it has been demonstrated that intermediate angles are more suitable for this purpose (80° to 100°)[22]. In contrast to the original LAH$_4$, despite its wide range of applications, it was not able to induce transduction of LV[23].

As it was presented before, some prerequisites have been determined for efficient peptides delivery systems. Nevertheless, determination of parameter for an optimal peptide for a specific cargo is still not possible. Hence, better understanding the mechanisms underlying the utilisation of these LAH$_4$ peptides would facilitate improvement and optimization of these delivery systems. Considering the diversity of interactions involved during the process of gene delivery, the biophysical investigation was divided in three parts: Study of the peptide-peptide interactions, peptide-lipid interactions and peptide-nucleic acid interactions.

Peptide-Peptide interactions: When VF1 peptide was investigated, the formation of fibrils was highlighted and a new parameter to take this into account was introduced[32]. Self-association propensities of LAH$_4$ peptides could be a key parameter to enhance gene delivery. The similarity of sequence and variety of biological activities presented by the family of LAH$_4$ peptides make it a suitable subject to study this effect. Indeed, the efficiency to enhance retroviral gene transfer has been studied for peptide nanofibrils, and a link between fibril morphology and transduction enhancement has been

suggested[36]. The importance of self-association of membrane peptide arises equally for antimicrobial activity[37].

With the aim to determine the molecular structure of the fibrils formed by VF1, the conditions of peptide aggregation have been investigated. The protocol to form homogenous fibrils suitable for NMR analysis of VF1 has been optimized. In parallel, expression and purification of VF1 in bacteria have been done in order to get $^{13}C^{15}N$ labelled peptide required for NMR experiments.

Peptide-Lipid interactions: Mechanisms underlying membrane destabilization are various. Modification of the conditions present in the endosome allows to reshuffle the interaction between the different components of the delivery system. Passage through an endocytotic pathway for LAH_4 peptides with different cargos has been demonstrated by studying the delivery activity when the acidification of endosomes is inhibited[17, 26, 31].

In this part, LAH_4L_1 peptide has been used to study the interaction with different membranes. In a first approach, the effect of increasing the peptide concentration and modification of the pH have been investigated in model membranes. This work resulted in a publication: "pH-Dependent Membrane Interactions of the Histidine-Rich Cell-Penetrating Peptide LAH_4L_1"[38]. Further analysis relative to this study will be presented. In a second approach, complex mixtures of membrane lipids have been used in order to be closer to biological membrane compositions.

Peptide-Nucleic Acid interactions: It has been demonstrated that interaction between peptides and DNA is mainly driven by electrostatic interaction[20]. Nevertheless, the hydrophobic angles of LAH_4 peptides are important for the delivery[17].

With the perspective to study interactions in complex mixtures involving peptide, DNA and membrane at an atomic level, preliminary investigations were done in order to obtain stable peptide:DNA complex. Then mixtures of peptide:DNA with model membrane were studied.

2

Methods:

Biophysical investigations use a wide variety of experiments. Methodologies are chosen depending of the time scale of the observable and the resolution needed. Investigation on complex systems requires the utilization of different techniques[39].

In this manuscript, different methods used are briefly described. Solid-state NMR will be more explained and more precisely for the characterization of membrane (peptide-lipids) systems, which will be introduced likewise.

2.1 Biophysical methods

Dynamic Light Scattering In this manuscript, this technique has been mainly used as a method to observe major changes of sample. It has been used to follow peptide aggregation and for determination of lipids vesicles size.

Dynamic light scattering (DLS) is a technique with a low-resolution determination of particle size. Autocorrelation curves are determined from the time dependence measurement of scattering intensity light. The passage of small particles in the beam induces quick disturbances and, de facto, a short time delay τ after autocorrelation. Then, a large particle results in a longer time delay (figure 2.1).

For monodisperse sample with a low polydispersity factor, the particule size information can be determined with the solvent diffusion coefficient for spherical particles. For polydisperse samples, a precise size determination is not possible, but it is possible to get an idea of the presence of wide different particle sizes or aggregates[40].

2. METHODS:
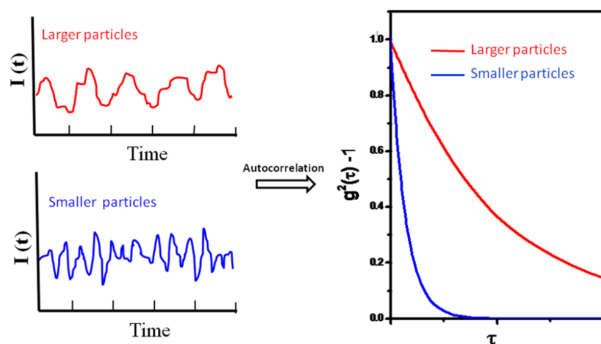
Figure 2.1: Principle of DLS measurement: on the left is represented the raw signal acquired and on the right the corresponding autocorrelation curves (adapted from [40]).

Fluorescence spectroscopy   In the chapter of peptide-peptide interactions, different approaches of fluorescence have been used in order to follow the aggregation of peptides under diverse conditions.

Fluorescence spectroscopy is a versatile tool widely used in biology. The sensitivity of the fluorophore to its environment allows to get information about structure (protein folding), dynamics and protein-protein or protein-membrane interactions. The experiment consists of an excitation of the system at a specific wavelength and the recording of its emission. Wavelength maximum, fluorescence intensity or fluorescence life-time can be interpreted, and are the sum of a multitude of microenvironmental effects. Modification of the signal can occur from external effects, like interaction with solvent molecules or with neighbouring molecules. Change of the signal can also occur by internal modifications at the level of amino acid side chain, polypeptide chains or/and because of the rotation of whole proteins [41]. The monitoring of different effects can be done with a broad variety of fluorophores, according to three different approaches:

- The intrinsic fluorescence of proteins, although limited, has the advantage to be not invasive. The signal of a Trp in a protein sequence allows to get information about its folding. It is thus possible to decipher if the indole group is exposed to solvent or embedded in a hydrophobic pocket [41].

- Extrinsic covalent probes allows one to get more specific information. For example, the development of more and more stringent organic fluorescent probes allow one to get information about structures and dynamics in biomembranes [42].

- Extrinsic noncovalent probes are suitable for probing protein structure, unfolding and aggregation. They are highly sensitive and particularly suitable for screening [43]. Nevertheless, cross tests are often necessary to confirm an effect like for the Thioflavine-T (ThT) used to detect amyloids without specifity [44].

Circular Dichroism   In this work, the circular dichroism (CD) measurements have been used to ascertain the degree of α-helical secondary structure of the LAH$_4$ peptide in different conditions.

CD measurement of proteins in the far ultraviolet (UV) allow one to get information about protein secondary structure. Molecule have to carry chiral chromophores to show circular dichroism [45]. Between 240 nm and 190 nm, peptide secondary structure information can be extracted [46] (figure 2.2).
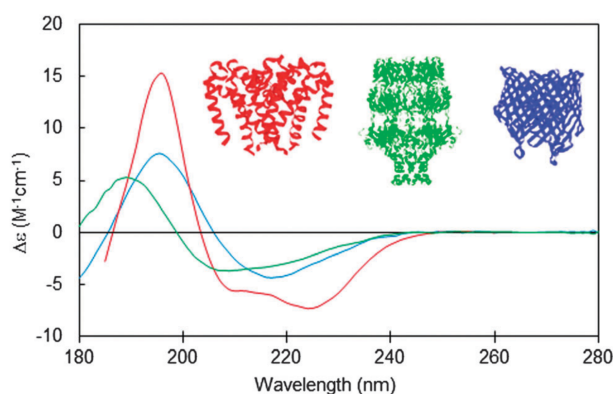
Figure 2.2: Typical CD spectra depending of the secondary structure and their corresponding proteins are represented: α-helical protein in red, mixture of α-helix and β-sheet in green and β sheet in blue (extracted from [46])

Each secondary structure is characterized by a specific dichroic signature: The spectrum of an α-helix has two minima at 208 and 222 nm and a maximum at 196 nm; β-strands have a maximum at 202 and a minimum at 219 nm.

When concentration is precisely known, percentages of secondary structure can be determined using dedicated software, like Dichroweb, which uses a data bank of protein secondary structures as reference [47]. In lipids model membranes, secondary structure and orientation with respect to the membrane can also be determined [46].

Liquid state NMR spectroscopy   In the manuscript, liquid state NMR spectra were acquired to support other methods, and mainly to follow the

2. METHODS:

complex formation of DNA and peptides during the titration of DNA into a peptide solution.

Nuclear Magnetic Resonance spectroscopy is a powerful technique for structure determination at atomic resolution, and to get information about dynamics[48]. Modulation of the phase and/or amplitude of successive radio-frequency pulses (pulse sequence) allows one to detect specific nuclei. The chemical shifts measured are related to differences of resonance frequencies of individual nuclei, depending on their local environments[49]. For biomolecules, the main nuclei observed are ^{1}H, ^{13}C, ^{15}N, ^{19}F and ^{31}P. Hence, due to the low NMR sensitivity and the low natural abundance of some of the nuclei, isotopic enrichment in ^{13}C and ^{15}N is usually done[50].

Investigation of structure and dynamics of membrane peptides is also possible by using membrane mimicking systems. Two common methods are using mixture of water and non-polar solvent or detergents , e.g. trifluoroethanol (TFE) or dodecylphosphocholine (DPC)[51].

2.2 Solid-state NMR

In this manuscript, solid-state NMR has been used for each chapter. Firstly, High Resolution Magic Angle Spinning (HR-MAS) or MAS solid-state NMR has been used with the aim to determine fibres structure. Then, for the following chapter, mainly static solid-state NMR spectra were acquired for the characterization of the effect of the peptide or a mixture of peptide-DNA complexes on lipids.

Similarly to liquid-state NMR, a wide range of structural and dynamic information can be accessed with solid-state NMR. However in the case of solution NMR, the anisotropy of the NMR parameters is not detectable because of the averaging due to the fast random movement of the molecules. However, this lack of information is compensated by very sharp transition and hence sharp spectral peaks. Because of the need of fast realignment, solution NMR is limited by the size of the complexes. The study of large complexes or extended lipid membranes is not possible due to the severe broadening of peaks.

In contrast, solid-state NMR allowed the study of extended assemblies such as fibres or small peptides associated with lipid bilayers. Additional information is obtained by solid-state NMR, such as anisotropic or orientation-dependent contributions of the chemical shift, dipolar and quadrupolar interactions. Nevertheless, this valuable information is associated with low resolution and broad lines are observed in solid-state spectra (figure 2.3, A)[52].
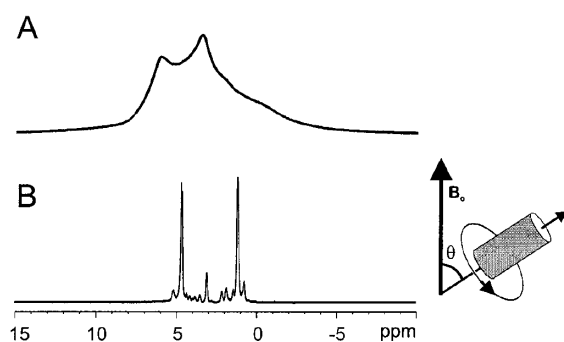
Figure 2.3: ^{1}H solid-state NMR spectra of phospholipid membranes: the same sample was acquired in the static mode or under MAS. Spectrum A shows broad line whereas MAS in spectrum B results in sharp peaks (extracted from[52]).

When needed, gain in resolution can be obtained by different methods. Specific pulse sequences, oriented sample preparation (described in the next

2. METHODS:

section) or magic angle spinning (MAS) can be used[53, 52].

Magic Angle Spinning MAS solid-state NMR allows drastic improvements in resolution, by removing information about molecular orientation in space or the size of the dipolar coupling[52]. Slow MAS NMR where sidebands are maintained, allows to conserve the information. By rapid rotation around an axis oriented at 54.74^o with respect to the magnetic field, it resultd in an averaging of the anisotropy of nuclear interactions and then leads to sharp peaks (figure 2.3 B).

Improvements in instrumentation and methodologies allowed highly resolved MAS spectra NMR, comparable to liquid-state NMR[54, 55].

Pulse sequences Spectra of low sensitivity nuclei like ^{15}N or ^{13}C are commonly acquired using cross polarization (CP). In this sequence, the magnetization from ^{1}H (higher polarization and shorter longitudinal relaxation, T1) is transfered to a low sensitive nucleus X. During simultaneous pulses in both channels - the cross polarization pulse -, the transfer is allowed and is optimal when a match in the amplitudes enables the same precession rate of both nuclei[51]. Then recording of the signal of the X nuclei is detected on the ^{1}H channel (figure 2.4).
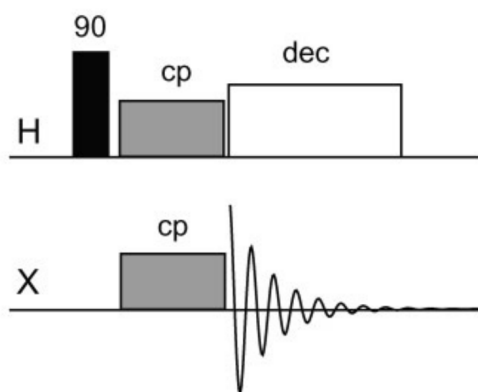
Figure 2.4: Sequence of cross polarization: the different pulses are indicated for the ^{1}H or X channels. The 90° pulse in the ^{1}H channel (black box) is followed by the CP spin-lock (grey boxes) and the acquisition is measured on the X channel, during which time ^{1}H is decoupled (white box) (extracted from [51]).

This CP sequence is a basic building block also used in more complex pulse sequences including 2D and 3D experiments, coupled or not with MAS NMR.

2.3 Solid-state NMR for studying membrane peptides

2.3.1 Model lipid membranes

Membranes are major component of the cells. Initially the membrane was considered as a rigid wall between inside and outside of a cell. The cell membrane was rapidly reconsidered as a dynamic entity, composed by numerous proteins, lipids and sterols organised in complex assemblies. The dynamics of this membrane is also complex, moving with fluid and gel phase, homogenous and heterogeneous areas like in lipids rafts[56].

In order to investigate, at a molecular level, the effect of peptides in lipid bilayers, different model systems are used. Lipids are amphiphilic molecules able to self-organise in vesicles, when reaching their critical micellar concentration. Lipids can be organized into three classes: glycerophospholipids, sphingolipids, and sterols[57]. The myriad of lipids comes from the possible modification of the head or the tail of the lipids (figure 2.5).
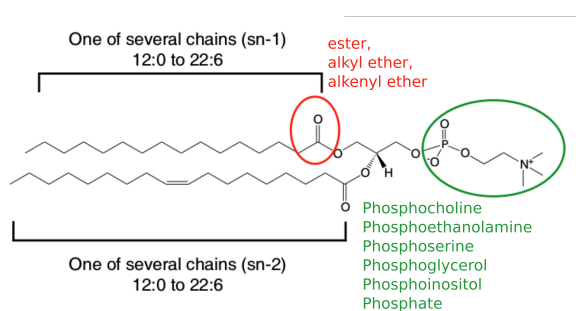
Figure 2.5: Glycerophospholipids with possible modifications: the variable positions are marked and their possible interchangeable functions indicated (adapted from[57]).

In order to facilitate biophysical analysis, simple lipid mixtures are used. The compositions are usually limited to one or two lipids. Model lipids are used to mimic the different kinds of membranes. The bacterial membranes are usually formed by a mixture of PG:PE (Phosphoglycerol:Phosphoethanolamine) lipids[58]. Eukaryote membranes are mimicked by the utilisation of zwitterionic PC (Phosphocholine) or PC:PG (PC:PS) (PS, Phosphoserine) mixtures to have charged membranes. Length and saturation of aliphatic chains play an important role in the dynamics of the membrane[59]. When arranged in bilayers, temperature is essential for the ordering of aliphatic chains and results in two possible phases: a gel phase, where lipids are well ordered, and a liquid phase, where aliphatic chains are disordered (figure 2.6).

2. METHODS:
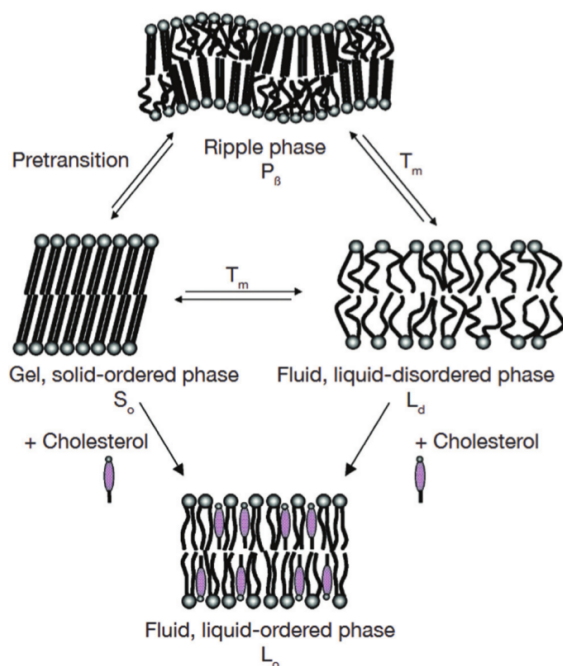
Figure 2.6: Representation of the different phases of bilayers: Changeover from gel (solid-ordered phase) to fluid (liquid-disordered phase) appears at the temperature transition. Intermediate state fluid, liquid-ordered phase is represented as the transition state of ripple phase (extracted from [60]).

The changeover from gel to fluid and back occurs at the transition temperature (T_m) which is specific for each lipid. The transition can be abrupt or smooth, but can be tuned by addition of other components. For a mixture of lipids, this transition is less clear, and co-existence of two phases can appear when close to the transition temperature (ripple phase). Molecules like cholesterol can also induce an intermediate state with a liquid-ordered phase. Both phases can bring information for the interaction of a molecule with a membrane as well the study of the effect on the phase transition.

Different kinds of "vesicles" are tuneable depending on the experiment:

- Micelles: self-organization of detergents. Micelles made of DPC are often used for liquid NMR. Micelles mimick membranes and have motional properties that are adequate for solution NMR experiment[61]. Limitations occur due to the structural constraints of these detergents. Dynamics or functionality of membrane proteins study in micelles are commonly reduced or abolish[62].

- Unilamellar Vesicles (UV): lipids organized as unilamellar bilayers can be formed at different sizes, depending on application. SUV (Small UV, d < 100 nm), LUV (Large UV, d > 100nm) or GUV (Giant UV, d = 10-

100 μm)[63]. Especially suitable for quantitative analysis because of their unilamellar bilayers allows to be directly exposed to added compound.

- Multi-Lamellar-Vesicles (MLV) are membrane models consisting of concentric phospholipid bilayers. MLVs are large systems composed of 10 to 12 bilayers that could exceed 1000 nm[64]. They have numerous advantages like easy preparation, stability and possibility to incorporate a wide variety of lipids. Despite not biological relevant, MLVs are commonly used in solid-state NMR because they allow to prepare highly concentrated samples[65].

Other systems like bicelles or nanodics allow to obtain wanted shape and size, bringing specific properties. Bicelles or nanodics allow the determination of proteins or peptides structures by NMR, but dynamic behaviour did not seem to be conserved, due to the constraint of the bicelles or nanodics[62]. Solid-state NMR structure determination can also be obtained by mechanically oriented membranes. Those oriented membranes can be obtained by spreading lipids on glass plate[66].

2.3.2 Application of solid-state NMR

Solid-state NMR is a suitable method for the study of membrane peptides. The effect of peptides on membranes can be studied through different ways, with static or MAS solid state NMR by looking at different nuclei. To look at the phospholipids (first section 2.3.2.1), MLV can be used to investigate different parts of the phospholipid bilayers. The phosphorus ^{31}P - very sensitive because of the natural abundancy of this nuclei - allows one to get information on the effect on the headgroup of the phospholipids. By using lipids deuterated on aliphatic chains, the effect of those peptides on the aliphatic chains can be monitored by ^{2}H NMR.

In order to look at the peptides (second section 2.3.2.2), ^{15}N labelling (full or partially) can be used to observe the structure or orientation of the peptide in oriented phospholipid bilayers.

2.3.2.1 Non oriented solid-state NMR

Static ^{31}P solid-state NMR The phosphorus group of the lipids offers a probe to monitor the effects of different molecules on the phospholipid head

2. METHODS:

group region. The spectra are acquired with a proton-decoupled ^{31}P Hahn-echo pulse sequence[67]. Utilization of an echo before the acquisition and a decoupling on the proton channel during acquisition result in an undistorted spectrum. Hence, the ^{31}P chemical shift anisotropy (CSA) of the phospholipids is measured and the possible proton-phosphorus dipolar coupling removed[64, 68].

In the specific case of phospholipid bilayers, CSA is mainly dependent of the phase of the phospholipids. Hence, the initially asymmetric CSA tensor defined by $\sigma_{11}/\sigma_{22}/\sigma_{33}$ can be represented by two elements $\sigma_{//}$ and $\sigma_{\perp}$ ($\Delta\sigma$ is the CSA defined as ($\sigma_{//}$ - $\sigma_{\perp}$))[69].
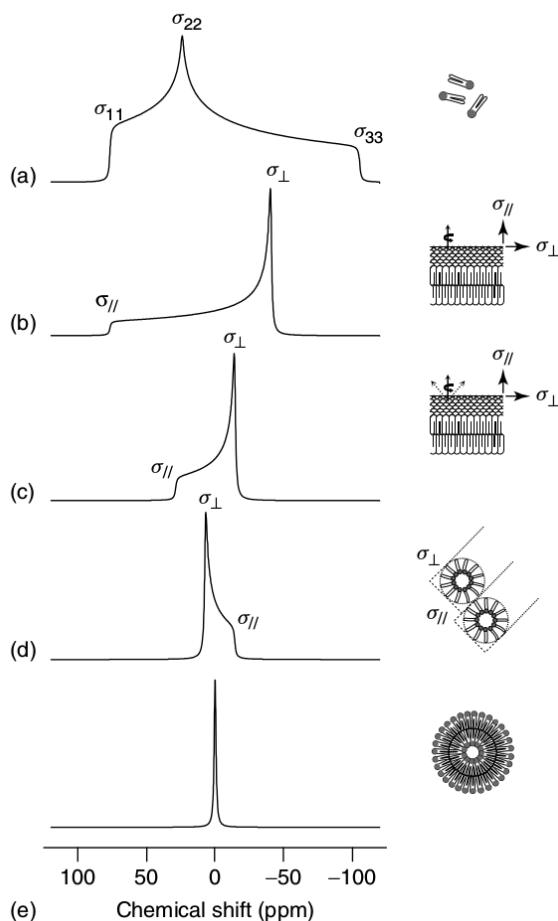
Figure 2.7: ^{31}P solid-state NMR spectra of non-oriented phospholipids in different phases: (a) static phospholipids, (b) bilayers in gel phase, (c) bilayers in fluid phase, (d) phospholipids in inverted hexagonal phase and (e) small isotropic vesicles (extracted from[69]).

Major phospholipid phase changes are easily observable, like between liquid phase to small isotropic vesicles, were an isotropic peak is observable. For phospholipid bilayers formed by MLV, subtle changes due to the addition of molecules can be monitored by determination of different parameters.

The order parameter S_2 is related to the form of the vesicles and allowed one to compare the CSA ($\Delta\sigma$) of a spectrum with the CSA ($\Delta\sigma_{ref}$) of a reference system, usually the phospholipids alone[69].

$$S_2 = \frac{\Delta\sigma}{\Delta\sigma_{ref}}$$

When submitted to a magnetic field, lipids (as peptides) have a diamagnetic susceptibility which is anisotropic. Hence, during the formation of assemblies like bilayers, the cooperative addition of this effect can lead to an orientation depending on the magnetic field[70, 71]. This propensity of vesicles to be oriented have been widely used for the determination of protein structures by solid-state NMR. Lipids arrangement like bicelles (ellipsoid form) are easily orientable and formed by mixing long-chain lipids with short-chain lipids or detergent molecules[72] (figure 2.8). Their morphology and their orientation are highly dependent on the composition, temperature and hydration. Thereupon, orientation dependance on the magnetic field is adjustable, through the addition of different molecules (e.g. lanthanides)[71].
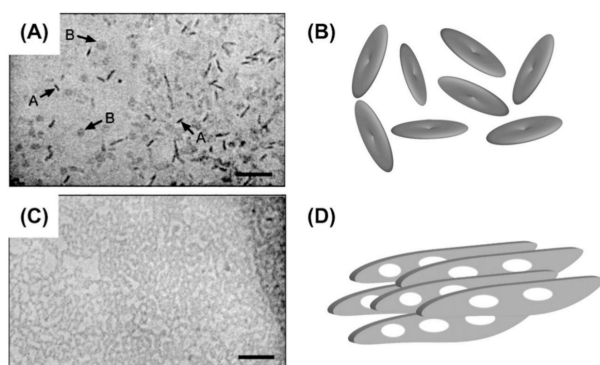
Figure 2.8: Pictures and corresponding morphology of lipid bicelles: two widely used bicelles are represented and their corresponding cryo-TEM (Transmission Electron Miscroscopy) micrograph are shown (extracted from[72]).

Whereas bicelles are usually depicted as well formed arrangements, in reality they can exhibit a wide range or morphologies[72]. As a consequence, depending of the homogeneity, those vesicles can be fully or only partially oriented. Vesicles formed by pure DMPC (1,2-dimyristoyl-*sn*-glycero-3-phosphocholine) lipids can present partial orientation[69].

The proton decoupled ^{31}P spectrum of partially oriented vesicles resultes in a deformed spectrum. Depending of the orientation of the vesicles, perpendicular or parallel to the magnetic field, the $\sigma_{//}$ or $\sigma_{\perp}$ components of the spectra are accentuated, respectively (figure 2.9).

2. METHODS:
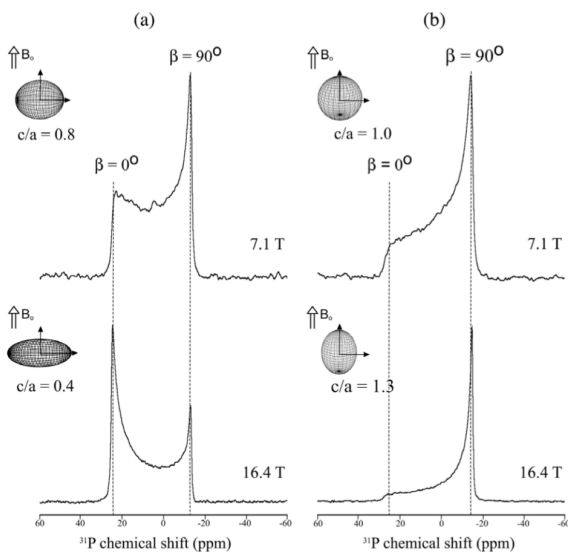
Figure 2.9: Modelisation of the liposome deformation induced by magnetic field and their corresponding ^{31}P spectra: liposomes are deformed into oblates (a) or prolates (b) shape, depending of their diamagnetic susceptibility. An increase of the strengh of the magnetic field resulted in the accentuation of the orientation (extracted from [71]).

An order parameter can be determined in order to quantify this orientation/deformation of phospholipidic systems[73]. The S1 parameter is extracted from the ^{31}P spectra, and by using the first spectral moment M_1, the isotropic chemical shift δ_{iso} and δ defined as $\delta = \delta_{//} - \delta_{iso} = -2\delta_\perp - \delta_{iso}$ where $\delta_{//}$ and $\delta_\perp$ are the chemical shifts measured for the phospholipids oriented parallel and perpendicular to the magnetic field direction, respectively.

$$S_1 = \frac{M_1 - \delta_{iso}}{\delta}$$

This value ranges from -0.5 to 1, corresponding to all the molecules oriented with their main axis perpendicular to B_0 and to all the molecules oriented in parallel[69], respectively.

^{2}H static solid-state NMR   Deuterium solid-state NMR is broadly used to monitor the effect of addition of molecules to membranes, e.g. cell penetrating peptides (CPP)[74]. The low natural abundance of only 0.01% and the wide variety of commercially available deuterium labelled lipids allowed to investigate specific effects[51]. Partially or fully deuterated chains lipids permitted to study effects along the different positions of the acyl chains.

The ^{2}H solid-state NMR spectra were acquired with the solid quadrupolar echo-pulse sequence[75]. The ^{2}H spectra are composed by signals from different

CD$_2$ and one CD$_3$ groups, each one contributing to a quadrupolar powder pattern, with the distance between the two main peaks, defining a characteristic quadrupolar splitting for each site (figure 2.10)[76].
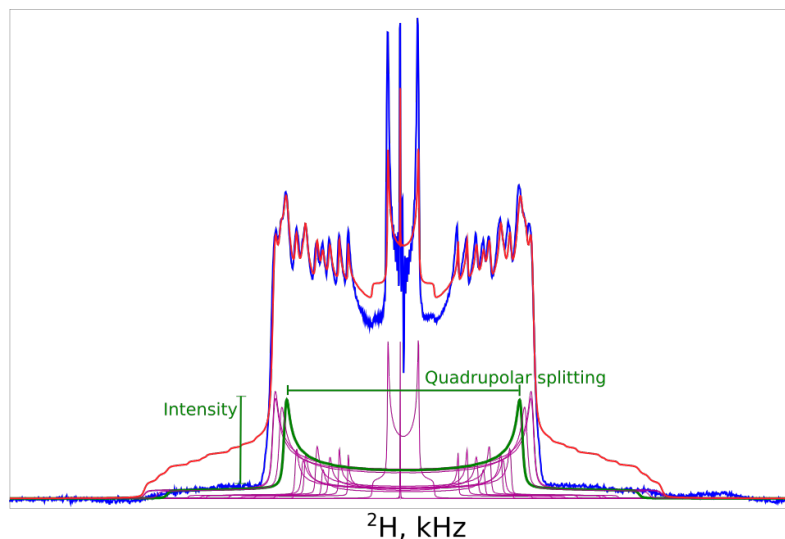
Figure 2.10: Typical ^{2}H solid-state NMR spectrum: the spectrum is composed by quadrupolar powder patterns of the different CD$_2$ and one CD$_3$ groups of the lipid aliphatic chains. The experimental spectrum is represented in blue and the red one is the sum of the individual patterns (in purple). One of this patterns is represented in green to show the two parameters optimised for the simulation, the quadrupolar splitting and the intensity.

The following equation was used to calculate the order parameter S$_{CD}$ for each of the C-D bonds:

$$\Delta\nu_Q = (\tfrac{3}{4})(\tfrac{e^2qQ}{h})S_{CD}$$

where $(\frac{e^2qQ}{h})$ is the static quadrupolar coupling constant equal to 167 kHz for a C-D bond, and $\Delta\nu_Q$ the observed quadrupolar splitting[77]. Without motions, the static splitting would amount to 125 kHz, but in a liquid crystalline bilayer, motions result in considerable averaging. Notably, the CD$_2$ groups exhibit more motional freedom in the hydrophobic interior when compared to the region of the carbonyl. Therefore, the order parameters tend to decrease for these segments towards the interior of the bilayer. This effect is also expressed by the deuterium order parameter, S$_{CD}$, representing the ratio between the measured and the maximal values (figure 2.11)[76].

For our study, the quadrupolar splitting of each C-D bond of the aliphatic chain of the labelled lipids was extracted using the TopSpin NMR software

2. METHODS:
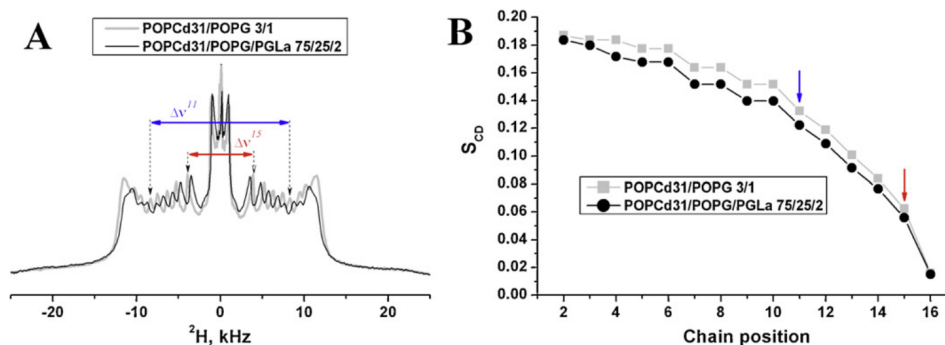
Figure 2.11: ^{2}H solid-state NMR spectra and the corresponding order parameter profile: deuterium order parameters S_{CD} are plotted in a position-dependent manner (extracted from [76]).

(SOLA (Solid Lineshape Analysis), version 2.2.4, Bruker Biospin). The QUAD all mode was used, where the full line shape of the spectrum of each CD_2 site was optimized by intensity, and the quadrupolar splitting was observed to obtain the best representation of the experimental data (figure 2.10).

2.3.2.2 Oriented solid-state NMR

Lipids have the advantage to be orientable systems. This orientation can be obtained magnetically (e.g. bicelles) or mechanically. By spreading phospholipids on thin glass plates, macroscopically oriented lipid bilayers can be obtained. Then, the peptides can be co-dissolved in this preparation, allowing to observe a peptide signal depending of its orientation in the membranes [51].

The ^{31}P NMR spectra from oriented samples are usually used as a quality control of the orientation of the phospholipids. When bilayers are well oriented, a sharp peak is visible (between 40 and 20 ppm, depending on the phospholipids used) and when lipids are disturbed or disorganised (by unsuitable sample preparation or by effect of peptides) intensities approximatively from the main peak to -20 ppm, are observable (figure 2.12) [78].

In these oriented bilayers, orientation of a peptide can be monitored with ^{15}N or ^{13}C by measurement of the dipolar coupling within a bond (^{1}H-^{15}N, ^{1}H-^{13}C) [51]. Hence, usually a single label ^{15}N is introduced to the backbone of a peptide. When the membrane normal is aligned parallel to the magnetic field direction of the NMR spectrometer, the ^{15}N chemical shift is a direct indicator of the approximate orientation of helical domains relative to the lipid bilayer
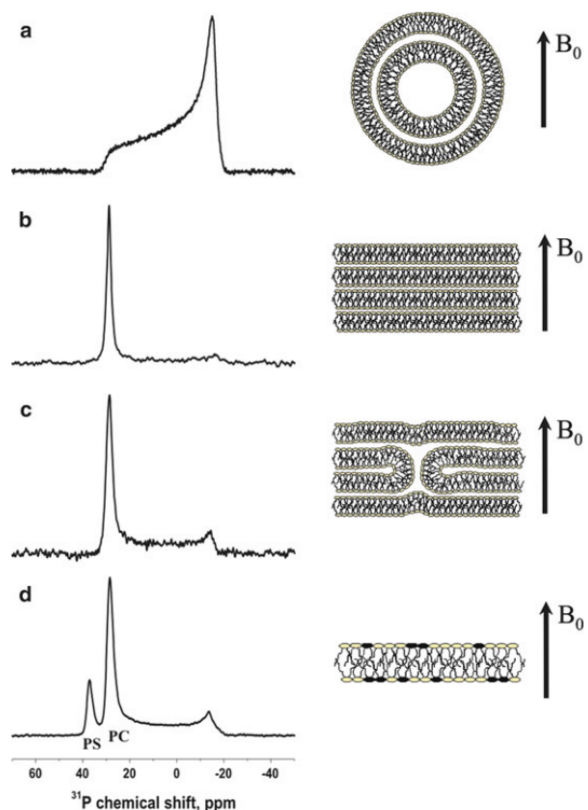
Figure 2.12: Typical line shapes of ^{31}P solid-state NMR spectra of different bilayer preparations: (a) non-oriented sample with classical powder pattern line shape, (b) a well oriented sample, (c) an oriented sample with small fraction of non-oriented lipids and (d) a mixture of phospholipids (PC, phosphatidylcholine and PS phosphatidylserine) (extracted from [78]).

and provides valuable information about the peptide topology and thus the peptide-lipid interactions (figure 2.13) [79].
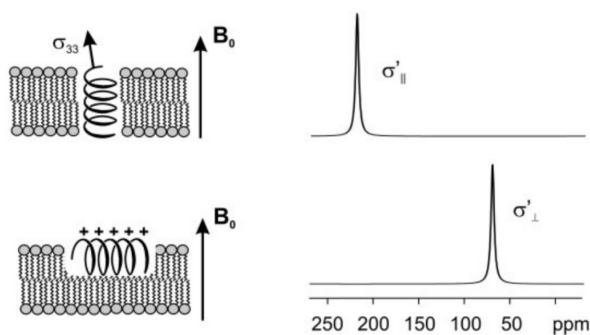
Figure 2.13: Representation of the ^{15}N signal obtained, depending of the orientation of the peptide: signals around 200 ppm and 80 ppm are obtained for a transmembrane and in planar orientation, respectively (extracted from [79]).

Whereas chemical shifts around 200 ppm are indicative of transmembrane alignments, helices that are oriented along the bilayer surface exhibit resonances of < 100 ppm [79].

2. METHODS:

3

Characterization of Peptide-Peptide Interactions:

Peptides are biomolecular building blocks suitable for biological applications because of their biocompatibility and readily production. Whereas specific functions are related to primary (specific amino acids), secondary or tertiary structures, during the last decades, quaternary structures have raised an increasing interest[80]. Indeed, higher-order assemblies such as complexes or large-scale self-assembled structures gave access to new function and possibility to create new materials (i.e. filaments/fibrils, hydrogels or surfactants)[81]. Self-assembly could also have an influence on the activity of membrane active peptides, like antimicrobial peptides (AMPs)[37].

In the field of gene delivery systems, peptide nanofibrils have been demonstrated to efficiently enhance retrovirus gene transfer[36]. Recent work highlighting enhanced LV transduction by VF1 (LAH_4A_4) fibrils opened new perspectives in the design of LAH_4 peptides for delivery systems. Enhancement of transduction appears through the ability to interact and concentrate viral particles. Pictures of the peptide incubated in culture medium (DMEM, Dulbecco Modified Eagle Medium) show an evolution from spherical complexes to annular and linear arrangements, with a periodicity of 10 nm after 1 hour[32] (figure 3.1).

Further investigation of the nanofibrils demonstrated a pH dependence of the secondary structure similar to most of the LAH_4 peptides[12]. A reversible α-helix is obtained, depending of the pH (unstructured at low pH and folded at neutral pH) with a transition above pH 6.1, close to the pKa of the histidines[32]. This reversibility is also an advantage from the point of view of gene

3. CHARACTERIZATION OF PEPTIDE-PEPTIDE INTERACTIONS:
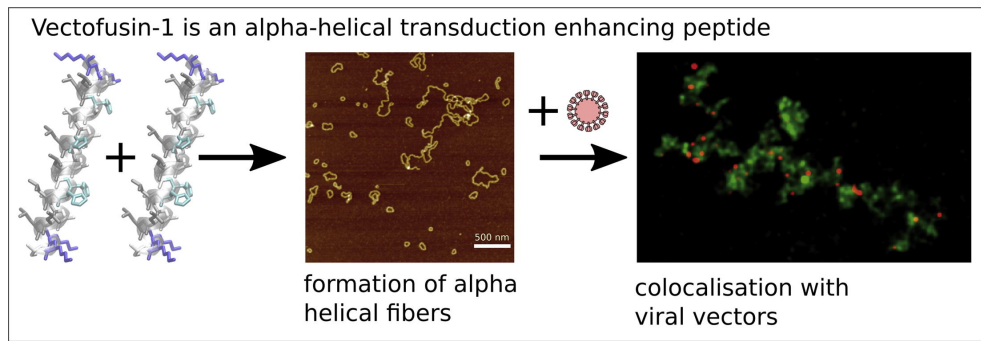
Figure 3.1: Summary of the behaviour of VF1 as enhancer of viral LV high-lighted by Vermeer et al.[32]: on the left VF1 is represented in α-helix conformation, in the middle AFM (Atomic Force Microscropy) picture of the fibrils formed by the VF1 and on the right confocal microscopy picture of the colocalisation of the peptide (in green) and viruses (in red) (extracted from [32]).

delivery. Indeed, in contrast to β-strand units, α-helix promotes hydrophobic interactions instead of hydrogen-bonding, allowing an easy reversibility of the assemblies[81].

The efficiency of VF1 to transduce different LV pseudotypes has demonstrated its efficiency[30,82]. In comparison, the LAH$_4$ peptide was inefficient to enhance gene transfer using LV vectors[23]. On the contrary, antimicrobial activity have been proven for LAH$_4$, but not for VF1[23]. Differences in activities for LAH$_4$ peptides have been studied, mainly by investigation of peptide-lipid interactions, but the importance of aggregation for the biological activity of these peptides has not been studied so far. As for other peptides used for delivery systems, thorough knowledge about their mechanisms of action would be needed, in order to an improvement of delivery systems[9,10]. Hence, investigation of LAH$_4$ peptide aggregation helps to develop more effective gene delivery systems.

The structural investigation of α-helical VF1 fibrils is interesting. For LAH$_4$ peptides, aggregation is mainly dependent on pH, similarly to the α-helical secondary structure. At low pH, the peptide is unstructured and mostly monomeric, and at neutral pH, the content of α-helix increases and aggregation occurs[13,32].

The α-helical coiled-coil structures are generally following the heptad-based pattern repetition (HPPHPPP), when considered as linear heteropolymers of hydrophobic (H: Ala, Leu) and polar (P: His, Lys) residues (only

residues presented in the LAH$_4$ sequence are listed)[83]. The LAH$_4$ peptide does not correspond to this canonical coiled coil motif (illustrated in table 3.1).

Table 3.1: Main peptides used in this manuscript: their amino acids sequences were indicated and their corresponding HP pattern.

Peptides	Sequences and HP patterns
LAH$_4$	KKALL ALALH HLAHL ALHLA LALKK A
	PPHHH HHHHP PHHPH HHPHH HHHPP H
LAH$_4$L$_1$	KKALL AHALH LLALL ALHLA HALKK A
	PPHHH HPHHP HHHHH HHPHH PHHPP H
VF1	KKALL HAALA HLLAL AHHLL ALLKK A
	PPHHH PHHHH PHHHH HPPHH HHHPP H

The driving forces of peptide interactions are mainly electrostatic and hydrophobic. Generally, the presence of negative and positive charged amino-acids on the peptides, at specific positions, stabilizes these large assemblies. Similarities in the LAH$_4$ peptide sequences are important, notably with a conserved number of charged amino-acids. Nevertheless, they contain only cationic amino-acids yielding this association highly dependent of the environment[84]. Hence, difference of aggregation for LAH$_4$ peptides would mainly be due to their hydrophobic propensity. Nevertheless, different parameters should be considered for the study of LAH$_4$ aggregation. Usually, for simplification, peptide secondary structure is considered as a perfect helix (100% α-helical instead of unstructured), but a mixture between the two secondary structures could actually trigger the interaction. Spontaneous formation of VF1 nanofibrils has been observed in rich cell culture media. Thereupon heterogeneous assemblies should have been obtained. The importance of phosphate ions has been indicated for VF1 fibril formation[32]. Nevertheless, biophysical investigations require homogenous samples for accurate analysis necessitating optimization of the VF1 fibrils formation conditions.

In this chapter, the peptide-peptide interactions of LAH$_4$ peptides have been studied. In a first part, the conditions of fibrillation are optimized. Then, different methods are tested to observe the aggregation. Finally, solid-state NMR spectra have been acquired, in order to study the fibril of VF1 at an atomic level.

3. CHARACTERIZATION OF PEPTIDE-PEPTIDE INTERACTIONS:

3.1   Material

Sample preparation

Fibril preparation: First assays were performed by dissolution of sample powder, and by increasing the pH through the addition of 0.1 or 0.5 M NaOH solution. The following assays were done using dialysis, to equilibrate the pH. Peptides were dissolved in water, and dialyzed against the desired final buffer. Dialysis bags of 0.5 to 1 MW were used (Spectra/Por, Biotech CE) and buffer was exchanged during at least 36 hours with four changes of buffer solutions. Optimal conditions of fibrillation were obtained by dialysis at a pH of 6.25 in 10 mM phosphate buffer. Samples were prepared directly from powder at a concentration of 2 mg/mL in water.

Since the post-fibrillation concentration is unknown, but is essential for specific measurements (mainly for DLS and CD measurement), the sample concentration was measured and modulated through dilution with similar buffer, until reaching a convenient signal.

For solid-state NMR, aggregates were pelleted by centrifugation at 13,000 g during 30 min, and transferred into an appropriate rotor.

Gel preparation: Gels were obtained by disolution of peptide powder directly at the wanted concentration. Then, increases of the pH were done with the addition of NaOH solution from 0.1 to 1 M. Effective polymerization was followed by visual inspection.

Sample measurements

Dynamic Light Scattering: Samples were measured in a quartz cuvette at 25^oC, using a Zetasizer NanoS from Malvern Instruments. The static light (laser He-Ne 633nm) diffusion is measured (according to Debye model) at 173°, allowing a measured range from 0.3 nm to 10 microns (diameter). The intensity size distributions, Z-average and Polydispersity Index presented are calculated from the correlation data by the Zetasizer Software (Malvern Instruments, 7.11 version).

Titration presented in the figure 3.2 has been done with VF1 peptide at 1 mg/mL in acetate buffer 100 mM starting at pH 4.8. The pH was increased by addition of 0.1 or 0.5 M NaOH solution. A small fraction of the sample was deposited on indicator strips to measure the pH.

Circular Dichroism: Samples were measured in a 1 mm quartz cuvette (Suprasil, Hellma Analytics) at 25ºC using a spectropolarimeter (Jasco J-810, Tokyo, Japan). Spectra were recorded from 180 nm to 260 nm with a data pitch of 1 nm, a standard sensitivity and a data integration time of 1 s. Scanning mode and speed were continuous at 50 nm/min. The spectra resulted from 10 accumulations.

Fluorescence spectroscopy: Fluorescence measurements were done in two different devices:

- Individual measurements were done in quartz cuvette at 25ºC using a FluoroLog-3.22 spectrophotometer (HORIBA, Kyoto, Japan).

For Thioflavin T (ThT, Sigma-Aldrich, Lyon, France) measurement: emission was scanned from 455 to 650 nm at an excitation wavelength of 440 nm. Slit sizes for excitation and emission were defined at 2 nm and the integration time of the photomultiplicator was set up at 0.3 sec. ThT stock solution was prepared at 1 mM and 10 μL of this solution was added to 1 mL of samples (= 10 μM final). The peptide concentration was at 0.25 mg/mL (in 20 mM acetate buffer) and the pH increased in a stepwise manner, by addition of 0.1 M NaOH (figure 3.7). Controls with only ThT or only peptide was performed with the same parameters. Augmentation of the pH did not result in any increase of the signal. The pH was measured by deposition of a small fraction of the sample on indicator strips.

For Blue emission measurement: emission was scanned from 370 to 600 nm at an excitation wavelength of 358 nm. Slit size for excitation and emission were at 3 nm and the integration time of the photomultiplicator was set up at 0.3 sec. The peptide concentration was 1 mg/mL (in 20 mM acetate buffer) and the pH increased in a stepwise manner, by addition of 0.1 or 0.5 NaOH solution (figure 3.8). The pH was measured by deposition of a small fraction of the sample on indicator strips.

- Multiple measurements were done with a multimode microplate reader CLARIOstar (BMG Labtech).

Peptide powder was aliquoted and dissolved with buffer just before measurements at two pH: 6.25 and 7.4, and at concentrations from 0.25 to 2 mg/mL. Buffer used was 10 mM phosphate at both pH, containing or not 40 μM of

3. CHARACTERIZATION OF PEPTIDE-PEPTIDE INTERACTIONS:

ThT. Excitation was done successively at 450 and 358 nm, and emission was recorded at 480 and 440 nm for ThT measurement or blue emission measurement respectively. One measurement per minute was done during at least 12 h.

Transmission Electron Microscopy: For each samples, a drop of 15 μL of sample was placed on the copper face on a TEM grid (CFT200-CU, Electron Microscopy Sciences, Hatfield, USA). After 2 minutes the drop was removed with a blotting paper and dried for at least 30 min. Then, grids were rinsed in order to remove salts from the buffer. Addition of 200 μL H_2O during 15 s was followed by drying with a blotting paper. This rinsing step was repeated successively two times, then the samples were completely dried during at least 30 min.

Staining was done by immersion of grids for 1 min in a solution of 1% of uranyl acetate. Finally, images were recorded with a transmission electron microscope (Hitachi 7500, Krefeld, Germany).

For samples prepared in DMEM (Dulbecco's Modified Eagle Medium, DMEM high glucose, GlutaMAX Supplement; Gibco, ThermoFisher), VF1 peptide was diluted to 12 μg/mL, similarly to cellular assays, and concentrated by using a SpeedVac system before being deposited on microscopy grids.

Liquid state NMR: VF1 was dissolved at 2.5 mg/mL in 10% D_2O and the pH was set at 5.5 by addition of 0.1 M NaOH. Spectra were acquired on a 600 MHz NMR spectrometer (Bruker Avance III) on a ^{1}H-^{19}F diffusion 5 mm probe at 298 K. Diffusion Ordered SpectroscopY (DOSY) experiment was acquired in 2D (2D stimulated Echo experiment using bipolar gradients and Watergate for water suppression). The NMRnotebook (NMRTEC, Illkirch - France) DOSY module was used for determination of the volume and the diffusion coefficient.

MAS Solid-state NMR parameters

Adamantane was used as external reference (38.2 ppm for the left peak corresponding to the CH_2) and to optimize the parameters on Bruker Avance 300 or 500 NMR spectrometers equipped with a 4 or 2.5 mm MAS probe head

(Bruker Biospin, Rheinstetten, Germany) with 12 or 25 kHz spinning at room temperature or 273 K, respectively.

Proton-decoupled ^{13}C solid-state NMR spectra[85] were acquired using a cross polarization sequence on optimal condition on a 300 MHz or 500 MHz instrument with the following parameters at 300 MHz or 500 MHz, respectively: the B1 fields, including for ^{1}H decoupling, were 76 kHz or 78 kHz, a contact time of 3000 μs or 1000 μs , 90° pulse between 3.9 or 2.5 μs; acquisition time, 62 or 82 ms; time domain data points, 4k; the recycle delay 3 s or 1 s and the number of scans between 17,668 to 79,070 or 16,384. A line broadening of 100 Hz or 25 Hz was applied before Fourier transformation.

The 2D ^{13}C-^{13}C spectra were acquired using a Dipolar Assisted Rotational Resonance (DARR) pulse sequence[86]. The spectra were recorded at 125 MHz with parameters optimised for the 1D ^{13}C. Two mixing times were used, 25 and 75 ms, the time domain data points and number of scans in the two dimensions were 2048 and 148, respectively. Spectra were processed using 100 Hz of line broadening, the effective time domain was reduced at 512 points.

3. CHARACTERIZATION OF PEPTIDE-PEPTIDE INTERACTIONS:

3.2 VF1 aggregation

Aggregation of peptides of the LAH_4 family is highly dependent on pH. The increase of the pH is associated with the deprotonation of the histidines and a higher propensity for hydrophobic interactions. DLS measurements (figure 3.2) allowed to follow this augmentation of size of aggregates.
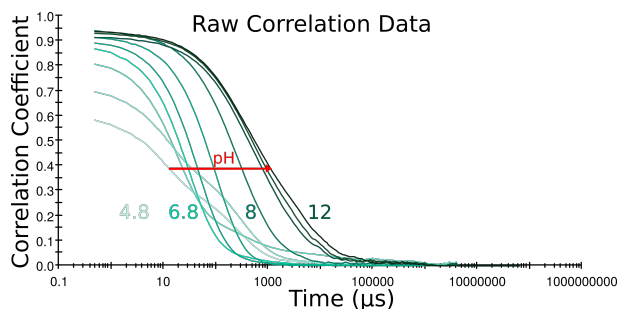
Figure 3.2: DLS measurement of VF1 with an increasing pH: the raw correlation data of VF1 is presented with colours of increasing darkness when the pH increases. pH values for some of the samples are indicated.

VF1 did not present a fully monomeric form at low pH. A high polydispersity was observed, even at low pH, as it was visible with the curve pH 4.8 presenting at least two components. DOSY measurements of VF1 at pH 5.5 corroborated this result. The species observed by liquid state NMR presented a diffusion coefficient of $1.4 \ 10^{-10} \ m^2.s^{-1}$, corresponding to a size of 24,400 $\mathring{A}^3$. Compared to the theoretical size of the peptide, this value corresponds to, at least, a dimer of peptides. Nevertheless, at low pH the aggregation did not seem to increase and slowly increases over time[32]. When the pH is increased below the pKa of the histidines, the particle size grows significantly. Above a pH 6.8, the size of the aggregates increase quickly until pH 8. Then, the aggregates reach a maximal size, corresponding to a correlation time around $10^5 \ \mu s$.

This high propensity of aggregation of VF1 was also observed by gel formation under some conditions. Gelification was observed for a pH of 7.5 around a concentration of 5 mg/mL in acetate buffer. When the pH or the concentration was higher, the gel was more and more rigid. The formation was reversible by lowering the pH. The TEM picture of a gel shows a network of peptides (figure 3.3).

The formation of this gel was immediate. Spontaneous formation of aggregates is not a good manner to form ordered/homogenous arrangements.

42
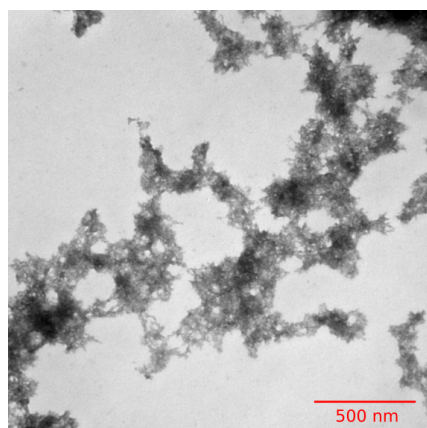
Figure 3.3: TEM picture of VF1 gel: the picture presented showns a network of peptides component the gel. Different density of gel were observed on the grid, the larger were totally impermeable to the beam and presented extended black piece.

Hence, for the formation of fibres, lower concentrations were used. The main parameter of aggregation was the pH, and the increase of it by pipetting seemed to be prohibitive for fibre formation. In order to increase slowly the pH, dialysis was chosen. An assay of dialysis against pH 7.4 was tried, nevertheless, depending on the conditions (buffer or concentration), fibres represent only a small fraction of the samples. A pH of 6.25, just above the pKa of the histidine, limits the aggregation.

This pH of 6.25 was also chosen because it could be suitable not only for VF1, but also for many other peptides of the LAH_4 family. The pKas of histidines of LAH_4 have been determined in DPC micelles between 5.4 to 6.0[11]. The pKas of the histidines of VF1 have been determined to range from 5.9 to 6.2 under similar conditions (unpublished data from Louic Vermeer). The pKas of histidines can be quite different, depending on the local environment[87]. Nevertheless, for LAH_4 derivatives, differences in histidines position along the α-helix did not significantly alter the pKa values.

The dialysis protocol at pH 6.25 in 10 mM of phosphate buffer was applied to VF1 and to LAH_4L_1. Samples before and after dialysis were measured by CD and DLS (figure 3.4).

Before dialysis, counter-ion exchange of the peptides (to exchange the trifluoroacetic acid (TFA) counter-ion: 3 exchanges in 4% acetic acid solution; peptide synthesis details in the Appendix) ensures acidic condition when resuspended in water, because of the cationic profile of the peptides. At low pH, CD measurements confirmed that both peptides are unstructured. In agreement with titration experiments presented in figure 3.2, at low pH, DLS

3. CHARACTERIZATION OF PEPTIDE-PEPTIDE INTERACTIONS:
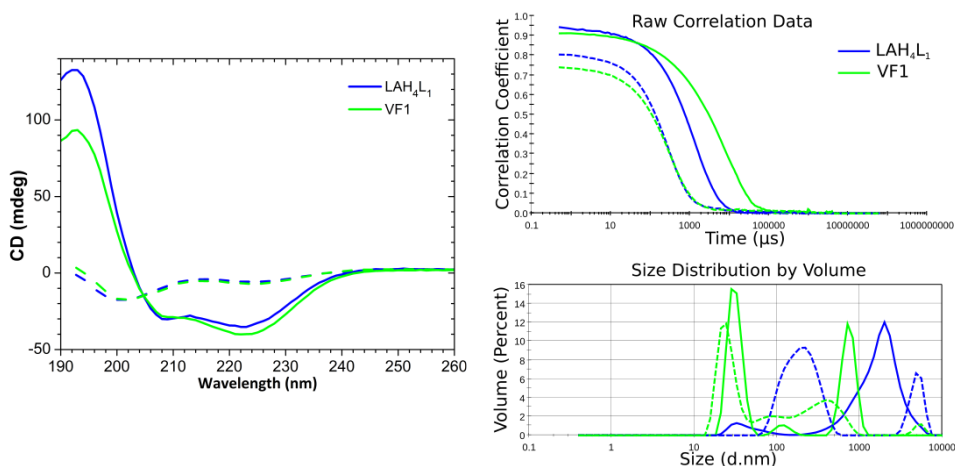
Figure 3.4: CD and DLS spectra of LAH4L1 and VF1: The dashed line corresponds to samples at low pH and the full line to the samples after dialysis at pH 6.25. Green and blue lines show to LAH_4L_1 and VF1, respectively.

experiments did not present fully monomeric peptide and a high polydispersity index (0.53 and 0.43 for LAH_4L_1 and VF1 respectively). After dialysis, both peptides LAH_4L_1 and VF1 presented an α-helical secondary structure. Correlation curves of DLS measurements indicated an increase of one and two orders for LAH_4L_1 and VF1, respectively (polydispersity index 0.59 for LAH_4L_1 and 1 for VF1). After dialysis, the two peptides measured by CD and DLS were observed by TEM (figure 3.5).
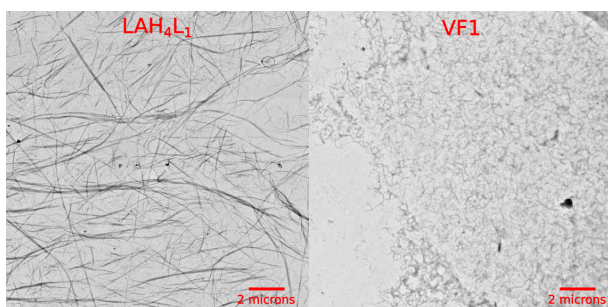
Figure 3.5: TEM pictures of LAH_4L_1 and VF1 fibres obtained after dialysis against 10 mM Phosphate buffer at pH 6.25.

In both cases, fibres were present on all the microscopy grids. For LAH_4L_1, straight elongated fibres of various lengths were observed. Fibres of VF1 were shorter, around 300 nm of length, and curvy.

It is interesting to note that LAH_4L_1 seemed to present bigger and less homogenous assemblies, but this is not correlated with the DLS measurement. This difference can be explained by a sedimentation of the larger species of the mixture. A difference in the appearance of the fibres by these two peptides can

44

be due to diverse reasons. Slight changes in peptide sequence can drastically change self-association and organization[88, 89]. The distribution of alanines and leucines of the VF1 compared to the LAH_4L_1 can allow a greater variety of arrangement between peptides, therefore, a less regular organization[90]. Different ratios of α-helix, breaks in the helix (as present for the LAH_4 peptide depending on the condition) can be the source of divergent packing[14]. Further investigation, and notably at an atomic level, would bring more information about the arrangement of peptides between each other. Nevertheless, this protocol could be applied to other peptides of the LAH_4 family, to determine if these peptides are all able to form fibres.

Further investigation with various conditions could be tried as well. For peptide-peptide interactions mainly driven by hydrophobic forces, salts are important for their arrangements[84]. This problem can be imaged by the great variety of arrangement observable in complete media. Biological assays are made in highly complex medium, needed for the growth of cells. Xvivo medium was used for VF1, and AFM pictures showed that the peptide formed globular aggregates[32]. Aggregates formed by VF1 were also observed in a DMEM medium, which is also often used for cellular growth (figure 3.6).
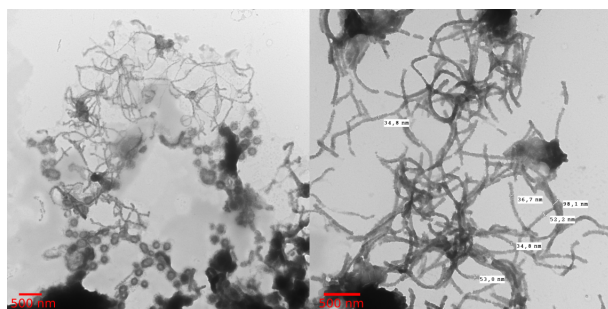
Figure 3.6: TEM pictures of VF1 fibres obtain in DMEM medium.

Different shapes were observed, and bigger arrangements, compared to the ones detected in Xvivo media[32]. If the biological activity of this peptides is dependent on the aggregation, some parameters could be detrimental. All the more that biological assays are performed in a wide variety of conditions depending of the cargo tested[10]. Hence, better knowledge about the peptide-peptide interaction of the LAH_4 family would be useful.

However, screening of conditions to study the different arrangements of these peptides needed an adapted methodology. In our study, assessment of

3. CHARACTERIZATION OF PEPTIDE-PEPTIDE INTERACTIONS:

the presence of fibres or not was possible only by TEM. Because of experimental constraint, mainly time of preparation and analysis, this method is not suitable for longer screening of fibrillation conditions. Hence, different methods of fluorimetry were tested. ThT fluorescence is an efficient method for the screening of conditions for amyloids fibres[91]. Nevertheless, positive indication of β-amyloids is always necessary, because of a lack of specificity[44]. By interacting with the hydrophobic part of β-sheets, the thioflavin induces a characteristic fluorescence signal. Hence, in our case, the presence of a hydrophobic surface due to the amphiphilic profile of the peptide when folded in α-helix could induce a signal.

As it was previously demonstrated, VF1 fibres did not show a ThT signal[32]. In our case, screening of concentration from 0.25 to 2 mg/mL at pH 6.25 or 7.4 in 10 mM phosphate buffer with a multimode microplate reader did not give any ThT signal. Nevertheless, a ThT signal was observed during pH titration of the VF1 (at 0.25 mg/mL) in presence of ThT (figure 3.7).
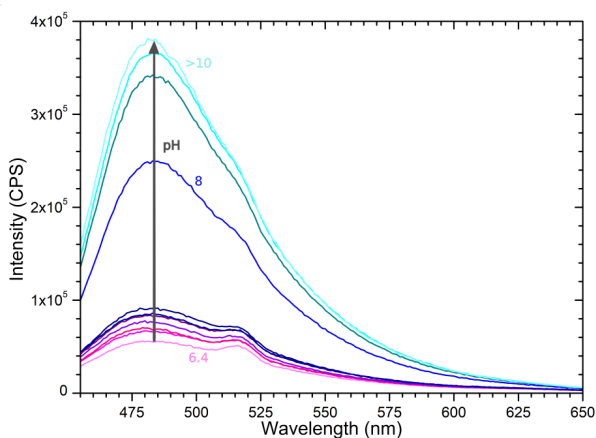
Figure 3.7: ThT measurement of pH titration of the VF1 peptide: the emission spectra were acquired from 455 to 650 nm and excitation was done at 440 nm. The pH measurement for some of the samples are indicated.

At the beginning of the titration, only a slow increase of the signal was observed. While reaching a pH of 8, the signal was 3 times more intense. Because pH can induces changes in the ThT molecule, negative controls are needed. Similar conditions with only ThT or only the peptide were tested, and augmentation of the pH did not result in an increase of the signal.

Under the condition tested, most of the samples is aggregated, but didn't form fibres. Nevertheless, it is interesting to observe a ThT signal with an α-helical peptide. Using the lack of specificity of the ThT, some conditions could be found in which ThT signal would be observed for VF1 fibres. Different

concentrations of ThT could be tested with fibres or aggregates in order to determine if a signature profile is observable to decipher the presence of fibres or aggregates.

Elsewhere, a library of molecules was used to determine the presence of β-amyloids[92]. Hence depending of their mode on interaction, some of them could be tested in presence of α-helical fibres. Otherwise, a fluorophore like ANS (8-anilinonaphthalene-1-sulfonic acid) or bis-ANS (4,4'-dianilino-1,1'-binaphthyl-5,5'-disulfonic acid) can be used to at least detect the lag phase of VF1 fibrillation[93].

Interestingly, the laboratory of David Fenard observed by confocal microscopy the photoluminescence of VF1 peptide. A maximum of emission around 518 nm was observed when excited at 488 nm[32]. Other studies of protein amyloids revealed an intrinsic fluorescence signal during aggregation[94]. Hence, emission fluorescence of the VF1 peptide was investigated and the maximum of intensity (from 370 to 600 nm) was observed for an excitation at 358 nm. Emission spectra were then acquired during pH titration of VF1 (figure 3.8).
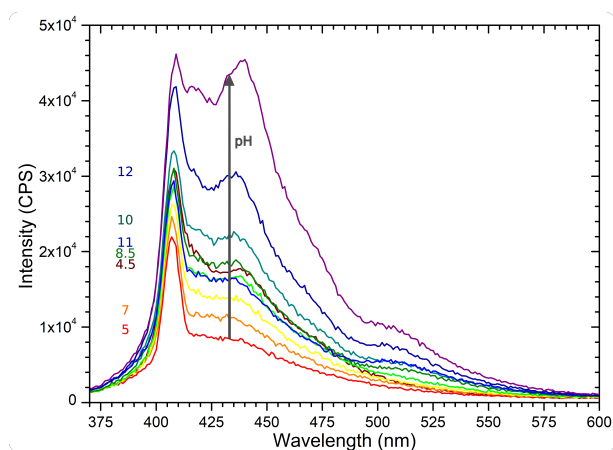
Figure 3.8: Emission spectra of pH titration of VF1: the emission spectra were acquired from 370 to 600 nm and excitation was done at 358 nm. The pH values for some of the samples are indicated.

An increase of the signal was observed when the pH was increased with a maximum at 440 nm. Different tests were done, mainly by variation of the buffer or the concentration of the peptide. LAH$_4$ was also tested, and like the VF1 peptide showed an increase of the signal parallel to the increase of the pH. Nevertheless, the intensity of the signal was very variable and not reproducible. Also, because aggregation of the VF1 is not fully controllable, it is impossible to correlate an increase of the signal with any kind of aggregation.

This kind of intrinsic emission is still not fully understood. It has been suggested that peptide electrons could be delocalized through hydrogen bonding. Fluorescence signal have been revealed to be significantly sensitive to the pH effect, or fibril structure[95, 96]. It may be possible to follow the VF1 fibrillation by following this intrinsic emission[97]. However, better control of the aggregation of the VF1 would be a prerequisite to use this method for screening, and a cross-validation method is needed. Utilising both intrinsic and extrinsic fluorescence (with fluorophore) experiment could bring a cooperative analysis to characterized and quantified peptide fibrillation.

3.3   Structural characterization of the fibrils

Arrangements of fibres are diverse and their influence on the biological activity is also questioned[36, 98]. The packing of mixed α-helical coiled-coil structure can occur in many different ways[90]. In our study, we decided to use solid-state NMR, which is particulary suitable for structural characterization of fibril assemblies, at an atomic level. Other methods like high-resolution NMR and X-ray diffraction fail, due to the size of the complexes and a lack of long-range order[55]. Divergences of fibres in backbone or sidechain conformations and supramolecular structure are observable by significant differences of ^{15}N and ^{13}C chemical shift in the solid-state NMR spectra[98].

However, for NMR analysis, isotopic labelling (^{15}N, ^{13}C) is necessary. For this purpose, VF1 was expressed in bacteria as a fusion protein, which after cleavage with formic acid, carries an additional proline at the N-terminus yielding pVF1 (details of expression and purification are presented in the following chapter 4).

The 1D ^{13}C solid-state NMR spectrum (in natural abundance) of pVF1 fibres was compared with spectra of VF1 powder at low pH and at pH 8 (figure 3.9).

Elevation of the pH resulted in broader peaks, when compared to the powder at acidic pH. On the contrary, aggregates from pVF1 fibrillation presented peaks as sharp as VF1. Some differences of peak chemical shifts are observable. Nevertheless, 1D experiments did not allow further interpretation of the results.

Figure 3.9: Spectra of pVF1 fibres compared to VF1 powder at low and high pH: 1D ^{13}C solid-state NMR spectra were acquired. The spectra of the fibre of pVF1, VF1 at low or pH 8 are coloured in green full line, blue full line or grey dash line respectively.

The VF1 peptide has been labelled on the methyl of the alanine 14 (^{13}C$_{beta}$) and 1D ^{13}C solid-state NMR spectra have been acquired. In this experiment, the fibres were recovered by centrifugation, and the supernatant was lyophilised in order to acquire a spectrum under similar conditions. A liquid state NMR spectrum of the supernatant was also acquired (figure 3.10).

When comparing the supernatant and the aggregates of VF1, their chemical shifts are mostly similar. The main difference was the peaks width, which is sharper for the fibres of VF1. Interestingly, concerning the labelled methyl ^{13}C$_{beta}$Ala14, for the VF1 fibres, the peak is splitted in two. This duplication of peak can correspond to specific arrangement of the peptide when assembled into fibres. Or it could be a result of two conformations of the peptide, resulting from a mixture of peptide in α-helix and random coil. As it is the case for LAH$_4$, depending on the conditions, in the central part of the peptide, amino-acids are in an helical or a hinged conformation[14]. Elucidation of the full structure of the peptide would allow to decipher if this difference resulted from intramolecular or intermolecular arrangements.

2D ^{13}C-^{13}C DARR spectra were acquired with the fibres of pVF1, fully labelled ^{13}C-^{15}N with two mixing times, 25 and 75 ms (figure 3.11).

In these 2D spectra, the different functional groups of amino acids are identified through their correlation peaks. The methyl of alanines around 15 ppm correlates with a peak around 55 ppm, corresponding to the Cα. The

3. CHARACTERIZATION OF PEPTIDE-PEPTIDE INTERACTIONS:
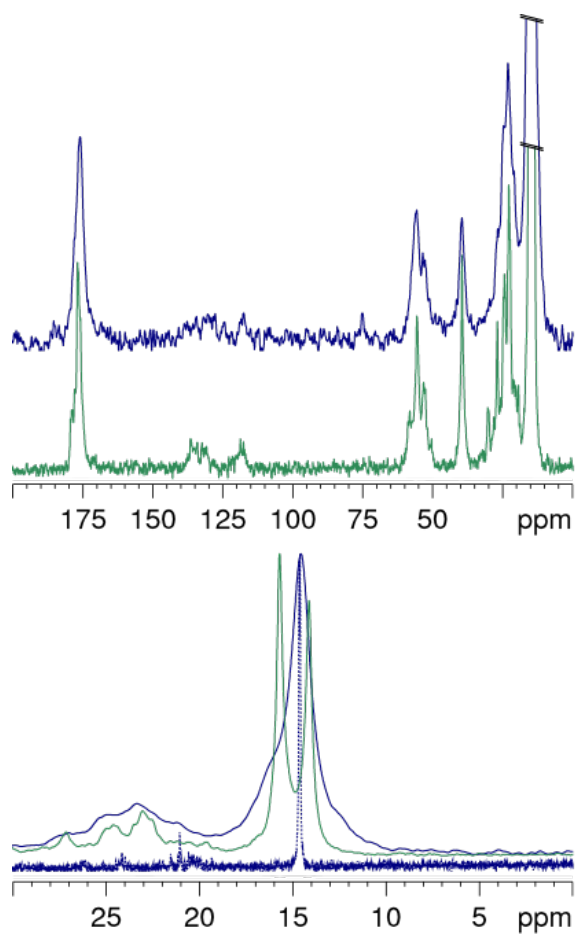
Figure 3.10: Spectra of VF1 fibres and the supernatant labelled in the ^{13}C on the C_βAlanine$_{14}$: The 1D ^{13}C solid-state NMR spectra of the fibre of VF1 or the supernatant of VF1 are coloured in green or blue, respectively. A liquid NMR spectrum of the supernatant of VF1 was also acquired and is indicated in blue dash line. A zoom on the methyl region is shown.
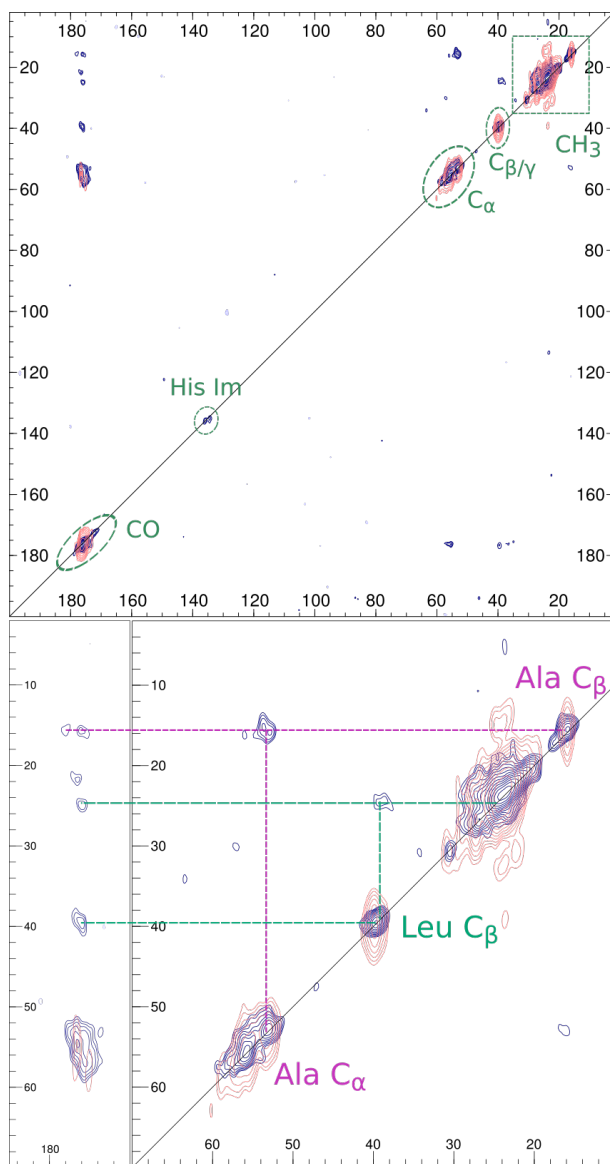
Figure 3.11: 2D ^{13}C-^{13}C DARR spectra of pVF1 fibres: two mixing time were used, corresponding spectrum are in pink for 25 ms and purple for 75 ms. In green are surrounded different amino acids group, CH_3, C_α, $C_{\beta/\gamma}$, Carboxyl group (CO) and imidazole group of the histidine side chains (His Im). A magnification shows the main correlation peaks, assigned to leucine or alanine.

3. CHARACTERIZATION OF PEPTIDE-PEPTIDE INTERACTIONS:

region around 25 ppm can be assigned to the methyls from leucine, by means of the correlation peak around 40 ppm, which correspond to the $C\beta/\gamma$ atoms. An assignment of the peptide is necessary for the identification of long-range correlation peaks. Because of the repetition of amino acids in the sequence as well as the similarity of environments, chemical shifts are clustered and did not allow the precise assignment. However the 2D spectra seem to arise from a morphologically homogeneous sample, with a single set of chemical shifts. This kind of samples is suitable for solid-state NMR, and further experiments are planned by the laboratory to determine the structure of the fibres[98]

Furthermore, chemical shift values are dependent of an amino-acid type and his secondary structure (Reference chemical shift average values are summarized in the table 3.2). Then by interpretation of the chemical shift of the alanines, the α-helical conformation of the peptide in the fibres can be confirmed for at least a part of the peptide.

Table 3.2: Chemical shift average values for C_β and C_α of the alanines in the different secondary structure conformation (Values are extracted from the Biological Magnetic Resonance Data Bank (BMRB))

	α-helix	β-strand	Random coil
C_α mean values (ppm)	55.2	51.12	52.1
C_α variance (ppm)	8.3	4.5	3.6
C_β mean values (ppm)	19.7	21.94	19.3
C_β variance (ppm)	6.3	5.4	4.0

As it will be presented in the next chapter, purification of pVF1 was problematic because of the coelution of the fusion protein TAF12 (chapter 4). Hence, the experiments were only done with a small fraction of peptide and other kinds of spectra will be acquired to determine the structure of the fibres. In parallel, in order to facilitate the assignment, experiment will be run with synthetic peptides specifically labelled at three or four consecutive amino acids.

3.4 Conclusion

In this chapter, the protocol for VF1 fibrillation has been optimised. Utilization of dialysis and lowering the pH to 6.25 (instead of a neutral pH as used for the biological assay) allowed to slow down the aggregation process, in order to have more homogeneous samples. These conditions allowed to have homogeneous VF1 fibres suitable for MAS solid-state NMR experiments. The α-helical secondary structure of alanines of the pVF1 on fibers have been confirmed (at least partially). A series of spectra will be acquired on different samples prepared with expressed peptide fully or synthetic peptide partially labelled to determine the complet structure of these fibres.

Hence, this protocol has been successfully applied for another peptide of the LAH_4 family, namely LAH_4L_1.

An efficient screening method to test more fibrillation conditions is still needed. Unfortunately, an easy protocol such as following ThT fluorescence signal as it is possible for β-amyloid fibres, is not practicable[92]. Utilization of other methods such as CD is not possible because the α-helical structure can be observed without fibres existence. DLS measurements allowed to follow the aggregation but do not provide the resolution required to distinguish fibres from other aggregates. However, methods like electrophoresis or gel filtration could be tested but are not suitable for conditions screening[91]. Hence, combination of the utilization of different fluorophores could be a good compromise[93].

Characterization of the aggregation of LAH_4 peptides could be beneficial. Experiment like the determination of the critical aggregation concentration (CAC) and application of the protocol of fibrillation could be applied more systematically[88]. This would be helpful for more reproducible and comparable results. Further investigation of the aggregation of LAH_4 peptides could allow to determine prominence of peptide-peptide interactions for biological application. Furthermore it would allow to follow the effect of aggregation in presence of membranes[99, 37].

3. CHARACTERIZATION OF PEPTIDE-PEPTIDE INTERACTIONS:

4

Expression and purification of pVF1 peptide:

Solid-state NMR spectroscopy is a suitable method to characterize assemblies like fibres, at an atomic level. This requires isotopic labelling of the peptide under investigation[50]. For a structural analysis by NMR, peptides are usually fully or partially labelled with ^{15}N and ^{13}C isotopes. The fully labelled peptides are synthesized in bacteria, growing in isotopically enriched minimal media. The expression and the purification of the pVF1 was adapted from the protocol developed in our laboratory for pLAH$_4$[100].

Because of their antimicrobial activity, cationic amphiphilic peptides like those from the LAH$_4$ family can't be expressed as a soluble protein. For that reason, the expression vector containing the sequence coding for the peptide includes the fusion protein TAF12. TAF12 guides the expressed product in the insoluble fraction of cells, allowing neutralization of the toxicity of the peptide[100, 101]. After induction of the expression of the construct in labelled media, cleavage of the insoluble part of bacteria (containing the fusion protein) allowed the recovery of the peptide from the expression product. The chemical cleavage with formic acid cuts the construct at a DP site and leaves an additional proline before the Vectofusin-1 sequence. Afterwards, the TAF12 and the pVF1 are separated by several purification steps to recover pure pVF1.

4. EXPRESSION AND PURIFICATION OF PVF1 PEPTIDE:

4.1 Materials and methods

Expression:

Expression: The expression vector pTIPX4-Vectofusin was built by insertion of the nucleotidic sequence coding for VF1 in the pTIPX4 (TAF12-mediated Insoluble Peptide eXpression) vector between the restriction sites BamHI and SacI. Competent bacteria (*E. coli*, OneShot BL21 Star (DE3), Invitrogen) were transformed with the pTIPX4-Vectofusin by heat shock. The transformation was done by incubation of 100 μL of bacteria suspension with 100 ng (100 ng/μL) of plasmid on ice for 30 min then, 30 s at 42°C and finally 2 min on ice. Transformed bacteria were incubated for 1h at 37°C under agitation (250 rpm) after addition of 250 μL of LB/YE (Lysogenic Buffer/Yeast Extract) medium. Thereafter, an aliquot of bacteria suspension was spreaded on agar plate (LB, Glucose 0.5% and 50 μg/mL Kanamycin) and incubated overnight at 37°C in order to have isolated colonies.

Culture: Preculture in minimal media (MM) was started from one of the colonies of the agar plate, and grown overnight under agitation (250 rpm). MM was composed of M9 salts ($Na_2HPO_4,2H_2O$ 8.5 g/L, KH_2PO_4 3 g/L and NaCl 0.5 g/L), NH_4Cl 0.5 g/L, Glucose 0.4%, $MgSO_4,7H_2O$ 2 mM, $CaCl_2,2h_2O$ 0.1 mM, Thiamine 0.01 g/L and Kanamycin 0.05 g/L.

For the culture, biotin 0.01 g/L (solution stock 4 g/L solubilised in 10% DMSO) and $FeSO_4,7H_2O$ 0.1 mg/L were added.

For isotopic labelling, $^{15}NH_4Cl$ or $^{15}NH_4Cl$ and $^{13}C_6$-Glucose were added as unique source of nitrogen or nitrogen and carbon. The bacterial culture was inoculated from the preculture to start at an OD_{600nm} of 0.02. The culture was incubated under agitation (250 ppm) at 37°C to the exponential growth phase of the bacteria (up to OD_{600nm} of 0.8). Thereafter, induction of the expression was triggered by addition of isopropyl β-D-1-thiogaLactopyranoside (IPTG, 1 mM), except for part of the culture, in order to have the non-induced reference as negative control. After 4h, cultures were centrifuged at 5000 g at 4°C (previously 10 mL of induced and non-induced cultures were put aside for localisation assays). Bacterial pellets were saved and kept stored at -20°C.

For the 10 mL aliquots of culture (I and NI), lysis and washing of the bacterial pellet were done to get different fractions for a localisation assay. The same procedure has been applied for the rest of the culture. The pellets

were resuspended in the lysis buffer (pH 8, 50 mM Tris-HCl, 100 mM NaCl, 5 mM Ethylenediaminetetraacetic acid (EDTA) and 0.5% Triton X100) (2 mL of lysis buffer for the 10 mL culture or 30 mL of lysis buffer/L of culture). Lysis of the cells was done with a sonication tip (MS72 microtip Bandelin SONOPULS) repeated 8 times, 1 minute at 50% of time cycle and 25% of power (the tubes were kept on ice during sonication to avoid thermal heating). At this step, 80 μL of the lysates were taken from the 10 mL culture, corresponding to the Total Extract. The lysates were centrifuged at 10,000 g during 30 min at 4°C. For the 10 mL culture, 80 μL of the supernatant were taken, corresponding to the soluble fraction. The pellet composed of the membrane and inclusion bodies (MIB) were saved and washed to remove the Triton X100. The pellets washes were done by 3 cycles of resuspension of the pellet in wash buffer (pH 8, 50 mM Tris-HCl, 100 mM NaCl and 5 mM EDTA) (at least 10 times more wash solution than lysis buffer (v/v)), and centrifugation during 30 min at 10,000 g at 4°C. MIB pellet was stored at -20°C until further purification.

Only for 10 mL of culture, the MIB pellets were resuspended in 2 mL of a denaturing solution composed of 8 M urea, 50 mM TrisHCl (pH 8.2) and 300 mM NaCl. This solution was incubated overnight in order to solubilize the inclusion bodies. From this mix, 80 μL of the solution were taken as insoluble fraction. Then, centrifugation at 16,000 g during 30 min at room temperature was done in order to recover the membranes in the pellet or the denaturated inclusion bodies solubilised in the supernatant.

Localisation assay: Expression of peptides using the fusion protein TAF12 should be recovered in the insoluble cell part. This insoluble fraction is composed of inclusion bodies and membranes. Following purification steps are dependent on the localisation and therefore required this assay. Locating of the expressed construct was performed on a Sodium Dodecyl Sulphate (SDS) Polyacrylamide Gel Electrophoresis (PAGE) 16% (adapted from the Schägger protocol[102]). Gel composition is indicated in the table below:

4. EXPRESSION AND PURIFICATION OF PVF1 PEPTIDE:

Component	Separating gel	Stacking gel
GB[a] 3X	3.3 mL	1.2 mL
Acrylamide:Bis-acrylamide 29:1	3.3 mL	0.4 mL
H_2O	2.29 mL	3.36 mL
Glycerol	1 mL	
APS[b] 10%	50 μL	40 μL
TEMED[c]	6 μL	4 μL
Vf and %	10 mL, 16%	5 ml, 4%

[a] Gel Buffer (GB) 3X, Tris 3 M, HCl 1 M and SDS 0.3 %, pH 8.45; [b] Ammonium peroxodisulfate (APS); [c] Tetramethylethylenediamine (TEMED)

Gels were run for 2 h at 150 V with anode and cathode buffer composed as following: anode buffer; Tris 0.1 M, pH 8.9 and cathode buffer; 0.1 M Tris, 0.1 M Tricine and 0.1% SDS, pH 8.25. The loading buffer deposited on the gel was composed as following (5X): 250 mM Tris HCl pH 6.8, 2% SDS (w/v), 0.1% Bromophenol Blue (w/v), 50% glycerol (v/v) and 500 mM Dithiothreitol (DTT). The different fractions were loaded on the gel from the 10 mL sampled extractions. The corresponding equivalent of bacterial culture were: 180 μL for the Total Extract, 250 μL for Soluble or Insoluble Fraction, 250 μL for Inclusion Bodies and 4.5 mL for Membrane pellet. The protein ladder Dual Xtra Standards (Precision Plus Protein, BioRad) was added as molecular weight reference on one band of the gel. Finally, gels were stained with Coomassie Blue.

Cleavage: Before further purification, a chemical cleavage was done in order to separate the pVF1 from the TAF12. MIB pellets were dissolved in 50% formic acid (v/v) (5 to 10 mL/L of culture) and incubated for 24h at 50°C. Formic acid cleaves between D and P and leaves a proline at the amino-terminus of VF1. Thereafter, the cleavage solution was evaporated using a rotary evaporator then lyophilised. Control of the cleavage efficiency was performed by SDS PAGE gel (see conditions 4.1). A small quantity of cleavage product and synthetic VF1 were dissolved in 1X loading buffer and loaded on the gel (figure 4.3).

Purification

For all the fractions, mass spectrometry analysis was performed using a Matrix Assisted Laser Desorption Ionisation - Time of Flight (MALDI-TOF, Bruker) mass spectrometer with an α-cyano (α-Cyano-4-hydroxycinnamic acid, Sigma-Aldrich) matrix dissolved in 30% of acetonitrile (ACN). When the high per-

formance liquid chromatography (HPLC) fractions were too diluted after a first mass analysis, the fractions were evaporated with a SpeedVad system and analysed again by MALDI-TOF.

Purification: Purification of pVF1 has been done on different devices by HPLC with C4 reverse stationary phase columns and an ACN (acetonitrile) gradient from 20 to 95%(solvent A: 10% ACN, 0.1% trifluoroacetic acid (TFA) in H_2O and solvent B: 100% ACN, 0.1% TFA). Systematically before sample injection on the column, the samples were centrifuged during 10 min at 10,000 g to remove potential aggregate or insoluble part. Different conditions are listed below (for the next section the terms, preparative, semi-preparative or analytical will be used to describe the different conditions used):

- Preparative HPLC (High Performance Liquid Chromatography) System (Gilson): with the column Jupiter 5 μm C4 300 Å(Phenomenex), flow: 20 mL/min [Preparative condition].

- Analytical HPLC System (Bischoff): with the column Jupiter 5 μm C4 300 Å(Phenomenex) (flow: 1 mL/min) [Analytical condition] or a semi preparative column ProntoSIL C4 5 μm C4 300 Å(flow: 7 mL/min) [Semi-Preparative condition].

Purification of the cleavage product was done following the analytical conditions with a 3 mL of equivalent of culture resuspended in water (figure 4.4). After optimization of the gradient, the pellet equivalent of 1.5 L of culture (MM unlabelled batch) was resuspended in water and purified under preparative conditions (figure A.1).

Further purification: Conditions of the coelution (section 4.3) are detailed below by following the order that it is mentioned in the text. The different conditions tested on the purified fractions containing both pVF1 and TAF12, were from the preparative purification done on the MM unlabelled batch (fractions 17, 18 and 21). The name of the fraction used corresponds to the fractions of the HPLC chromatogram presented in figure A.1.

- Elution of reference synthetic peptides LAH$_4$, VF1, pVF1 and the pLAH$_4$ from bacterial expression were done by solubilisation of peptides at 2 mg/mL in 500 μL of solvent A (figure 4.5). Semi-preparative conditions were used.
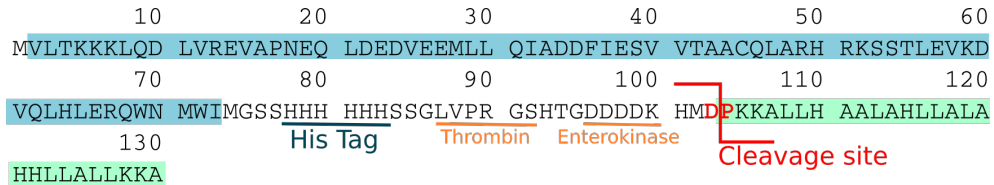
4. EXPRESSION AND PURIFICATION OF PVF1 PEPTIDE:

- Purification of the mixture of synthetic peptides and fraction 21 (VF1 + F21, figure 4.6) was done with the semi-preparative conditions. Around 1 mg of fraction 21 was solubilized in 500 μL of solvent A. This solution was used to solubilize $\sim$ 0.5 mg of synthetic VF1.

- Tests of the effect of different solvents were done with semi-preparative condition after solubilisation of peptides at 2 mg/mL in 500 μL. Fraction 17 was used for HFIP (Hexafluoropropan-2-ol), 10% ACN, 50% formic acid. Fraction 18 was used dissolved in water (figure 4.6) and in denaturated condition in 6 M of GuCl.

- The His-tag present between the TAF12 and VF1 sequences was used to test affinity purification by nickel column chromatography (figure 4.1). 1 mg of fraction 18 was dissolved in denaturating condition (6 M GuCl, 50 mM Tris, 300 mM NaCl, pH 7) then incubated with 100 μL of Ni-NTA beads (His-Bind Resins nitriloacetic acid (NTA), Novagen). It has to be noticed that during solubilisation of the mixture under the denaturating condition, a pellet was visible. The resin was equilibrated first in 1 mL of H$_2$O then by two exchanges with 1 mL of the initial buffer. The sample was applied and incubated for 1 h. Continuous mixing was assured by turning the sample upside down at 25 rpm, fractions were taken after centrifugation at 15,000 g for 10 s. Successive elutions were achieved with the same initial buffer, supplemented by increasing concentrations of imidazole at 20, 165, 330 mM and 1.5 M. Last incubation step was done in initial buffer with 5 mM of EDTA to ensure that all proteins were eluted from the resin. Finally, each fraction was purified with semi-preparative HPLC condition.

- Size exclusion purification was done with a gel filtration column (HiPrep 26/60 Sephacryl S-100 HR, GE Healthcare) coupled to a FPLC system (Fast protein liquid chromatography, DuoFlow Chromatography System; Bio-Rad). Isocratic elution of the sample (10 mg of the fraction 18 solubilized in 5 ml of H$_2$O) was done with an acetate buffer at 100 mM, 150 mM NaCl at pH 5. Fractions were pooled (figure 4.7), evaporated with a SpeedVac system and purified in semi-preparative HPLC conditions in order to remove the salt and analyse it.

4.2   Expression and purification of the pVF1

The pTIPX4-Vectofusin vector allows to overexpress the construct composed of the fusion protein TAF12 (composed of a part of the coding sequence TAF12 protein, different enzymatic cleavage sites and a His tag) and pVF1 (figure 4.1).

```
           10          20          30          40          50          60
MVLTKKKLQD  LVREVAPNEQ  LDEDVEEMLL  QIADDFIESV  VTAACQLARH  RKSSTLEVKD
           70          80          90         100         110         120
VQLHLERQWN  MWIMGSSHHH  HHHSSGLVPR  GSHTGDDDDK  HMDPKKALLH  AALAHLLALA
          130
HHLLALLKKA
```

His Tag   Thrombin   Enterokinase   Cleavage site

Figure 4.1: Sequence (one letter) of the construct with coloured major component: TAF12 or pVF1 are highlighted in blue and green respectively. The two specific enzymatic cleavage sites and the His-tag are underlined, and the cleavage site of formic acid is indicated in red.

The fusion protein TAF12 allows to address the construct in the inclusion bodies. However, a part of the construct can be recovered from membranes. Hence, the control of expression and localisation of the construct was assessed by SDS PAGE gel (figure 4.2).
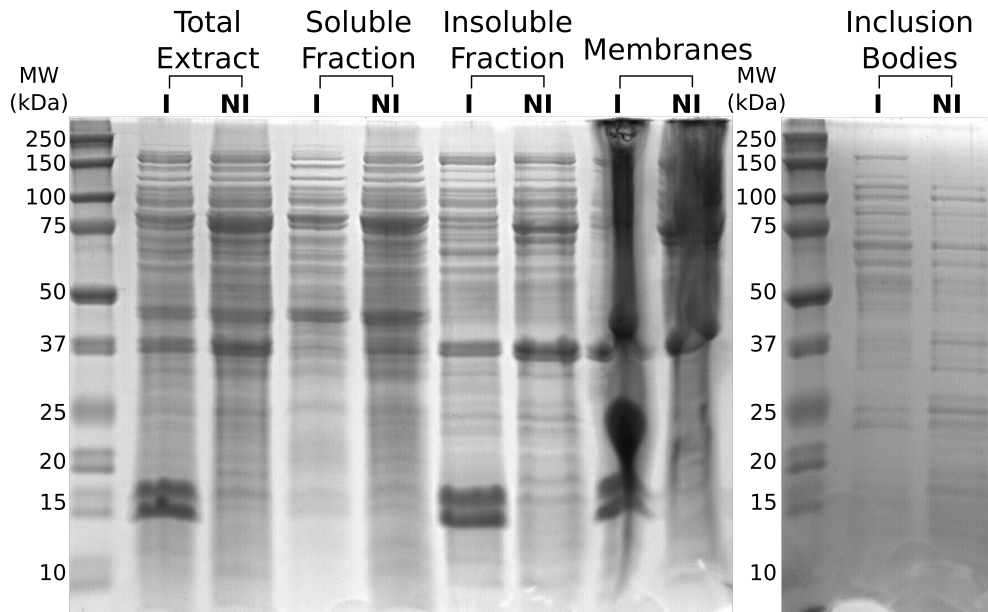
Figure 4.2: SDS PAGE gel of the localisation assay: the different culture batches are indicated by induced (I) or non-induced (NI) and the type of fraction loaded on the gel ais indicated. The molecular weights corresponding to the protein ladder are indicated at the left of the lane.

Different fractions of extraction were compared between a batch of bacte-

4. EXPRESSION AND PURIFICATION OF PVF1 PEPTIDE:

ria whose the expression was induced (I) or non-induced (NI). The presence of the construct is assessed by the presence of a band around 15 kDa (MW of TAF12-pVF1 = 14727 Da). This band was present in the induced fraction of the total extract (corresponding to the bacterial lysate) as well as in the insoluble fraction (composed of the membranes and inclusion bodies). The band was well defined in the induced membranes fraction, validating the presence of the expected product. The line of the induced inclusion bodies was less visible, partly due to the low amount of product loaded (equivalent of culture: 250 μL for inclusion bodies and 4.5 mL for membranes). Nevertheless, the inclusion bodies fraction was also used for the following step in order to recover a maximum of peptide. Furthermore, the use of all the insoluble fractions allowed to avoid an additional step of purification. On the contrary, this band was not present in the soluble fraction or in any of the non-induced fractions.

These data were comparable with those obtained for pLAH$_4$. Two other sets of culture were expressed in minimal medium enriched in isotopes to obtain full ^{15}N labelled and full ^{13}C^{15}N labelled peptides.

The cleavage with 50% formic acid allowed to separate the TAF12 from the pVF1. Control of the efficiency of the cleavage was done by SDS PAGE gel (figure 4.3).
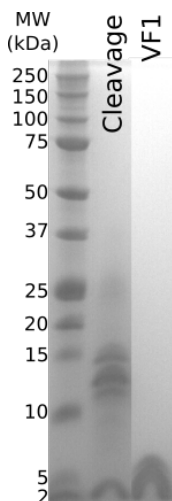
Figure 4.3: SDS PAGE gel of cleaved product: VF1 was deposited as reference and the molecular weight corresponding to the protein ladder are indicated at the left of the lane.

The presence of the peptide was compared with VF1 synthetic peptide (MW of 2779 Da for VF1 or 2876 Da for pVF1). A band around 15 kDa should correspond to the uncleaved construct TAF12-pVF1. Two other bands were present between 10 and 15 kDa. One band should correspond to TAF12

(MW of TAF12 = 11,869 Da). For the other band, different possibilities are conceivable, like the product of another recombinant protein, or TAF12 interacting with pVF1. Another band between 10 to 15 kDa was also observed in the pLAH$_4$ expression. A wider faint band was visible at 25 kDa and could correspond to a dimer of TAF12 or TAF12-pVF1. Albeit the presence of the uncleaved product TAF12-pVF1, the cleavage time was not extended as this was unsuccessful when preparing pLAH$_4$. In this case, when the cleavage was exceeding 24h, an increased quantity of a formylated adduct of pLAH$_4$ was found.

The cleavage product was purified by HPLC on a reverse phase column and the fractions were analysed by SDS PAGE gel electrophoresis (figure 4.4).

Bands around 3 kDa in the gel were indicative of an elution of the peptide in fractions 9 to 11. Nevertheless, the presence of other proteins corresponding to the TAF12, and the uncleaved product TAF12-pVF1 were also observed in lanes 8 to 13. Mass spectrometry analysis confirmed the coelution of VF1 and TAF12 in these fractions. The elution of pVF1 started around 50% of solvent B until 52%, when the fusion protein TAF12 was eluted from 50% of solvent B and lagged at least until 53%. The slope of the gradient was 1% per minute. In comparison, the one used to purify pLAH$_4$ was around 5.25% per minute. Elution of the pLAH$_4$ was around 45% of ACN and the TAF12 was eluted trailing from 54 to 62%.

Observation of coelution of the pVF1 and TAF12, and differences of elution compared to the pLAH$_4$ required further analysis. Hence, adaptation of the protocol was required to get purified pVF1. Despite high similarities of sequences, peptides can have differences of polarities, leading to different retention times on reverse phase columns. Elsewhere, bacterial expression complexity of the media and in our case, the presence of TAF12 can also induce modifications of the elution profile. In the next section, further comparisons of pVF1 and pLAH$_4$ are presented. Different purification methods were tested to eliminate the problem of coelution of TAF12 and pVF1. HPLC and mass spectrometry were used to characterize the fractions.
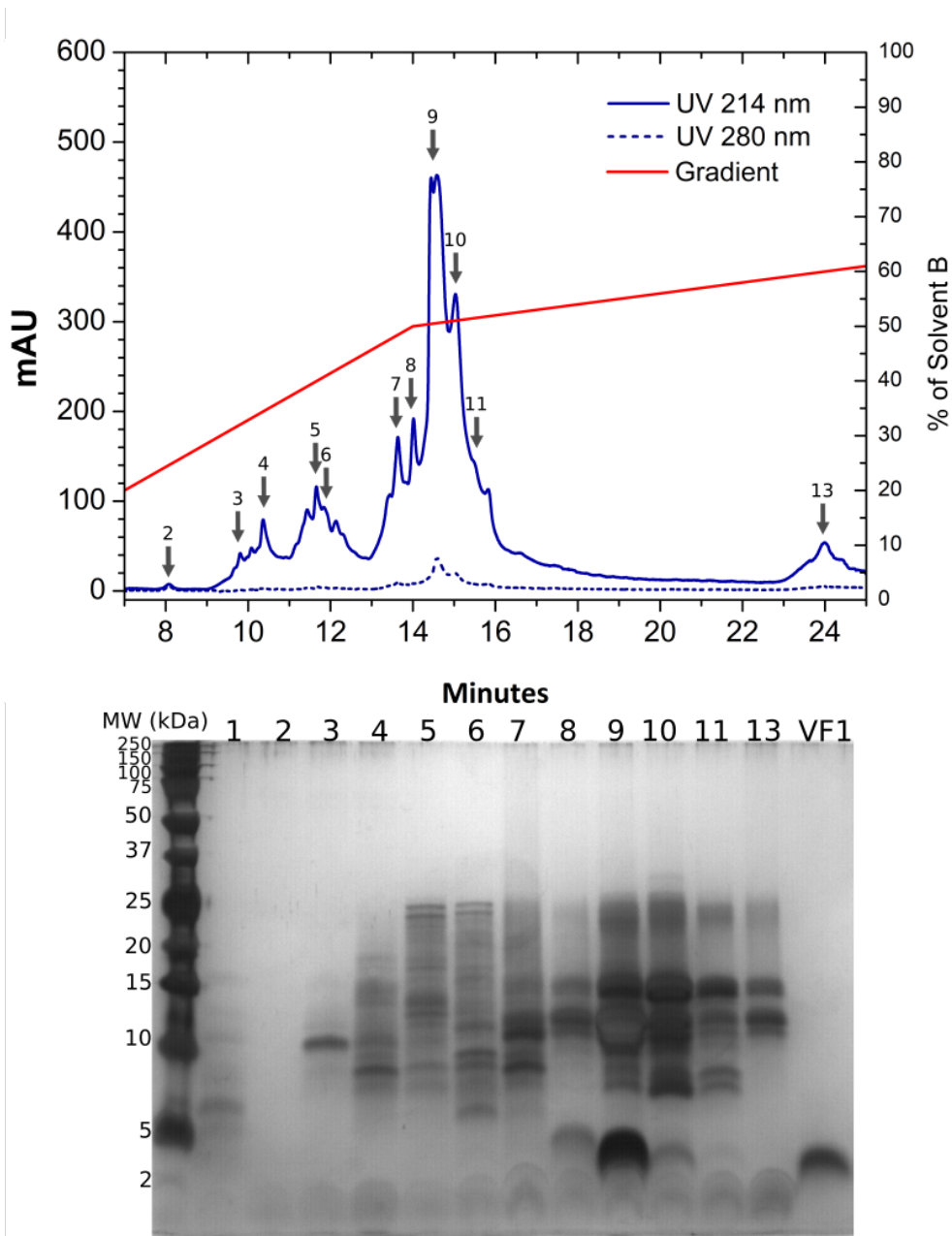
Figure 4.4: HPLC chromatogram and the corresponding SDS PAGE gel: Reverse phase (C4) HPLC chromatogram of the purification of the TAF12-pVF1 cleavage solution. The gel SDS PAGE (silver staining) of the corresponding fraction. Fraction 1 corresponds to the injection peak and the synthetic peptide VF1 was added as positive control to assess the presence of the peptide.

4.3   Separation of pVF1 and TAF12

Our expressed peptide possesses an additional proline at the N-terminus due to the chemical cleavage step. Moreover, the C-terminus of our synthetic peptide is amidated instead of having a free carboxy group, allowing a better solubility. In order to compare elution profiles of $pLAH_4$ and pVF1, different peptides were purified: LAH_4, $pLAH_4$ (expressed), VF1 and pVF1 (figure 4.5). It has to be noted that for the following study, the column was changed for the semi preparative one and the slope of the % of B solvent was lowered from 50% on to 0.5%/min.
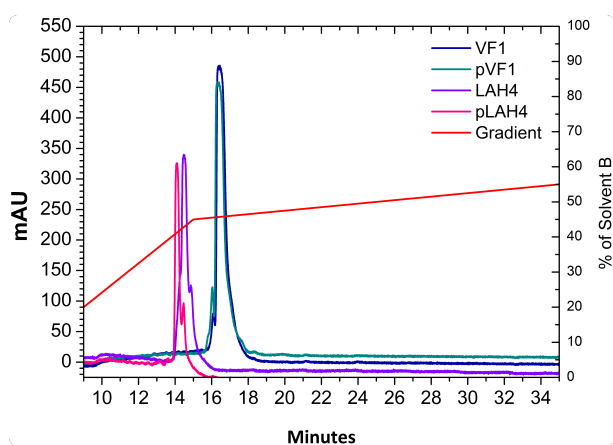
Figure 4.5: Reverse phase HPLC (C4) chromatogram of different LAH_4 and VF1 peptides: the UV measurement at 214 nm of the synthetic peptide VF1, pVF1 and LAH_4 and the expressed peptide $pLAH_4$ were compared.

Both LAH_4 and $pLAH_4$ were eluted at 45% of solvent B while VF1 and pVF1 were eluted around 50.5 and 51%, respectively. It is interesting to note that the $pLAH_4$ elutes slightly before LAH_4. Hence, the difference of elution was related to the peptide and not of the bacterial over-expression conditions.

The repurification of the fraction 18 resuspended in water gave the same profile than previously (figure 4.6). The lowering of the slope of the slovent gradient and changing of the column (semi-preparative instead of analytic) allowed a better separation of peak with VF1 at (18 min), VF1 and TAF12 at (20 and 21 min) and TAF12 and TAF12-pVF1 at (22 min). However, this peak resolution from an analytic application was not reachable for preparative quantities. Hence, another method to separate pVF1 from TAF12 was necessary. Although a part of the pVF1 was recovered at 18 min, a significant part was still eluted in the peak at 20 min and 21 min, together with the TAF12.

In order to determine if the coelution of the pVF1 and TAF12 was due to a specific interaction between the two components, synthetic VF1 was mixed

4. EXPRESSION AND PURIFICATION OF PVF1 PEPTIDE:

with fraction 21 from a previous purification containing both TAF12 and pVF1. This mixture was purified by HPLC (figure 4.6).
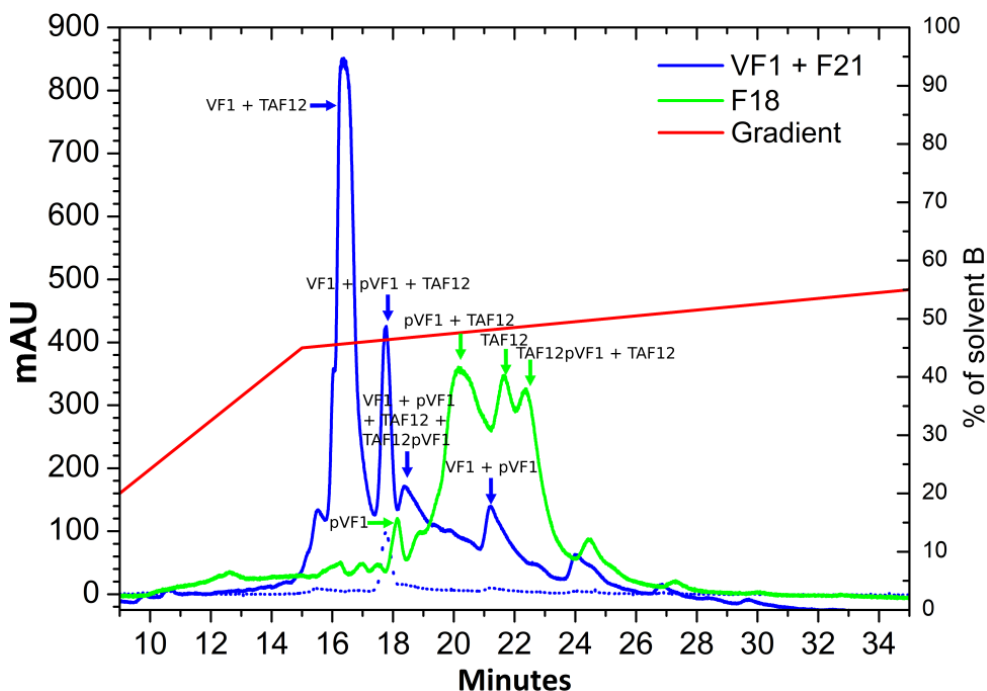
Figure 4.6: HPLC profile of the repurification of fraction F18 (green line, absorbance at 214 nm) and the mixture VF1 + F21 (blue lines). Full or dashed lines indicate the UV absorbance at 214 or 280 nm, respectively. Arrows indicate the components found by mass spectrometry.

The first elution peak at 16 min corresponds to VF1. Nevertheless, mass spectrometry indicated that TAF12 was also present. The elution of TAF12 at a lower percentage of solvent B (lower retention time: around 16 min instead of 18 min) with VF1 could be indicative of an interaction between these two components. The second peak at 18 min presents the same composition than the first one with pVF1 in addition. Interestingly, the absorbance at 280 nm indicates that TAF12 was present in this fraction. Moreover the addition of VF1 into the mixture f21 induced a shift of both the pVF1 and the TAF12 peaks. In order to confirm this effect, it could be interesting to proceed to the same experiment with LAH_4 instead of VF1. Complementary thermodynamic experiments like isothermal titration calorimetry (ITC) would allow to get information about the specificity of the interaction between TAF12 and VF1.

The purpose of the following experiments was to modify initial conditions in order to disrupt the interaction between pVF1 and TAF12. To this end,

the solvent for the solubilisation of the mixture (TAF12 + pVF1) was changed prior to HPLC purification. Neither HFIP, 10% ACN, nor 50% formic acid allowed to separate pVF1 and TAF12, even if there is a shift in the different elution profiles. Similarly, denaturation condition (in 6 M GuCl) unable to separate pVF1 an TAF12, and the same profile as obtained for the f18 was observed (figure 4.6).

Other strategies were also tested. TAF12 was designed with another tag for different purification protocol. Affinity purification was tested using the His-tag present between TAF12 and pVF1 (figure 4.1) despite the 4 histidines present in the sequence of the pVF1. The mixture TAF12-pVF1 was loaded on nickel beads and competitive affinity elutions were done by using increased concentrations of imidazole. Unfortunately, TAF12 and a small amount of pVF1 was recovered in the flow-through and only smaller peptides than pVF1 were eluted with imidazole. The presence of smaller fragments could be due to the nickel assisted cleavage of the (Ser/Thr)-Xaa-His site present just before the His tag of the TAF12[103].

However, it was noticed that solulisation of the mixture in salt (50 mM TrisHCl, 100 mM NaCl with or without 5 mM EDTA) resulted in the presence of aggregates, even under denaturating conditions. Aggregation propensity of the VF1 could be used as purification by salts precipitation methods. Different salts mixtures could be tested in order to precipitate only the pVF1 nevertheless, resolubilisation conditions should be found as well.

Finally, size exclusion chromatography was used in order to repurify and separate the mixture of TAF12 and pVF1 (figure 4.7).

In addition to separate by size, size exclusion purification was also used because of conditions (100 mM Acetate pH 5 and 150 mM NaCl) that could allow to modify potential electrostatic interactions between TAF12 and pVF1. The profil of FPLC was presenting low intensities, nevertheless, 5 fractions were pooled and further analysed by HPLC. This also permits to remove salts. Products were eluted only in fractions 2 and 3 (figure 4.7). The HPLC profile of fraction 2 was close to the purification profile of the mixture of TAF12 and pVF1 (figure 4.6). A mixture of TAF12 and pVF1 and the uncleaved product TAF12pVF1 were eluted from 18 to 22 min. Differently, for the fraction 3, the elution of a single peak at 18 min contains pVF1. Hence, size exclusion purification was efficient to separate pVF1 and TAF12. Nevertheless, this

4. EXPRESSION AND PURIFICATION OF PVF1 PEPTIDE:
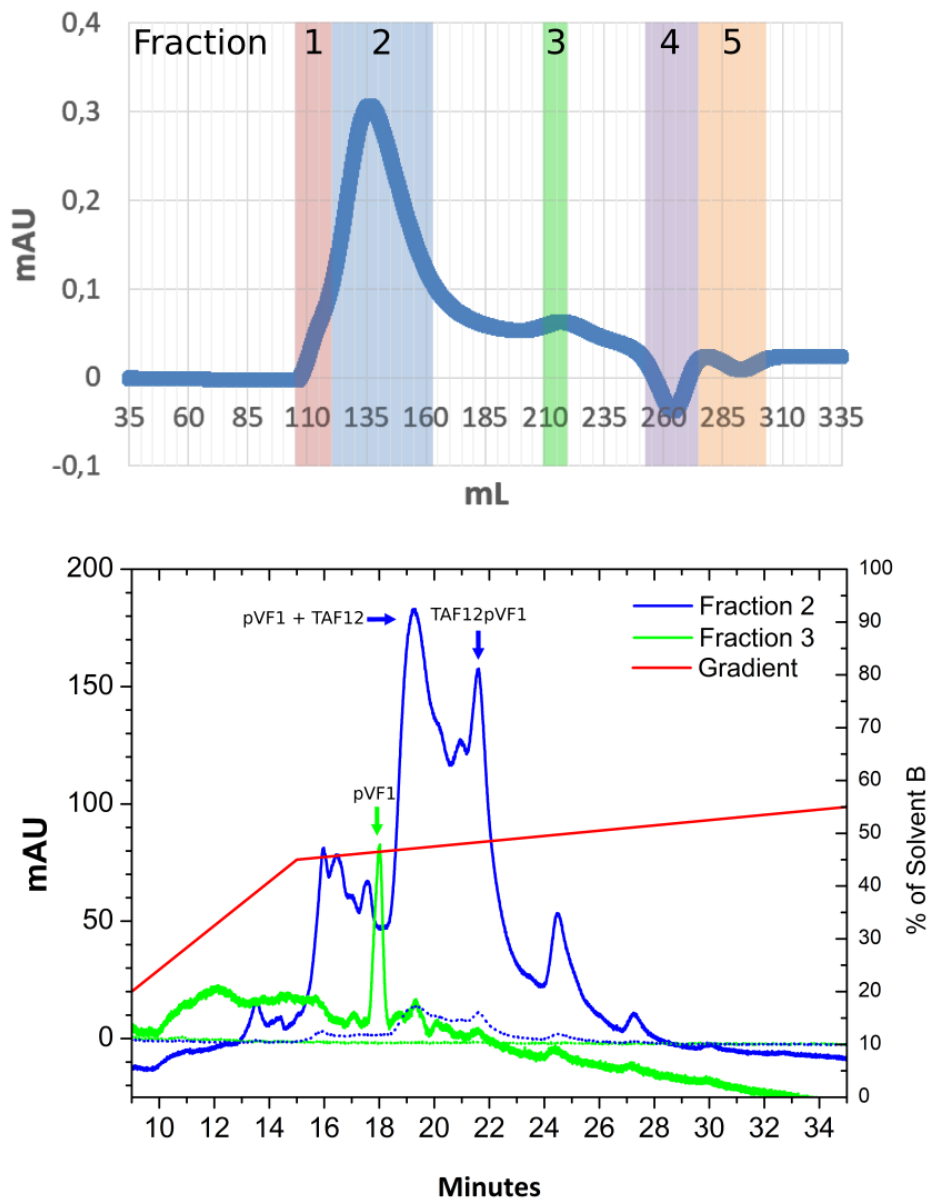
Figure 4.7: Purification of the mixture of TAF12 and pVF1, FPLC and the corresponding HPLC profiles: In the FLPC profile, pooled fraction are indicated in red, blue, green, purple and orange. Below, the HPLC chromatogram of FPLC fractions 2 and 3 are presented. The full or dash line correspond to the UV 214 or 280 nm respectively. Arrows indicate the components determined by mass spectrometry.

separation was only partial because pVF1 was still eluted in the presence of TAF12. Optimization of the condition could allow to gain total separation of pVF1 and TAF12. Other purification methods could be used, like ion chromatography. Indeed, the theoritical isoelectric point of the pVF1 and TAF12 are enough different, 10.48 and 5.58, respectively. Then, purification with cation exchange column could be test.

4.4 Conclusion

As for the $pLAH_4$, the construct containing the pVF1 was well expressed in the insoluble fraction of the cells. Nevertheless, after cleavage between the fusion protein TAF12 - essential for the overexpression - and pVF1, the purification of these products was not possible by reverse phase HPLC purification alone as it was done with the $pLAH_4$. Interaction of pVF1 with TAF12 causes a shift in the elution time and a coelution of both components with a more hydrophobic solvent when compared to LAH_4 (45% of solvent B for LAH_4 and 50% of solvent B for VF1, the latter being closer to the elution percentage of the TAF12).

Different methods were tested in order to avoid the coelution of TAF12 and pVF1. Neither solubilisation of the mixture (TAF12 + pVF1) in different solvent before HPLC purification, nor affinity purification were working. Size exclusion separation revealed to be efficient for this purpose. Nevertheless, other methods should be used to purify pVF1. Indeed, only partial recovery of the peptide was possible and this method was time consuming due to the limited amount that can be loaded on the gel filtration column. Other methods like cation exchange or salts precipitation should be tested. The VF1 peptide presents a high propensity to reversibly interact with membranes thus the use of detergent could be possible as well. Characterization of the interaction between pVF1 and TAF12 would be helpful. Otherwise, if the interaction is too high, another fusion protein should be tested[101].

5

Characterization of Peptide-Lipid Interactions

Understanding of interactions between peptides and the cell membrane is a challenging problem. Cell membranes are complex arrangements because of the diversity of membrane components and their differences of assortment. Small uncharged molecules can pass through the membrane passively, while active mechanisms transport charged molecules. Other mechanisms are necessary for the membrane crossing of bigger and charged molecules like amino acids, peptides and nucleosides[104]. In the development of drug delivery systems, the utilization of CPPs turned out to be a powerful tool to transport molecules through membranes[105]. Despite good efficiency, the mechanism of action are still unclear and make improvement of drug delivery systems tricky. CPPs are composed by plenty of different amino-acids. Most of these peptides are charged and amphipathic[8]. Cationic amphiphilic α-helical peptides, such as the LAH$_4$ family, have good propencities to bind to membranes. The abilities of LAH$_4$ peptides to interact and disturb membranes have been first studied because of their antimicrobial activities[12]. Nevertheless, the cell penetrating propensity of these peptides was then used to help cargo to cross the membrane[17]. The capacity to disturb a membrane, cross it or fuse with it requires different mechanisms of interaction between peptide and lipids. However, the interaction between peptide and lipids shouldn't be that different when AMPs and CPPs are compared to each other[106]. The various biological applications of the LAH$_4$ peptide family, despite their similarities of sequences, makes it an interesting candidate to go further in the comprehension of the mechanism of interaction between peptides and lipids.

5. CHARACTERIZATION OF PEPTIDE-LIPID INTERACTIONS

Gene delivery systems used with LAH_4 peptides can be subdivided in two categories depending of their mechanisms of delivery. For cargo like nucleic acids or naked viruses, after endocytosis in a cell, the disruption of the membrane is necessary to release the cargo in the cytosol[107]. For an enveloped virus, the release of the virus in the cytosol goes by membrane fusion between the endosomal and viral lipids[108]. The two possible mechanisms are: disruption/perturbation of the membrane and membrane fusion (figure 5.1).
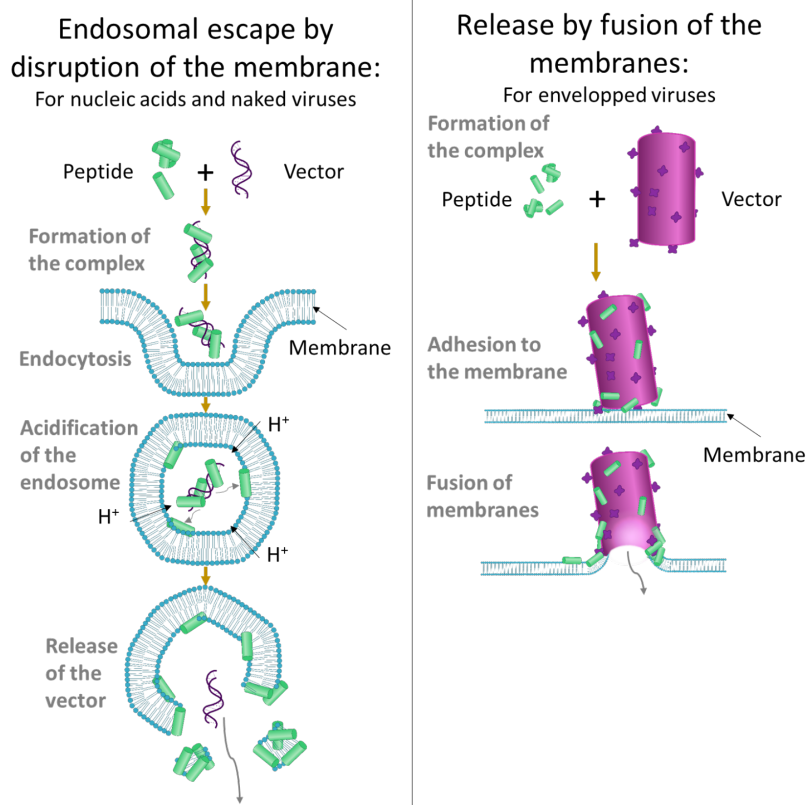
Figure 5.1: Schematisation of the mechanism occurring during gene delivery depending on the cargo used.

During maturation the endosome is subject to many important modifications. Hence, biophysical investigations require simplification in order to study the main effect. First of all, the pH decreases drastically from 6.8-6.1 in the early endosome to 6.0-4.8 in the late endosome[109]. Quantitative analysis of the interactions between LAH_4 and DNA demonstrated that when lowering the pH from neutral to 5.5, only half the amount of peptides is involved to form the lipid:DNA complex[20]. Hence, during the maturation of the endosome, an

increase of the peptide:lipid ratio follows the decrease in the peptide:DNA ratio. Secondly, during the maturation from early endosome to late endosome, the composition of the membrane changes[110] (figure 5.2).
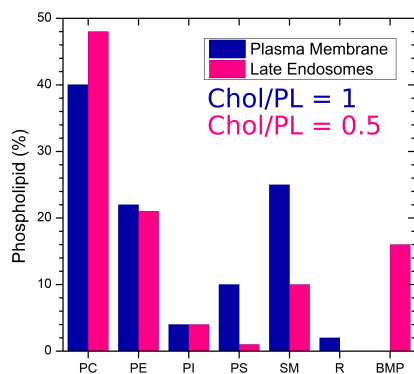
Figure 5.2: Lipid composition in plasma or late endosomal membranes: the histogram represent the amount of main phospholipids present in the two membranes. PC (phosphatidylcholine), PE (phosphatidylethanolamine), PI (phosphatidylinositol), PS (phosphatidylserine), SM (sphingomyelin), R (remaining lipids) and BMP (bis(monoacylglycero)phosphate) (adapted from [110]).

The amount of sterol and charged lipids decreases while the amount of uncharged lipids increases. The interaction of LAH_4 with lipids is driven by electrostatic interactions in a first instance then by van der Waals and hydrophobic interactions[111]. Although LAH_4 peptides do not appear to have specific affinity for specific lipids, a thermodynamic study of LAH_4L_1 indicated that electrostatic interactions are important elements for the membrane selectivity and could explain the higher propensity to interact with bacterial membranes instead of eukaryotic cells[112].

Interactions between peptides of the LAH_4 family and lipids have been well characterized. Hence, in this chapter the study of the LAH_4L_1:lipids interactions have been investigated with the purpose to reproduce the main events occurring during gene delivery. Conditions have been chosen to mimic the effects of the pH modification and the lipid reorganization. To study the effect of increasing the peptide concentration, MLVs of model membranes were prepared at neutral and low pH with different LAH_4L_1 concentrations. The effects on the lipids were followed by ^{31}P and ^{2}H static solid-state NMR. In similar condition, oriented bilayers were prepared in order to observe the orientation of LAH_4L_1 by ^{15}N solid-state NMR.

Then, the impact of various membrane compositions was investigated by comparison of different lipids mixtures with or without LAH_4L_1 at pH 5 and

pH 7.4. A mixture of POPC:POPS (POPC, 1-palmitoyl-2-oleoyl-*sn*-glycero-3-phosphocholine :POPS, 1-palmitoyl-2-oleoyl-*sn*-glycero-3-phospho-L-serine) was used to mimic the plasma membrane of the early endosome. Late endosome conditions were reproduced by using a POPC:POPG (POPC:POPG, 1-palmitoyl-2-oleoyl-*sn*-glycero-3-phospho-(1'*rac*-glycerol)) mixture (POPG was chosen instead of BMP, Bis(Monoacylglycero)Phosphate). For those mixtures, the effects of cholesterol and sphingomyelin were explored. All conditions were analysed by ^{31}P static and slow MAS solid-state NMR. The orientation of LAH$_4$L$_1$ in mechanically oriented membranes of total extract from *E. coli* was investigated by oriented ^{31}P and ^{15}N solid-state NMR.

5.1 Material

Preparation of MLVs

Different mixtures of lipids were prepared and solubilized in CHCl$_3$/MeOH (2:1 v/v). The quantities of lipids used for each sample were weighed to reach a hydration level of 90 % defined by $h(\%) = \frac{m_{H_2O}}{m_{H_2O}+m_{lipids}}$. Either $\approx$ 5 or 13 mg were added depending on the capacity of the 3.2 (45 μL) or 4 mm (96 μL) MAS rotors, respectively, used as containers. The amounts of LAH$_4$L$_1$ (previously solubilized in CHCl$_3$/MeOH 2:1 was added to obtain the desired molar peptide/lipid (% P/L) ratios. The solvent was gently evaporated under a stream of nitrogen to obtain a lipidic film along the walls of a glass tube. The film was dispersed in MilliQ water and the pH was equilibrated at $\approx$ 5 or 7.4 by adding 0.1 or 0.5 M of NaOH, and then lyophilized. Because of the acidic conditions during the purification of the peptide and the small sample volume, this initial adjustment assures an accurate equilibration of the pH of the final sample without the need to modify the volume and concentrations after the addition of the buffer. Samples were lyophilised and stored at -20°C. Just before experiment, the samples were suspended in either 100 mM Tris buffer (pH 7.4) or in 100 mM acetate (pH 5). Finally, the multilamellar vesicles (MLVs) were equilibrated by three freeze/thaw cycles (1 min in liquid nitrogen or 10 min at -80°C, 1 min at ambient temperature, and 10 min at 45 or 50 ^{o}C, vigorous vortexing). Before acquisition, the samples were stored at 4°C.

Different batches of samples discussed in the first section 5.2 are summarized in the table below:

Lipids	DMPC^a	DMPC	DMPC	POPC	POPC:POPS
Molar P/L %	0, 1, 2, 4	0, 1^c, 2, 2.7, 4^b, 8, 20	0, 2, 4, 8, 5.9, 12.5, 20	0, 2, 8, 20	0, 2, 4, 8, 20
pH	7 and 5.5	7.4 and 5	7.4 and 5	5	7.4 and 5

^{a} the peptide was dissolved in TFE instead of CHCl$_3$/MeOH and the batch was prepared with a buffer concentration of 10 mM.

$^{b\ c}$ were completed by 10 and 20 μL of buffer respectively.

The table below summarizes the different mixtures of lipids prepared (section 5.3). All the samples were studied at both pH 5 and 7.4 at ratio of 2 mole %. MLVs were stored at -20°C between the static and slowMAS experiments.

Lipids	PC:PG/S	PC:PG/S:Chol	PC:PG/S:Chol:SM
Ratio	7:3	4:3:3	4:2:3:1

Samples comprising both peptides and POPS were turbid.

5. CHARACTERIZATION OF PEPTIDE-LIPID INTERACTIONS

Preparation of oriented samples

From 20 to 40 mg of lipids, depending on the lipids and the desired P/L ratio, were dissolved in $CHCl_3$/MeOH 2:1 v/v in order to have between 1 to 2 mg of peptide. The peptide ($[^{15}N$-$Leu_{14}]$-LAH_4L_1) was dissolved in TFE for DMPC and POPC samples or in $CHCl_3$/MeOH 2:1 for the Total Extract samples, and added to the lipid mixtures. The pH was adjusted by addition of microliter amounts of 0.1 to 0.5 M NaOH. The solvent was evaporated under a stream of nitrogen until the obtention of a viscous mixture and was spread onto 15 to 25 ultra thins glass plates (W*L, 8*12 mm, Marienfeld). For oriented samples prepared from the MLV mixture (section 5.2), after vortexing, the samples were spread onto glass plates and followed the same step than usual samples. Plates were dried first by exposure to air, then at least 1 h under vacuum to remove any traces of organic solvents. The glass plates were placed in a hydration chamber at 93% relative humidity for at least 2h. After equilibration, the glass plates were stacked on top of each other, wrapped with Teflon tape, and the stack closed at 3 sides of a plastic bag then hydrated again. The bags were sealed just before the NMR measurement. Uniaxially oriented samples prepared are summarized in the table below:

Lipids	DMPC	POPC	Total Extract *E. coli*
Ratio	2, 4%	2%	1%
pH	5 and 7	5 and 7	<5 and >7

The ratio of the Total Extract were approximate because the exact composition of the Total Extract is unknown, hence, the MW were estimated to be 800.

In the same manner, two samples with POPC or Total Extract *E. coli* at low pH were prepared with the $[^{15}N$-$Leu_{15}]$-$[3,3,3,-^2H_3$-$Ala_{14}]$-$h\Phi 19W$ peptide at P/L = 1% (dissolved in $CHCl_3$/MeOH 2:1)[113].

NMR parameters

The external references have been used to reference chemical shifts and optimize the parameters: H_3PO_4 (0 ppm) for ^{31}P spectra, D_2O (0 ppm) for ^2H spectra and $^{15}NH_4Cl$ (39.3 ppm[114]) for ^{15}N spectra.

Static solid-state NMR

Proton-decoupled ^{31}P Hahn-echo spectra[67] of MLVs were obtained on a Bruker Avance 500 or 300 NMR spectrometer equipped with a 4 or 3.2 mm MAS probe

head (Bruker Biospin, Rheinstetten, Germany) without spinning. Temperature was set at 37°C and 7°C for DMPC samples, 30°C for POPC/POPS and POPC samples or at 37°C and 15°C for the lipid mixtures. The following parameters were used (acquisition parameters are indicated for the 300 MHz or 500 MHz spectrometers, respectively) : 90° pulse between 2.45, 2.5 and 6.45 or 5 and 6.12 μs; echo delay, 37 μs or 100 μs; acquisition time, 10 ms or 40 ms; time domain data points, 2048 or 8192; spectral window, 100 kHz; number of scans, between 3538-17,918 or 96-1024 with the 4 mm probe and 160-4558 with the 3.2 mm probe; recycle delay, 3 s or 10 s; and continuous wave ^{1}H decoupling around 28 or 60 and 40 kHz.

For ^{2}H static solid-state NMR a solid quadrupolar echo-pulse sequence[75] was used with the following parameters (acquisition parameters are indicated for the 300 MHz or 500 MHz, respectively): 90° pulse, 3.4 μs or 8 μs; echo delay, 50 μs or 40 μs; acquisition time, 16.4 ms or 6.5 ms; dwell time, 0.5 μs or 0.1 μs; time-domain data points, 32,768 or 65,536; spectral window, 1,000 kHz or 5,000 kHz; number of scans, between 9200-46,823 or 2750-190,000; and recycle delay, 0.3 s.

The spectra (both ^{31}P and ^{2}H) were processed with a line broadening of 100 Hz before Fourier transformation.

Slow MAS solid-state NMR

Proton-decoupled ^{31}P spectra of MLVs were obtained on a Bruker Avance 500 or 300 NMR spectrometer equipped with a 4 mm MAS probe head (Bruker Biospin, Rheinstetten, Germany) with 1.5 kHz spinning at 37°C or 15°C. The following parameters were used (acquisition parameters are indicated for the 300 MHz or 500 MHz, respectively): 90° pulse between 3 or 7 μs; acquisition time, 28 or 164 ms; time domain data points, 2048 or 32,768; spectral window, 6.25 kHz or 36.5 kHz; number of scans, between 1557-2048 or 625-1024; recycle delay, 5 s; and continuous wave ^{1}H decoupling around 30 or 40 kHz. The spectra were processed with a line broadening of 10 Hz before Fourier transformation.

Oriented solid-state NMR

The ^{31}P solid-state NMR spectra were acquired on a Bruker Avance 300 spectrometer equipped with a static solid-state NMR probe with a flat coil[66].

5. CHARACTERIZATION OF PEPTIDE-LIPID INTERACTIONS

Proton-decoupled ^{31}P Hahn-echo spectra were acquired with the following parameters: 90° pulse between 7.5 to 8.45 μs; echo delay, 10 or 30 μs; acquisition time, 82 ms; time domain data points, 8192; spectral window, 36.5 kHz; number of scans, between 256 to 22,292; recycle delay, 5 s; and continuous wave ^{1}H decoupling around 32 kHz. A line broadening of 50 Hz or 100 Hz was applied before Fourier transformation.

The ^{15}N solid-state NMR experiments of the peptide were performed on a Bruker Avance 300 or 750 spectrometer equipped with a static solid-state NMR probe with a flat coil. Proton-decoupled ^{15}N solid-state NMR spectra were acquired using a cross polarization sequence with a contact time of 600 μs on the 300 MHz instrument[85] or 150 μs on the 750 MHz instrument using a multi-CP sequence[115]. The following parameters are indicated for the 300 MHz or 750 MHz instruments, respectively: the B1 fields, including for ^{1}H decoupling, were 18 kHz or 75 kHz, the recycle delay 1 s, the spectral width 25 kHz or 100 kHz, the pre-acquisition delay 26 μs or 6.5 μs, and the number of scans 162,000-310,995 or 10,000 to 95,000. A line broadening of 150 Hz or 300 Hz was applied before Fourier transformation.

DLS measurements

The NMR DMPC samples were diluted 1000 times and measured in a quartz cuvette at 25^oC using a Zetasizer NanoS from Malvern Instruments. The static light (laser He-Ne 633nm) diffusion is measured (according to Debye model) at 173° allowing a measurement range from 0.3 nm - 10 microns (diameter). The intensity size distributions, Z-average and Polydispersity Index presented are calculated from the correlation data by the Zetasizer Software (Malvern Instruments, 7.11 version).

Total lipids extraction

The protocol of extraction was adapted from "A Rapid Method of Total Lipid Extraction and Purification"[116]. The solvent extraction procedure was applied to commercial yeast, *Saccharomyces cerevisiae*. In the extraction of materials, the hydration level is important to adjust the different ratios of solvent in order to ensure good phase separation. Hence, 6 g of yeast were first lyophilised. The dry yeast, 2.1 g, was mixed in a solution of $CHCl_3$:MeOH:H_2O 1:2:0.8 and sonicated in a bath for 10 minutes. The phase separation was obtained by

the addition of $CHCl_3$ and H_2O to reach the ratio $CHCl_3$:MeOH:H_2O 2:2:1.8 and then sonicated for 4 minutes. The solution was filtered on a Buchner funnel $n^o = 3$ with a paper filter (Schleicher and Schuell 595, 110 nm diameter) and transferred in a separating funnel. After 30 minutes of decantation, the lower phase was recovered and evaporated under a stream of nitrogen. After lyophilisation, 23 mg of product were recovered. This extract was solubilized in $CHCl_3$:MeOH 1:1 and spread onto 16 glass plates (8*12 mm, Marienfeld), and exposed to air overnight. Thereafter the plates were placed in a hydration chamber (relative humidity of 100%) at 37^oC for at least 2h. After equilibration, the glass plates were stacked on top of each other, wrapped with Teflon tape, and closed at 3 sides by plastic bags, and then hydrated again. The bags were sealed just before the NMR measurement.

5.2 Study of the interaction between LAH_4L_1 and model lipids

In this first part, investigation of the effect of LAH_4L_1 on MLV has been done by interpretation of large effects. In this section, the study about the detergent model was mainly discussed from the experiment on POPC:POPS 3:1 MLVs and compared with DMPC MLVs prepared with additional ratio P/L (figures are presented in the appendix).

5.2.1 Mechanism of interaction: Detergent model

To investigate the macroscopic behaviour of model lipid bilayers as a function of P/L, proton-decoupled ^{31}P solid-state NMR spectra were acquired. Two model membranes were studied, a POPC:POPS 3:1 mixture (figure 5.3) and DMPC phospholipid bilayers (figures A.2 and 5.12).

In the absence of peptide and at 30°C the POPC:POPS 3:1 spectra exhibit the typical symmetric chemical shift anisotropy of phospholipid membranes in their liquid crystalline states[117]. Main features of the reference spectra (without peptide) are indicated in Figure 5.3 by a green or blue dash line for the high intensity peak ($\delta_\perp$) or the low intensity shoulder ($\delta_{//}$) respectively. At both pH, the superposition of powder pattern line shapes of POPC and the one of POPS results in spectra with a main intensity at about -17 ppm and the less well-defined discontinuity around 30 ppm. Orientations and conformations of phospholipids headgroup have been demonstrated to be sensitive to electric charges surface[118]. Slight differences were visible between the two references (pH 7.4 or pH 5), hence the two series were compared independently.

First of all, the macroscopic phase of the vesicles were visible from a quick view. At pH 7.4 for POPC:POPS MLVs, symmetric powder pattern line shapes were observed up to peptide concentrations of 8%. Increasing the concentration to 20% of LAH_4L_1 resulted in an increase of the $\delta_{//}$ (signal around 29 ppm). The higher amount of lipids aligned with the long axis parallel to the magnetic field direction is an indication of an oblate orientational distribution of the lipids[73]. The same tendency under similar conditions was observed with DMPC lipids (figures A.2 and 5.11). The powder pattern line shape was conserved until a LAH_4L_1 concentration of 8%. At higher concentration (P/L $\leq$ 12.5%),the $\delta_{//}$ shoulder around 25 ppm was accentuated, which indicate a
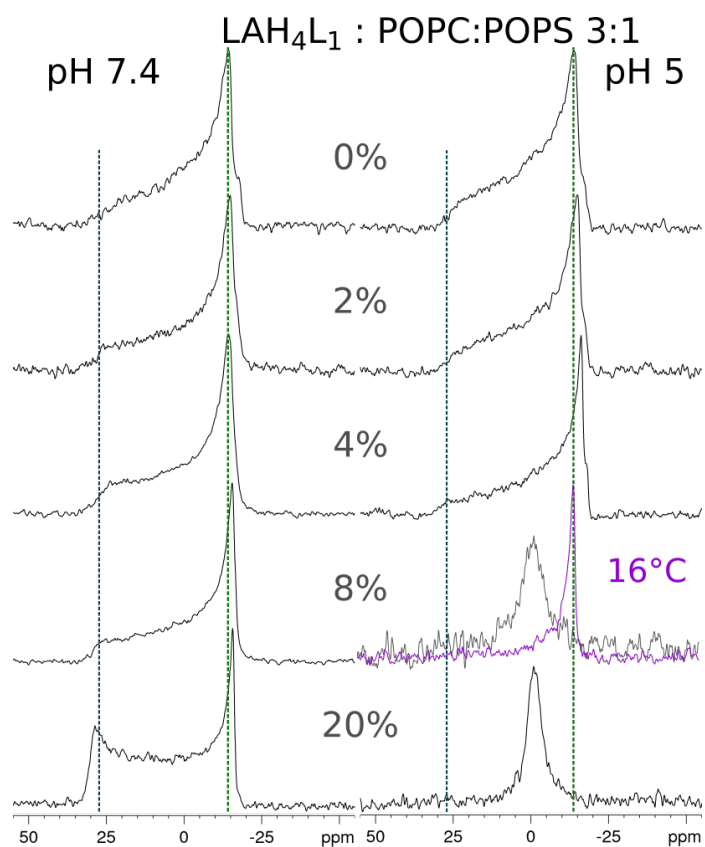
Figure 5.3: Increasing concentration of LAH$_4$L$_1$ in MLVs of POPC:POPS 3:1 studied by ^{31}P solid-state NMR: Samples were prepared at pH 7.4 (left column) and pH 5 (right column). All spectra were acquired at 30°C excepted for P/L 8% pH 5 acquired at 16°C (indicated in purple). The blue and green dash lines represents the $\delta_{//}$ and $\delta_\perp$ of the reference spectrum (0% P/L) respectively.

parallel lipid orientation. Nevertheless, this effect was less pronounced with DMPC vesicles than for POPC:POPS vesicles.

When studied at pH 5, POPC:POPS MLVs (figure 5.3), the classical powder pattern line shape was preserved until a P/L ratio = 4%. At higher peptide concentrations, an isotropic peak was observed, suggesting supramolecular assemblies such as micelles or isotropic bicelles that tumble fast enough to average the chemical shift anisotropy[64, 72]. Lowering the temperature to 16°C for the sample P/L 8% resulted in a deformed spectrum. A decrease of intensity from 25 to -10 ppm is observed representing a prolate distribution of phospholipid alignments perpendicular, relative to the magnetic field direction[73]. The effect of the increase of peptide with DMPC lipids at pH 5 was comparable (figures A.2 and 5.12 (third column)). The powder pattern line shape was observed until a P/L = 5.9%; at P/L of 8 and 12.5%; a deformation in the spectra, which is typical of prolate distribution, was present, and finally at the highest concentration of 20% , the spectra presented an isotropic peak characteristic of small vesicles.

Different models of interaction between cationic amphipathic peptides and membranes have been described. The equilibrium of this interaction is dependent on many parameters, such as the composition of the membrane, the temperature or the concentration of peptides[119]. The characterization of the macroscopic phase as a function of the concentration of these peptides and composition of the membrane give a broader picture of the effect of a peptide. The observation of the macroscopic phase of the Mag2 peptide by ^{31}P solid state NMR allows to observe the detergent-like properties of this amphipathic peptide[120]. The detergent-like properties were already suggested for the antimicrobial activity of the LAH$_4$[12]. Moreover, the deformation of the membrane by the LAH$_4$ at high peptide concentration was observed by solid-state NMR[16].

Furthermore, the study of the interaction of the LAH$_4$L$_1$ with an increasing concentration confirmed the detergent-like properties at low pH. For this system, a combination of two effects is needed to observe this property: the increase of quantities of peptide beside lipids and the lowering of the pH. Hence, the addition of peptide at pH 5 induces, as a first step, a high deformation of the membrane emphasised, by the presence of oriented bicelles, then, at high ratio P/L, it lead to the lysis of the membrane depicted by the observation of

an isotropic peak. In contrast, at neutral pH, the addition of peptide did not induce the disruption of the membrane, even at the highest ratio.

5.2.2 Detailed analysis of LAH$_4$L$_1$:lipids vesicles

In the following section, deeper analysis of different parameters has been done
with the complementary acquired spectra.

The orientation was mainly discussed with the POPC:POPS series and
an additional series of vesicles formed with POPC (pH 5 only). Then, the
transition temperature was studied from different batches of DMPC vesicles.

5.2.2.1 Monitoring of the vesicles deformation

In a second time, a supplementary analysis of the ^{31}P spectra presented in
the previous section was done in order to go further in the study of the effect
induced by LAH$_4$L$_1$. Monitoring of the vesicle deformation can be done by the
determination of the S$_2$ order parameter which is related to the form of the
vesicles. This order parameter is relative to dynamic properties of the lipids
and their orientation in the magnetic field. It varied from 1 to 0 for systems
with dynamics similar to the reference (lipids alone) to an isotropic system[73].
Spectra without peptide were used as a reference for each series (figure 5.4).
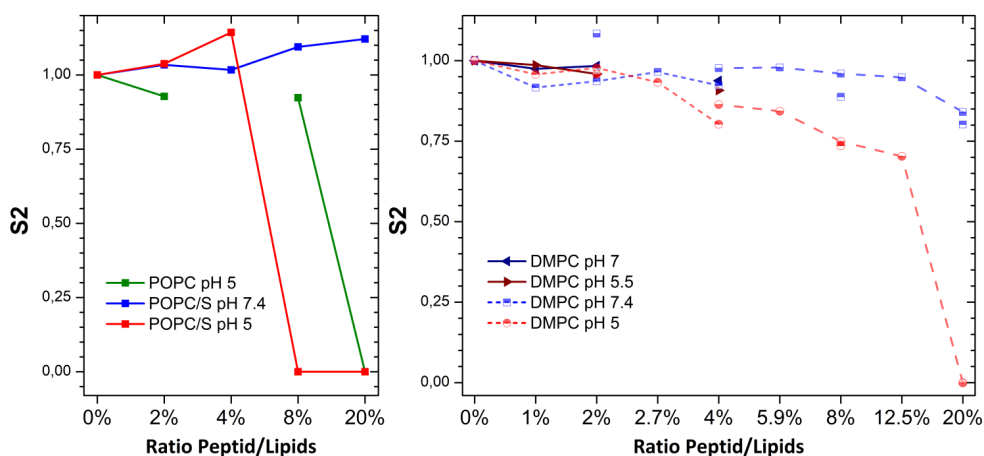
Figure 5.4: Graph representing the S2 order parameter: The different series of
samples were plotted as a function of peptide concentration.

For both MLVs with peptide at pH 7.4, the parameter slightly differed
when compared to the MLVs alone (it increases to 1.1 for POPC:POPS and
decreases to 0.8 for DMPC). As expected, at pH 5, the vesicle deforma-
tion was more important (with an increase to 1.15 at P/L 4% of peptide
for POPC:POPS and decrease to 0.7 at P/L 12.5% for DMPC). At higher
peptide concentration, the value of zero correspond to the isotropic spectra

observed. The comparison between DMPC batches showed a variation of the parameter for similar conditions. Bigger deformation at low pH was expected, due to the in planar conformation, allowing the interaction with more phospholipid heads and thus, potentially leading to more vesicle shape modifications[38](section 5.2.3).

Hence, LAH$_4$L$_1$ induces deformation of the vesicles in both membranes (POPC:POPS or DMPC) but two tendencies were observed depending on the lipids composition. For POPC:POPS, the effect of increasing peptide concentration was related to an increase of the order parameter S2. On the contrary, for DMPC (and POPC), the S2 value was decreasing with addition of peptide.

The order parameter S2 is calculated from the ratio between the $\Delta\sigma$ of the sample compared to that reference system (2). The ^{31}P spectra observed are a sum of different effects provided from global or local effects, making delicate its thorough interpretation. In ^{31}P solid-state NMR, modifications promoted by negative charges, e.g. from POPS, induced a decrease of the $\Delta\sigma$ parameter[118]. Elsewhere, structural changes generated by addition of cation, e.g. from LAH$_4$L$_1$, are different in zwitterionic or in anionic/zwitterionic lipid bilayers[121]. It is known that the mechanisms of interaction of the LAH$_4$ peptides are dependent on the membrane composition[111, 112]. Hence, it is interesting to observe that this effect could be monitored with the determination of the S2 order parameter. Nevertheless, further investigation should be done to confirm this observation with, for example, different series with various POPC/POPS ratios. Also, cross validation with other methods developed to observe a local effect on the membrane could be used, like spectrofluorometry with a specific dye probe[42].

5.2.2.2 Monitoring of the lipid chains by ^{2}H solid-state NMR

^{2}H solid-state NMR allows to monitor the effect of different components on the aliphatic lipids chains. By following the quadrupolar splitting of the different segments CD$_2$ and one CD$_3$, perturbations of the lipid chains are observable (details in chapter 2).

Then, complementarily to the ^{31}P spectra, to assess the effect of an increasing concentration of peptide at the level of the lipid fatty acyl chains, ^{2}H

solid-state NMR spectra were acquired from the same unoriented samples carrying a fraction of lipids containing fully deuterated palmitoyl ($^2H_{31}$-POPS, figure 5.5) or myristoyl ($^2H_{54}$-DMPC, figure A.2) chains.
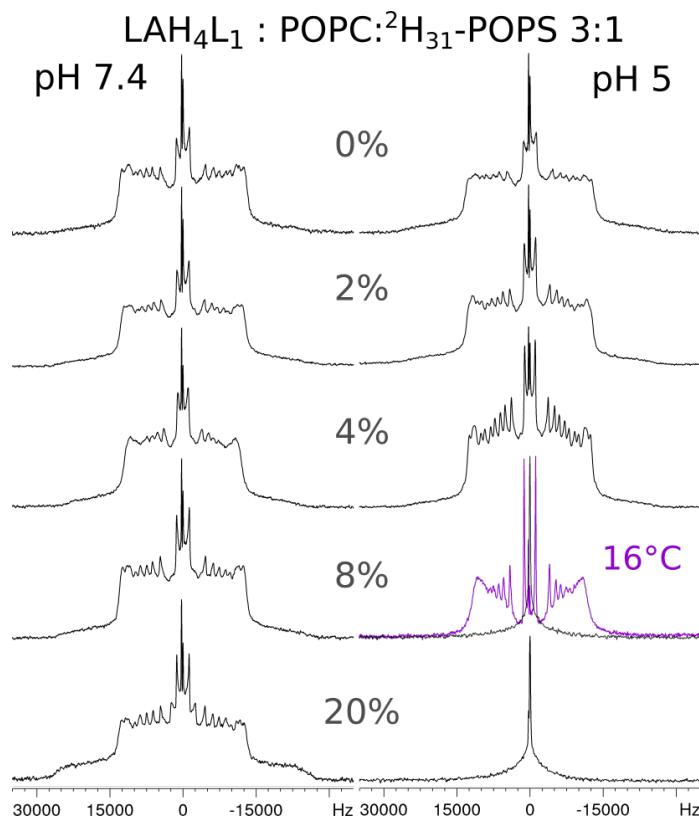
Figure 5.5: Increasing concentration of LAH_4L_1 in MLVs of POPC:$^2H_{31}$-POPS 3:1 studied by ^2H solid-state NMR: samples were prepared at pH 7.4 (left column) and pH 5 (right column). All spectra were acquired at 30°C excepted for P/L 8% pH 5 acquired at 16°C (indicated in purple).

The ^2H solid-state NMR spectra of POPC:$^2H_{31}$-POPS 3:1 at pH 7.4 changed in two complementary ways upon addition of peptide at 2 and 4%. First, the individual resonances defining quadrupolar splittings broaden, and second, the quadrupolar splittings decrease. When more peptides are added (P/L = 8 and 20%), the effect is reversed, with a narrowing of the individual resonances and an increase in the quadrupolar splitting. Furthermore, at a P/L ratio of 20%, a second set of peaks is observed and the shoulders are accentuated (until around 27 and -27 kHz), confirming an oblate orientational distribution, as observed for the corresponding ^{31}P spectrum. A gain in spectral resolution associated with the line narrowing is also observed at pH 5 at P/L ratios of 2 and 4%. As observed for the corresponding ^{31}P spectrum, from a pep-

tide concentration of 8%, an isotropic peak is observed. For the sample at 8% of peptide concentration, lowering the temperature to 16°C resulted in a spectrum with prolate distribution of lipid alignments.

When the deuterium solid-state NMR spectra of ^{2}H$_{54}$-DMPC were investigated (figure A.2), they parallel the orientational distributions of the corresponding ^{31}P solid-state NMR spectra as well as many features described above for the POPC:^{2}H$_{31}$-POPS 3:1 membranes.

From those ^{2}H solid-state NMR spectra shown in figure 5.5 and figure A.2, the quadrupolar splittings were extracted and the order parameters S$_{CD}$ plotted against the carbon position of the labelled lipids (figure 5.6).
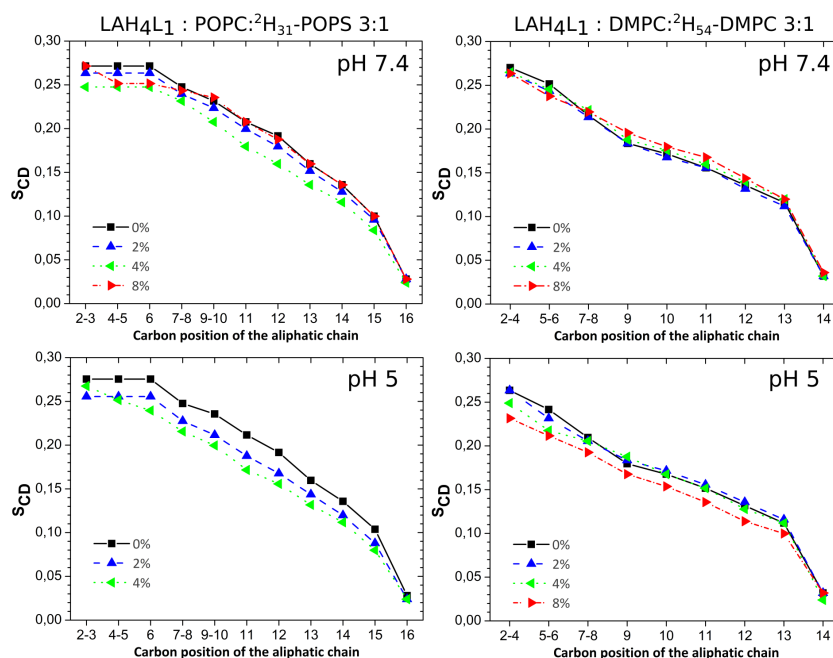
Figure 5.6: The deuterium order parameter as a function of carbon position of POPC/^{2}H$_{31}$-POPS 3:1 (A and B) and ^{2}H$_{54}$-DMPC (C and D) in the presence of increasing amounts of LAH4-L1 at pH 7.4 (A and C) or at pH 5 (B and D). The temperature was set to 30°C for POPC/POPS and 37°C for DMPC.

At pH 7.4, when LAH$_4$L$_1$ is added to POPC/^{2}H$_{31}$-POPS 3:1 membranes at P/L 2 and 4 %, a modest decrease of the order parameters was observed for all the C-^{2}H$_2$ positions. For the sample at P/L = 2 %, the shift is less pronounced than at the higher peptide concentration of 4 %. However, when the peptide concentration was further increased to 8%, the order parameters

were again close to the reference values, excepted for 4-6 carbon positions, which remain lower than the reference. At pH 5, the decrease in order parameters was more pronounced, except for positions 2-3 at 8% of peptide, where order parameters near the reference value were observed. When compared to $^2H_{31}$-POPS embedded in a POPC membrane, the effects were less pronounced for $^2H_{54}$ DMPC. At pH 7.4, addition of peptides causes only small changes in the order-parameter profile, with a small decrease for the first C-$^2H_2$ positions and a small increase from carbon position 7 onward. At pH 5, a decrease in the order parameter was observed for the first carbon segments at P/L = 4%, and decreases throughout the fatty acyl chains only for the sample at 8% of peptide.

### 5.2.2.3 Monitoring of the vesicles Deformation/Orientation

The deformation of vesicles /orientation of bicelles in the magnetic field is dependent on numerous parameters like the buffer, the hydration, the temperature and the type of lipids[71, 122]. Therefore, the sample preparation was systematically varied by the type of lipids, the temperature and the pH used. The temperature has an important effect on all lipids investigated while pH changes (in a biological pH range) affect mostly the peptide and POPS but not the zwitterionic vesicles. DMPC and POPC:POPS are different by the length and saturation of the aliphatic chains and by the presence of anionic phospholipids (POPS). To complete the analysis of the deformation/orientation of DMPC and POPC:POPS vesicles/bicelles, an additional serie of sample was prepared with POPC lipids. The different results of this part are discussed all together in a general conclusion at the end of this part.

Monitoring of the POPC vesicles Deformation/Orientation

The POPC serie was prepared and studied at pH 5 with a NMR spectrometer operating at 7.05 Tesla (^1H 300 MHz) (figure 5.7).

The detergent effect of LAH$_4$L$_1$ was also present with POPC vesicles. Indeed, at 8 mole% of peptide concentration, an oriented spectrum was obtained and membrane solubilisation happened at a P/L = 20 mole%, with an isotropic peak detected in both the ^{31}P and ^2H spectra. The samples with peptide were less stable, than without peptides, depicted by the isotropic peak visible in the ^{31}P spectra at P/L = 2%; also observable with ^2H spectra in which the
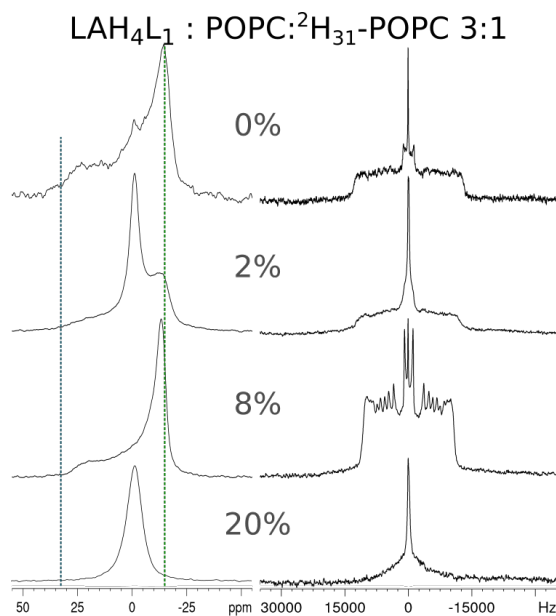
Figure 5.7: Increasing concentration of LAH$_4$L$_1$ in MLVs of POPC:^{2}H$_{31}$-POPC 3:1 studied by ^{31}P and ^{2}H solid-state NMR spectroscopy (300 MHz spectrometer): Samples were prepared at pH 5 and all spectra were acquired at 30°C. The blue and green dashed lines represent the $\delta_{//}$ and $\delta_\perp$ positions of the reference spectrum (0% P/L), respectively.

distinction of individual quadrupolar splittings was not possible (P/L 0 and 2%). The strength of the magnetic field is important for the orientation or deformation of vesicles[71]. In our case, lowering of the magnetic field from a 11.75 (^{1}H 500 MHz) to 7.05 Tesla resulted in a partially oriented spectra at P/L = 8%. Interestingly, this orientation was obtained at 30°C instead of 16°C for POPC:POPS vesicles.

Monitoring of the vesicles Deformation/Orientation: S1 order parameter

In order to quantify the orientation/deformation of the vesicles, the S1 order parameter was analysed (details in chapter 2). This value went from -0.5 to 1 for all the molecules oriented with their main axis perpendicular or parallel to B$_0$, respectively[69]. The parameter was estimated for the different series of samples (figure 5.8).

The S1 parameters show that the orientation/deformation of POPC/POPS vesicles, was more accentuated at pH 7.4 (lipids parallely oriented S1 = 0.1) than at pH 5 (S1 from -0.15 to -0.2). On the contrary, with DMPC vesicles the orientation was higher at pH 5 (S1 = -0.3 at pH 5 and 12.5% of peptide) and lower at pH 7.4 (S1 = -0.1). Nevertheless, the magnetic orientation of DMPC was more sensitive than POPC/POPS vesicles. This results in a big-

5. CHARACTERIZATION OF PEPTIDE-LIPID INTERACTIONS
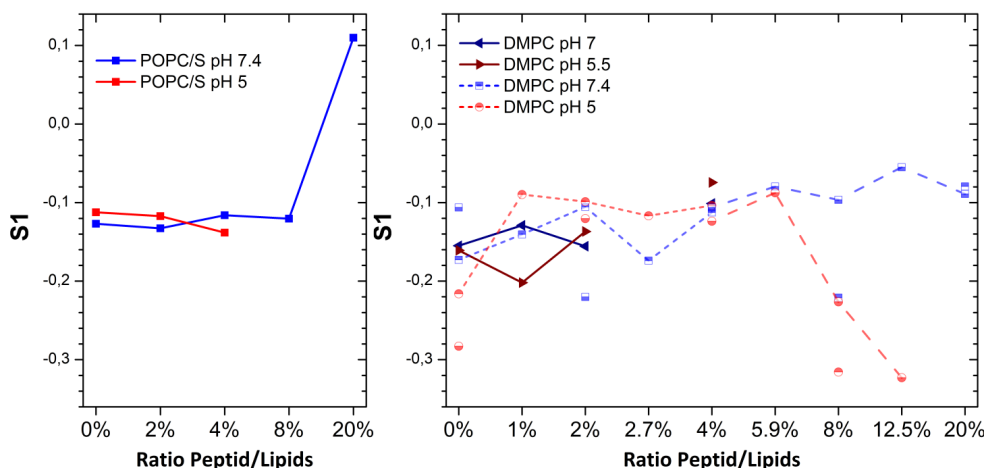
Figure 5.8: Graph representing the S1 order parameter: The different series of samples were plotted following the increased peptide concentration.

ger variation of the S1 parameter for DMPC.

Investigation of temperature dependency of the oriented samples

Lipid dynamics is highly dependent on the temperature as well as the orientation of the bicelle. Temperature dependency of bicelle orientation can be related to bicelles morphology (oblate: pH 5 P/L 8% and prolate: pH 7.4 P/L 20%).

The ^{2}H spectra of POPC:POPS pH 5 at 8% of LAH$_4$L$_1$ were acquired at different temperatures, with decreasing temperature (left column figure 5.9) or with increasing temperature (right column figure 5.9).

When the temperature was reduced from 28°C to 16°C, the isotropic peak was replaced by a spectrum with distinguishable quadrupolar splittings at 16°C. An intermediate broad spectrum is presented at 20°C. When the temperature increased from 16°C and 20°C, spectra characteristics of a well oriented vesicles parallel to the magnetic field is presented. When heated to 28°C, the spectrum exhibited a superposition of an isotropic contribution and distinguishable narrow quadrupolar splitting. This spectrum indicates the presence of different bicelles: oriented bicelles and isotropics micelles/bicelles that tumble fast enough to average the chemical shift anisotropy.

The observation at different temperatures of this sample showed the versatility of the bicelles orientation and revealed a temperature hysteresis of the system. Depending on the strength of the magnetic field and the propensity
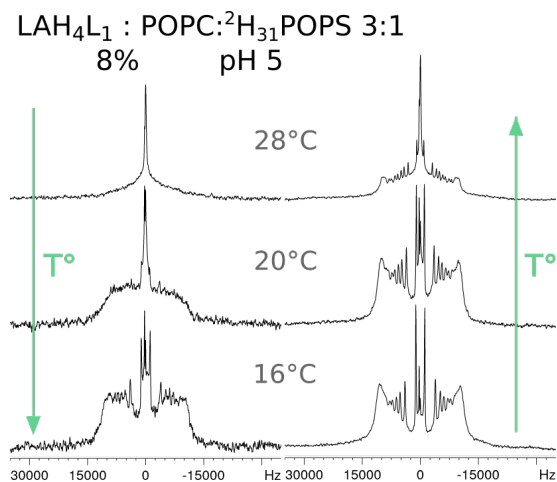
Figure 5.9: Temperature study of MLVs of POPC:^{2}H$_{31}$POPS 3:1 with 8% of LAH$_4$L$_1$ at pH 5 by ^{2}H solid-state NMR (500 MHz spectrometer). On the left, spectra acquired after decrease of the temperature are shown and on the right, the spectra acquired after increase of the temperature are shown.

of orientation, the orientation and disorientation of vesicles has been shown to be also time dependent[123]. However, here time dependency for orientation/disorientation seemed too short to be established.

Temperature screening from 10° to 40° was applied to the sample with 20% of LAH$_4$L$_1$ at pH 5. Spectra with isotropic peak were obtain, which indicates that solubilisation of the membrane in isotropic micelles/bicelles was temperature independent (not shown).

Orientation of the sample with 20% of LAH$_4$L$_1$ at pH 7.4 was investigated at different temperatures (figure 5.10).

In contrast to pH 5, lowering the temperature to 10°C resulted in the loss of the orientation. Starting from 14°C, increasing the temperature resulted in an augmentation of the oriented vesicles fraction. Apparition of peak around 4 kHz and large shoulders confirmed the oblate orientation. When the same sample was recorded at 60 ^{o}C, individual peak intensities became distinguishable, even within the shoulder.
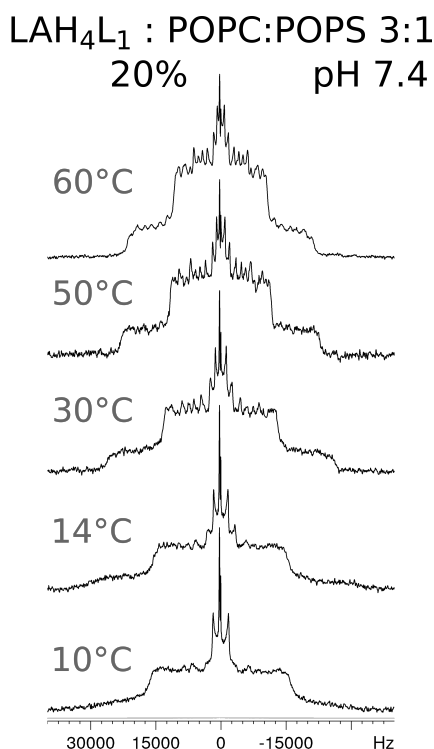
Figure 5.10: Temperature study of MLVs of POPC/POPS with 20% of LAH_4L_1 at pH 7.4 by ^2H solid-state NMR (500 MHz spectrometer). Spectra were acquired from 10^oC to 60^oC.

Conclusion about the monitoring of the vesicles Deformation/Orientation:
The orientation within a magnetic field is dependent on the cooperative addition of the diamagnetic susceptibility of the molecules component the vesicles/bicelles. Magnetic sensitivity of DMPC makes it a suitable lipid to form bicelles or nanodiscs for structural investigations[72]. At the contrary of DMPC, orientation of lipids with longer aliphatic chains, like POPC or POPC/POPS, is less favorable[71]. Then the observation of the same orientation with POPC lipids and at a lower magnetic field indicated than the peptide is responsible of the deformation/orientation of the lipids.

In our conditions, it is interesting to observe different vesicles orientation, parallel or perpendicular, with only differences in pH or peptide concentrations. Indeed with POPC/POPS vesicles, a perpendicular orientation (oblate) was observed at pH 7.4 at 20% of LAH_4L_1 or a parallel orientation (prolate) at pH 5 at 8%. Hence, this effect could be attributed to the diamagnetic anisotropy propensity of the peptide. Magnetic anisotropy of peptide can be attributed to the diamagnetic anisotropy of the planar peptide bonds. The regular arrangement (axial alignment) of the peptide bonds in α helix induce a large anisotropy[70].

This observation would fit with the peptide orientation in planar (IP) at

low pH and transmembrane (TM) at high pH, in membranes[124].

Temperature dependency of vesicle/bicelle orientation can be related to their morphology. Bicellar samples presented a wide variety of morphology dependence to the q ratio. This q ratio, usually defined for bicelle preparation, is a ratio between a long-chain lipid and a detergent[72].

In our case, difference of behaviours with the temperature and presence of orientation at different ratio depending ot the pH have been observed (oblate: pH 5 P/L 8% and prolate: pH 7.4 P/L 20%). Nevertheless, it is interesting to note that the orientation is independent on the chain length and phospholipid charge (DMPC myristoyl or POPC:POPS palmitoyl). It could be interesting to study the organization of the peptide in this two different cases. In front of the known orientation of the peptide in membrane (IP at pH 5 and TM at pH 7.4[124]), a belt model at pH 5 and a picket fence model at pH 7.4 was considered[125]. Structural characterizations would be necessary to assess these models[125, 126].

5.2.2.4   Monitoring of the vesicles temperature dependency

The utilisation of DMPC lipids allowed an easier study of the vesicles in their liquid or gel phase. The transition temperature of the DMPC is 24°C whereas the one of POPC and POPS are -2°C and 14°C, respectively.

Monitoring of the transition temperature   The transition can happen over a range of 1°C in homogeneous systems. Nevertheless, transitions are modified by addition of components like cholesterol or proteins[127].

The impact of LAH$_4$L$_1$ in the transition temperature of DMPC at different concentrations was studied by the acquisition of ^{2}H spectra at different temperatures. This effect was followed at $\pm$ 13°C around the transition point of DMPC at a pH of 5.5 and 7 (figure 5.11 and the corresponding ^{31}P spectra figure A.3).

In the ^{2}H spectra, the effect of the transition temperature is visible by a significant broadening of quadropolar splittings. Below the transition temperature, the effect of the temperature is only visible by a global shift of all the splittings, getting smaller with the increase of the temperature until reaching a plateau around 37°C. In contrast, below the transition temperature, only a wide quadrupolar splitting corresponding to the methyl group of the aliphatic chain, was distinguishable. The transition from resolved to broad spectra was sharp for the reference samples without peptide. Interestingly, the transition appeared at different temperatures, 22°C and 24°C for the references at pH 7 and 5.5, respectively. Addition of LAH$_4$L$_1$ did not change the transition temperature at pH 5, nervertheless at pH 7 the transition was smoothed. At pH 5.5, transitions were also gentle with addition of the peptide, but temperature transitions were shifted at P:L = 1% (26°C) and 4% (22°C). However, this difference for the sample at 1% of peptide was attributed to a degradation of the sample. It has been noticed that faster degradation of samples over time was more frequent at low concentration of peptide (1 or 2%).

In general, slight differences were visible with smoother transition for samples with peptides. However, any major modifications were distinguishable as it can been observed for other components like cholesterol[128].
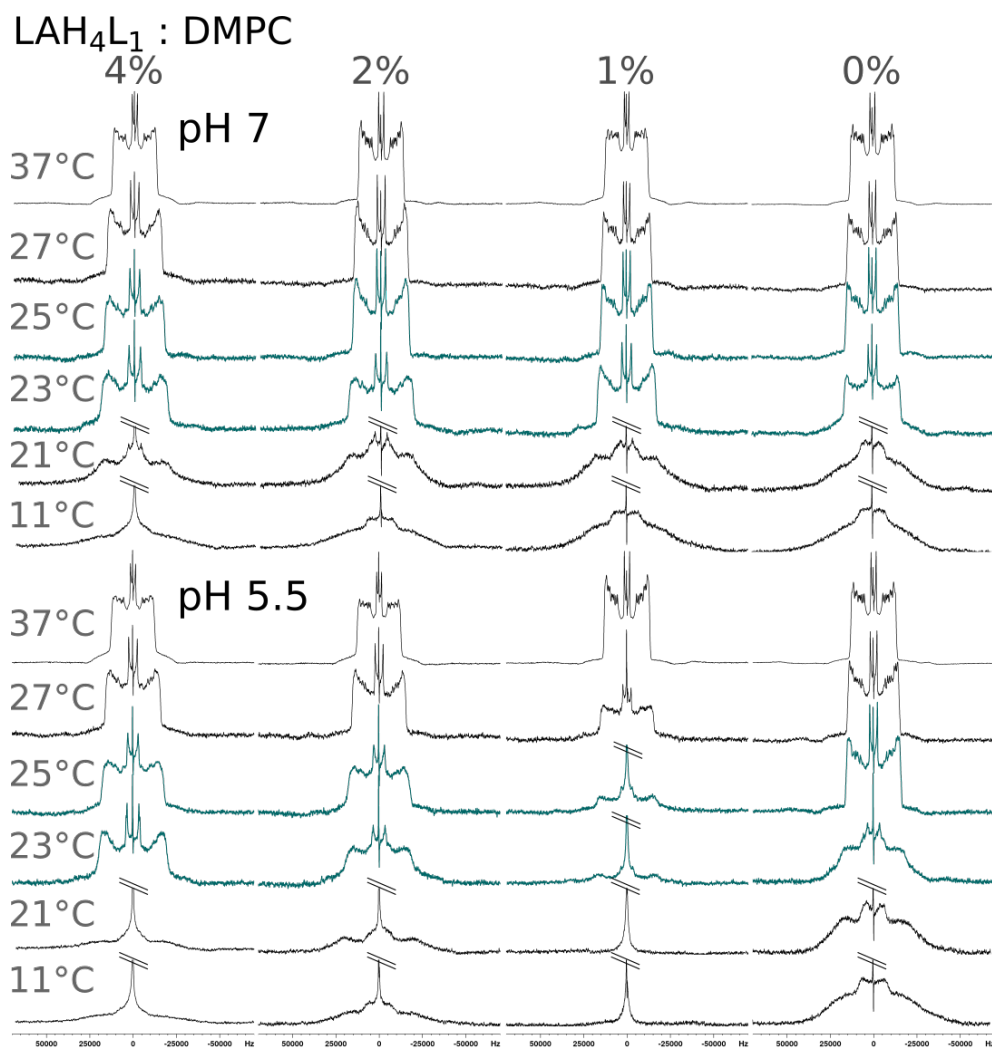
Figure 5.11: Temperature study of MLVs of DMCP with increased concentration of LAH$_4$L$_1$ by ^{2}H solid-state NMR. Samples were prepared at pH 7 and 5.5, all spectra were acquired from 37°C to 11°C. The spectra just below and beside the theoretical transition temperature were coloured in blue.

5. CHARACTERIZATION OF PEPTIDE-LIPID INTERACTIONS

Monitoring of the vesicles in fluid or gel phase   In their gel phase, lipids with aliphatic chains are fully extended, which is changing the dynamics of the bilayers[127]. Hence, additional information can be obtained from studies in both lipid phases (gel and liquid). The MLVs of DMPC with increased concentration of LAH_4L_1 were studied by ^{31}P solid-state NMR at 37^oC and 7^oC (figure 5.12).
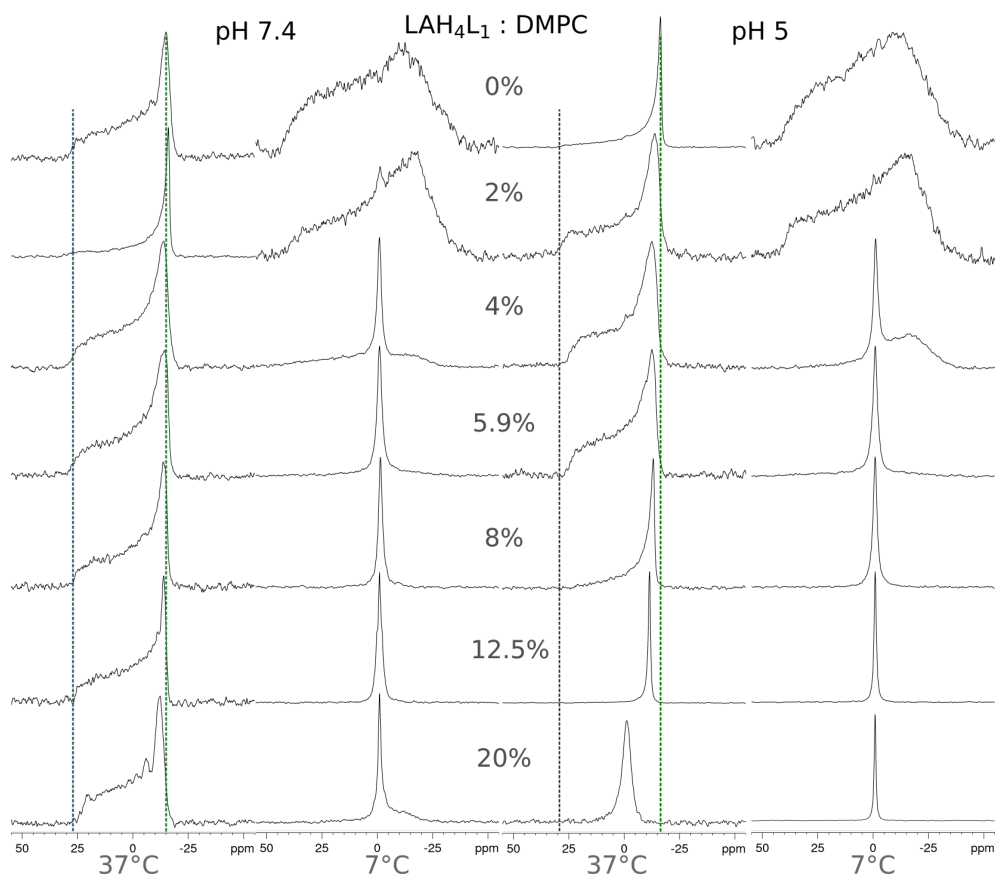
Figure 5.12: Increasing concentration of LAH_4L_1 in MLVs of DMPC studied by ^{31}P solid-state NMR: Samples were prepared pH 7.4 (two left column) and pH 5 (two right column) and spectra were acquired beside and below transition temperature of DMPC at 37^oC (first and third rows) and 7^oC (second and fourth rows). The blue and green dash lines represent the $\delta_{//}$ and $\delta_{\perp}$ of the reference spectrum (0% P/L) respectively.

When the temperature is lowered to 7^oC, for both pH, the chemical shift anisotropy increased to 68 ppm in the absence of peptide and at P/L = 2%. For a peptide concentration of 4% and at both pH, a sharp isotropic line shape appeared, suggesting a micellar or isotropic bicelle arrangements. This isotropic peak in the gel phase could indicate that the temperature transition

96

is going through a rippled effect. It is interesting to observe that the presence in this ripple phase persisted well below the transition temperature[129].

Monitoring of the size vesicles at the transition temperature   This study was completed with size determination of DMPC vesicles by DLS. Diluted NMR samples with increased concentration of LAH$_4$L$_1$ were measured at 23°C, just beside the transition temperature (figure 5.13).
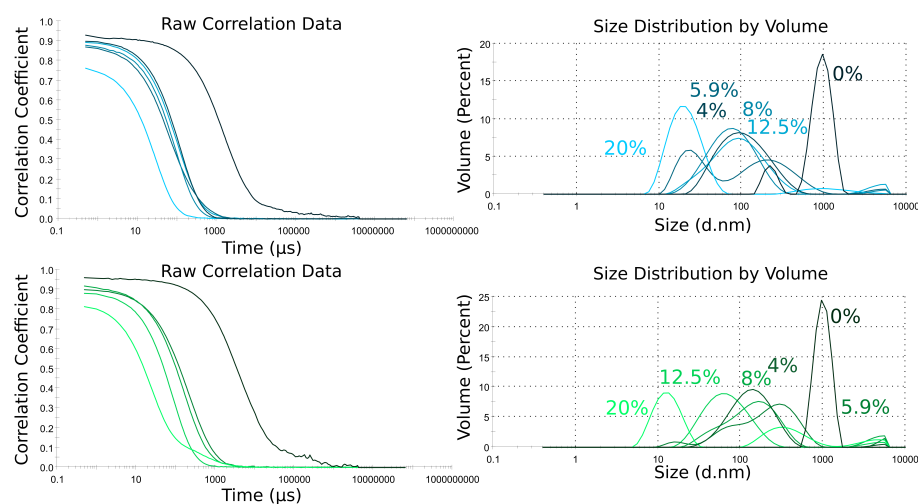
Figure 5.13: DLS curves of MLVs of DMPC with increased concentration of LAH$_4$L$_1$: Correlation curves (left) and size distribution are presented (right). The colours from dark to light green (pH 7.4) and from dark to light blue (pH 5) represent the data obtained from the lowest to the highest P/L ratios.

Whereas the DMPC vesicles exhibited a large hydrodynamic diameter around 1000 nm at both pH, the addition of LAH$_4$L$_1$ resulted in at least a 10-fold reduced size of the vesicles. At the highest ratio of 20%, the size of the aggregates reached the 10 nm range. Parameters (Z-Average and Polydispersity Index (PdI)) and appearance were summarized in Table below:

% P/L	Z-Average		PdI		Aspect	
pH	7.4	5	7.4	5	7.4	5
0	2678	1079	0.882	0.704	Milky	
4	108	84	0.340	0.294	Milky	
5.9	141	49	0.537	0.796	Untransparent	
8	114	65	0.444	0.277	Untransparent	Transparent
12.5	59	75	0.332	0.415	Transparent	Transparent [a]
20	22	20	0.546	0.287	Transparent	Transparent [b]

[a] Gelly at ambient temperature, liquid at 0°C. [b] Gel highly polymerised at ambient temperature, liquid at 0°C.

5. CHARACTERIZATION OF PEPTIDE-LIPID INTERACTIONS

Despite a decrease of the polydispersity of the samples containing peptides, this index was relatively high. Modification of the aspect is another marker of macromolecular properties changes. It has been noticed that samples of bicelles were optically transparent[120]. Two samples at pH 5 with P/L = 12.5 and 20% were transparent and viscous at room temperature. This optical observation can be correlated with vesicles deformation, and paralleled the observation of oriented ^{31}P spectra[130] (figure 5.12).

Both NMR and DLS agreed that, with the stepwise addition of LAH$_4$L$_1$, the structures diminish in size to reach a 10 nm hydrodynamic ratio at P/L = 20% at both pH. Study of lipid-peptide interactions in the gel phase allowed to observe additional effects[131, 129]. Absence (P/L = 2%) and presence of a ripple phase (P/L = 4%) could indicate an additional effect of the peptide for these concentrations. This effect, quite local, could be induced by the tendency to the peptide to be aggregated at the surface of the membrane. Also, this effect should be accentuated at pH 7.4 when the peptide presents more propensity of aggregation[99]. Hence, because NMR allows to look at global instead of local effects, this behaviour could be confirmed by other methods.

5.2.3 Study of LAH$_4$L$_1$ in mechanically oriented model membranes

The ability of lipids to form oriented bilayers between glass plates allows one to study other parameters than presented in the previous part. Interestingly the ^{31}P spectrum for LAH$_4$L$_1$ in POPC:POPS 3:1 at a P/L = 4% presents a big disordering effect of the lipid bilayer. This effect is observable with the presence of an important peak around -15 ppm indicating a disordering of lipid headgroup.

In order to study this effect samples presented in the previous section were spread on glass plate and the ^{31}P spectra acquired (figure 5.14). The samples used were the MLVs of POPC:POPS 3:1 and POPC (5.3 and 5.7, respectively).
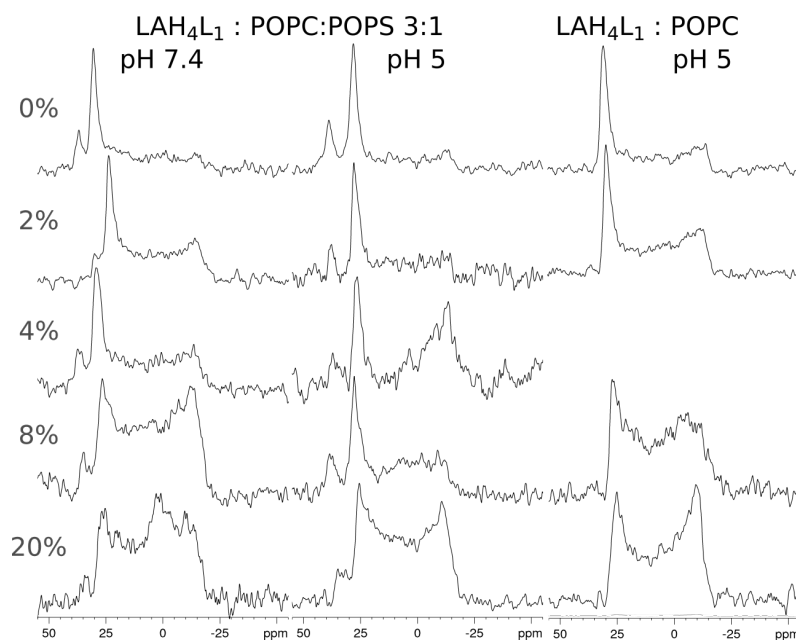
Figure 5.14: ^{31}P oriented spectra of POPC:POPS or POPC with an increased concentration of LAH$_4$L$_1$: the sample were prepared at pH 7.4 and 5 for POPC:POPS or only pH 5 for POPC.

The percentage of intensities, corresponding to the liquid crystalline state aligned with the lipid long axis parallel to the magnetic field, is indicate Table 5.1.

Unlike the classical preparation, the spreading of MLV on glass plate induced much less oriented samples, as visible with only 59, 67 and 51 % of orientation for the reference samples without peptide[78]. With the increase

Table 5.1: Table of the percentage of intensity corresponding to the fraction of oriented lipids on the spectra presented in the figure 5.14.

Lipids	POPC:POPS 3:1		POPC
pH	7.4	5	5
P/L 0%	59	67	51
P/L 1%	59	67	51
P/L 2%	85	51	38
P/L 4%	47	36	
P/L 8%	27	45	26
P/L 20%	26	30	25

of the peptide concentration to P/L = 20%, the proportion of well oriented lipids decreases to only 26, 30 and 25 %. This decrease of orientation goes with the increase of peptide except for the sample pH 5 ratio 8% in POPC:POPS membranes.

Mechanically oriented membranes are often used to study peptide orientation. By ^{15}N labelling the peptide at a single position, the investigation of the orientation of the peptide in the membranes is possible. LAH_4L_1 in POPC:POPS 3:1 membrane, like LAH_4, presents an in planar orientation (IP) depending on the membrane at pH 5 and is transmembrane (TM) at neutral pH[124, 11].

Nevertheless, the membrane orientation of peptide is highly dependent on the conditions, e.g. buffer or lipids. It has been demonstrated that transmembrane alignment of LAH_4 peptide is favoured by utilization of dimyristoyl phospholipids instead of palmitoyl phospholipids. Also, TM orientation of the peptide is obtained with the addition of citrate buffer, even at low pH. In citrate buffer, LAH_4 is dimerized allowing the insertion in the membrane even in acidic condition[132].

Orientation of LAH_4L_1 has been thoroughly studied in different membrane mixtures of palmitoyl chain lipids, composed of different ratio of POPC:POPS[124]. In our case, the orientation of LAH_4L_1 was studied with different phospholipids chains: in POPC or DMPC lipids (figure 5.15).
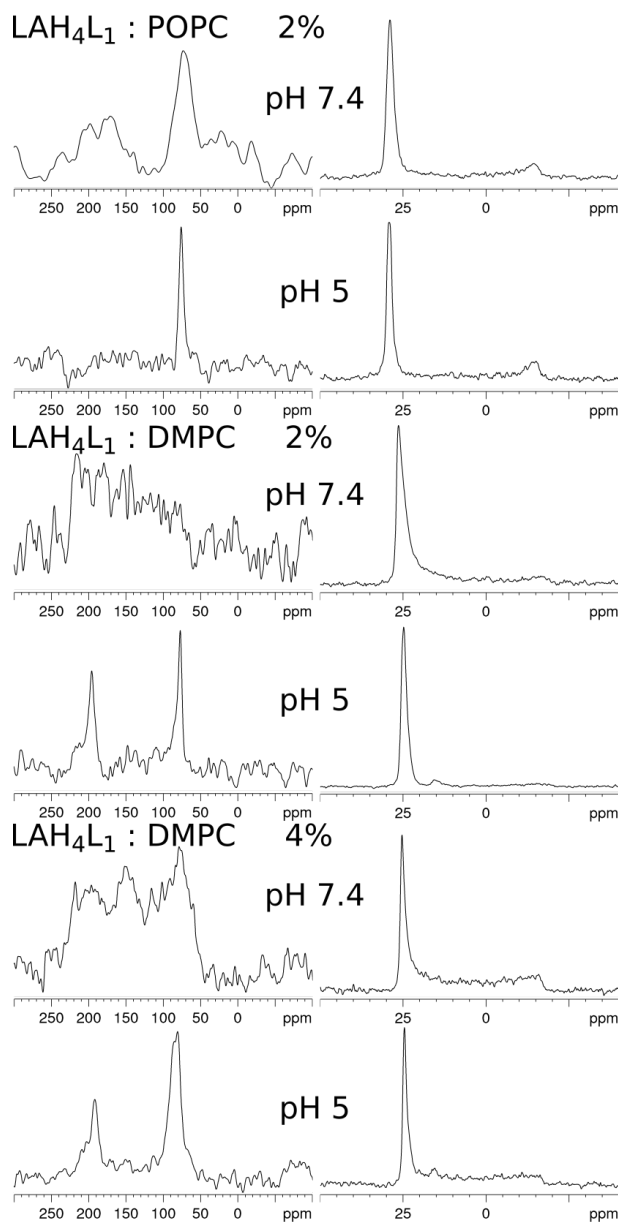
Figure 5.15: Proton-decoupled ^{15}N and the corresponding ^{31}P solid-state NMR spectra of [^{15}N-Leu$_{14}$]-LAH$_4$L$_1$ reconstituted in POPC or DMPC bilayers oriented with the normal parallel membrane to the magnetic field direction. In the first row, are shown the ^{15}N spectra (acquired on a 300 MHz for the POPC samples pH 7.4 and 750 MHz spectrometer for the other samples) and the second row correspond to the ^{31}P spectra (acquired on a 300 MHz spectrometer). One peptide concentration was used for POPC, P/L = 2% and two for DMPC membranes: P/L = 2 and 4%. The pH (pH 7.4 or 5) are indicated on the figure.

5. CHARACTERIZATION OF PEPTIDE-LIPID INTERACTIONS

Table 5.2: Chemical shift of the ^{15}N oriented spectra of the figure 5.15 and the percentage of IP-TM orientations.

Lipids	POPC		DMPC	
P/L	2%	2%	2%	4%
pH	7.4	5	5	5
IP	73±2 ppm	76±1 ppm	78±1 ppm	83±2 ppm
LWHH	27 ppm	6.5 ppm	7 ppm	16 ppm
TM	175±5 ppm		196±1 ppm	192±1 ppm
LWHH	56 ppm		10 ppm	16 ppm
IP-TM	55-45 %		52-48 %	65-35 %

Table 5.2 summarises the spectra description of the oriented sample (figure 5.15). When reconstituted into DMPC at pH 7.4, a broad distribution of resonances extends from 235 ppm to 50 ppm. Notably, all the ^{31}P NMR spectra of POPC and DMPC were well-oriented.

The orientation of LAH$_4$L$_1$ in membranes is energetically dependent on small contributions. In presence of anionic lipids, the electrostatic attraction favours the interaction with POPS and enable the partial insertion of the α-helix. Nevertheless, in presence of zwitterionic lipids like POPC, biophysical investigations suggest that the interaction with neutral membranes follows a different mode of interaction. Indeed, the apparent binding constant is two orders of magnitude less than for POPS. Also, the α-helix secondary structure decreases from 88% with POPS to 52% with POPC[112]. So, it is not surprising to observe a reduction of transmembrane alignment at pH 7.4 in POPC membrane instead of in POPS membrane.

The DMPC lipids are different from POPC by the length of the aliphatic chains and their saturation (saturated chains for DMPC). In these lipids, the TM alignment is favoured as it is easily visible at pH 5. The influence of lipids on the peptide orientation is known for LAH$_4$ and has been demonstrated for other peptides, e.g. the antimicrobial peptide PGLa[132, 133]. Nevertheless, at pH 7.4, when the TM orientation should be more favourable because of the deprotonation of the histidines, a broad distribution of all orientations is visible whereas the ^{31}P spectra remain well oriented.

Hence, other parameters should be considered to explain these multiple orientations. Peptide aggregation can be considered to describe the broad distribution of orientation[134]. Considering the lower affinity for zwitterionic membrane and the weaker constraint due to the saturated chains of DMPC, in this conditions (at pH 7.4) peptide-peptide interactions within membranes could be accentuated[99].

In view of the aggregation propensity of these peptides presented in the previous chapter (chapter 3) and the potential effect on the biological activity, this aspect could be more investigated, regarding the peptide-lipid interactions[37].

5.3 Study of the interaction between LAH$_4$L$_1$ and complex lipid mixtures

The LAH$_4$ peptide family presents affinities for anionic lipids, e.g. POPG or POPS, because of electrostatic interactions[16]. During the maturation of the membrane from the early to the late endosome, the bilayer is subject to a rearrangement of its phospholipids. In the case of drug delivery systems trapped in an endosome, these modifications in addition to the modification of the pH can induce a redistribution between the peptide and its cargo as well as between the peptide and the lipids[20].

Nevertheless, lipid models commonly used for biophysical investigation are much different in composition and proportion from cell membranes. Hence, in the following section, different mixtures of lipids have been used in order to study the peptide effect in systems closer to real membranes.

5.3.1 Interaction of the LAH$_4$L$_1$ and lipid mixtures

In this section, different mixtures of lipids where prepared in order to be closer to the composition of real endosomal or late endosomal membranes[110]. The MLVs prepared are summarized in the table below:

Lipids Ratio	POPC:POPG/S:Chol 4:3:3		POPC:POPG/S:Chol:SM 4:2:3:1	
	pH 7.4	pH 5	pH 7.4	pH 5

Based on a POPC membrane, POPS was added to reproduce the early endosome or POPG to fit with the late endosome composition. POPG was chosen instead of Bis(Monoacylglycero)Phosphate (BMP), because BMP is an expensive lipid and is a structural isomer of PG[135]. Cholesterol is a major component of the eukaryotic membrane. Hence 30% of cholesterol was added to the lipid mixtures[56]. Furthermore, the sphingomyelin is also subject to a drastic decrease during the maturation of the endosome, hence it was added in one of the series.

The MLV were analysed by ^{31}P static and MAS solid-state NMR. Spectra were acquired at two different temperatures (37°C and 15°C) with the aim to follow the evolution of the CSA parameters. The static ^{31}P spectra of the MLV at pH 7.4 and pH 5 are presented in figure 5.16.

LAH$_4$L$_1$: Lipids   2%
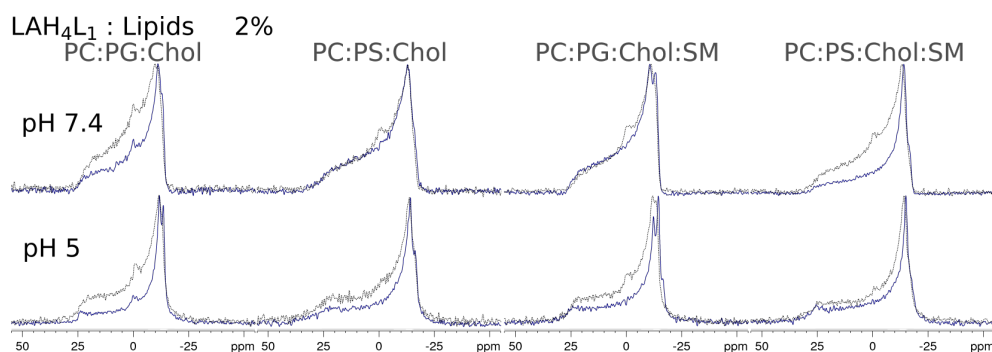
Figure 5.16: Static ^{31}P solid-state NMR spectra of MLVs of different lipid mixtures at pH 7.4 and pH 5. All the spectra presented here were acquired at 37°C. The spectra in blue correspond to membranes containing LAH4-L1 and the spectra in black dash lines are the reference spectra of lipids without peptide.

Each spectrum was compared to the reference without peptide. At pH 7.4, PC:PS:Chol and PC:PG:Chol:SM were almost similar, except for the small isotropic peak present in the reference samples. The reference sample PC:PG:Chol presented a spectrum with a shape between liquid and gel phase with a pronounced shoulder (between 25 to -10 ppm). The differences between spectra with peptide and reference seemed to be more important at pH 5 for all of the mixtures tested. The decrease of the shoulder intensity could indicate a bigger deformation of the vesicles when the peptide is present. Spectra acquired at 15°C were similar to those acquired at 37°C, but differences were less pronounced (figure A.4).

In lipid mixtures, the ^{31}P CSA represent the sum of the spectrum of each lipid, hence, the extraction of the parameters needed to be done by simulation of the different components of the spectrum. Good overlap of theoretical and acquired spectrum were not reachable.

Under these conditions, extraction of the CSA was not possible, thereupon, slow MAS-NMR spectra were acquired in order to have a second dataset to extract this parameter.

The slow MAS ^{31}P solid-state NMR spectra are presented in the following figure 5.17 (acquired at 37°C and the other acquired at 15°C in the figure A.4).

The spinning allows to determine more easily the isotropic value for each lipid. The PC:PG mixture presented two separate peaks as it was also visible in the static spectra, with chemicals shifts around -1 ppm and 0 ppm for

5. CHARACTERIZATION OF PEPTIDE-LIPID INTERACTIONS
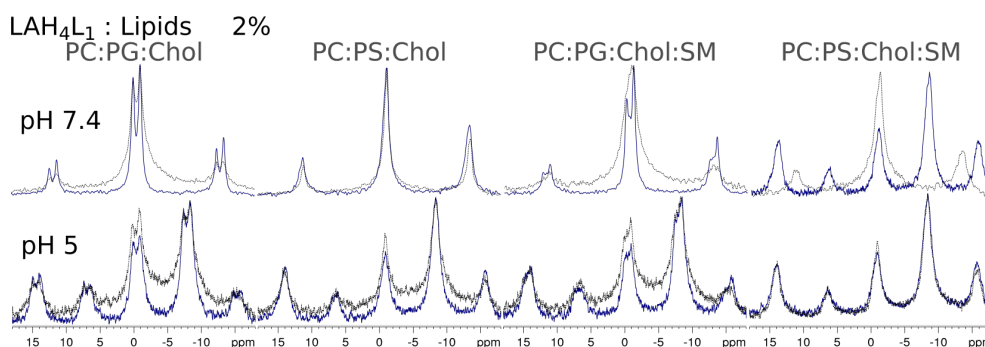
Figure 5.17: ^{31}P solid-state slow MAS spectra (1.5 kHz spinning) of MLVs of the different lipids mix at pH 7.4 and pH 5. All the spectra presented here were acquired at 37°C. Spectra pH 7.4 excepted PC:PS:Chol:SM with peptides were acquired on a 300 MHz and all the other on a 500 MHz. The spectra in blue are with LAH4-L1 and the spectra in black dash line are the reference without peptide.

POPC and POPG respectively. The peak corresponding to the SM around -0.5 ppm is also distinguishable. Nevertheless, for the mix with POPS, the chemical shift around -0.8 ppm of POPS appeared like a shoulder as well as when SM was added to this mixture, yielding to difficulties to determine the isotropic value peak. The simulation of the spectra in order to extract the CSA parameters was not possible, as for the static spectra.

The isotropic chemical shift was plotted, depending on the temperature (figure 5.18). The evolution of the isotropic value at two different temperatures for a sample was compared to the reference (only lipids).

The samples with POPG at pH 7.4 are quite similar, with a decrease of the isotropic value around 0.1 ppm from 37°C to 15°C. The reference with SM presents a shift of POPG slightly bigger than 0.2 ppm. At pH 5, an increase around 0.1 ppm is observable between the two temperatures, in all the cases, excepted for the reference with SM, with a decrease around 0.1 ppm. In a general manner, neither the differences induced by the temperature are notable nor the differences between POPC and POPG are significative.

The comparison of isotropic value in samples with POPS is more sensitive to the different conditions. At pH 7.4, the reference with cholesterol increases when the one with the peptide decrease. The reference with SM decreases when with peptide, it was increasing. At pH 5, a slight decrease is visible in all the conditions. Nevertheless, the shifts seemed to be more important for
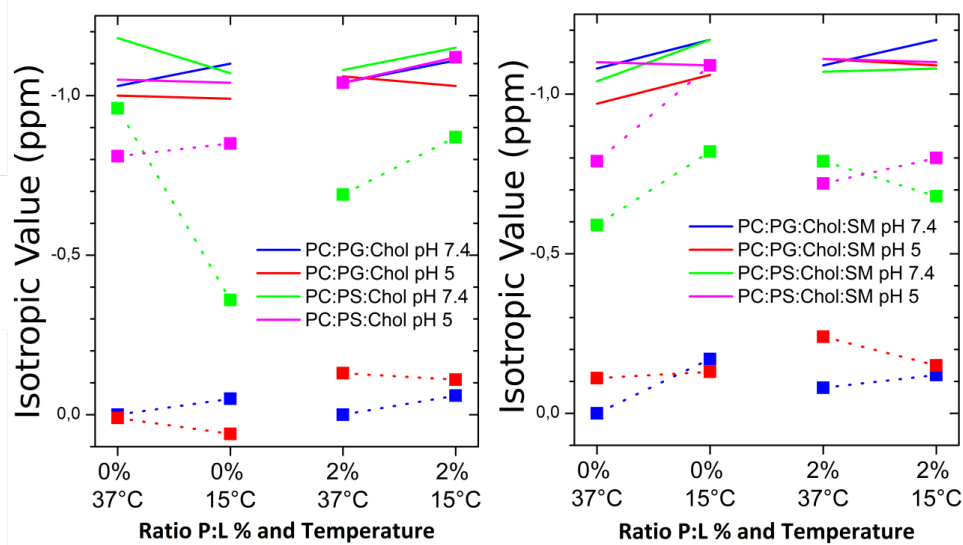
Figure 5.18: Graphs of the isotropic value extracted from the slow MAS ^{31}P spectra. The samples are indicated by the colour in the legend. The two first or two last rows of each graph represent the value without or with peptide, respectively. The full line represent the value measured for POPC when the dashed line the value for POPG/PS.

POPS (at least 0.2 ppm) than for POPC (0.1 ppm).

Interpretation of these results was impossible. In a general observation, as expected, anionic lipids (POPG or POPS) seemed more sensitive to the different conditions. Nevertheless, samples with POPS did not appear to converge. While no quantification was done, spectra with LAH$_4$L$_1$ seemed presenting sharper peak and more stable time compare to their references without peptide.

Further investigation would be necessary to extract precise information. Nevertheless, others methods should be tested in first instance, to determine the stability, temperature dependency or homogeneity.

5.3.2   Interaction of peptides with total extract lipids

To get rid of the preparation of plenty of lipids mixture, and to fit as much as possible with real membranes, the idea was to use membranes extracted from cells. The advantages would also be to use different kinds of membrane, like plasma membrane, early endosome or late endosome[136].

The extraction of membrane can be done by various methods. The solvent extraction is a fast and easy technique for the membrane extraction. This approach was used on 5 g of lyophilized Yeast, allowing to recover 50 mg of product. This solution was spreaded on glass plate and the ^{31}P spectrum was acquired (figure 5.19).
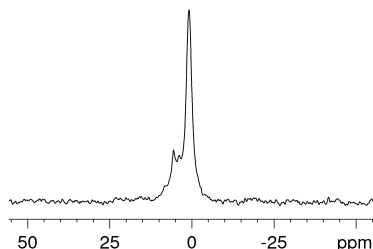
Figure 5.19: ^{31}P spectra of the total extract from Yeast spread on glass plate.

The spectrum results in a predominant isotropic peak at 0 ppm. Two smaller peaks are present at 5 and 2.5 ppm along a shoulder at 8 ppm. The presence of phosphorus could indicate the presence of phospholipids, even if other cell products can contain phosphorus[137]. However, this product doesn't seem to be orientable on glass plate. Further investigation should be done in order to determine for which reason this product is not orientable.

A commercial Total Extract of *E.coli* was used to prepare oriented samples. As presented in the previous part, the orientation of the LAH$_4$ and LAH$_4$L$_1$ can be diverse, depending on parameters like membrane composition or buffer[132] (section 5.2.3). Hence, in parallel samples were prepared with the hΦ19W under similar conditions (the sequence is presented on the table below). This highly hydrophobic peptide preferentially adopts a transmembrane orientation in presence of membrane. It is a derivative from LAH$_4$, where histidines were removed, and a tryptophan amino acids was added as 1 additional lysines at each terminis[113].

LAH$_4$L$_1$	KKALL AHALH LLALL ALHLA HALKK A
hΦ19W	KKKAL LALLA LAWAL ALLAL LAKKK

Orientation of LAH$_4$L$_1$ at low and neutral pH in total extract of *E.coli* was compared to the orientation of hΦ19W, reconstituted in POPC membrane or in total extract of *E.coli* (figure 5.20). The total extract of *E.coli* is mainly composed of PE, PG and CA (57.5, 15.1 and 9.8 wt/wt% respectively). In the Table 5.3, is summarised the spectra description of the oriented samples in total extract (figure 5.20).
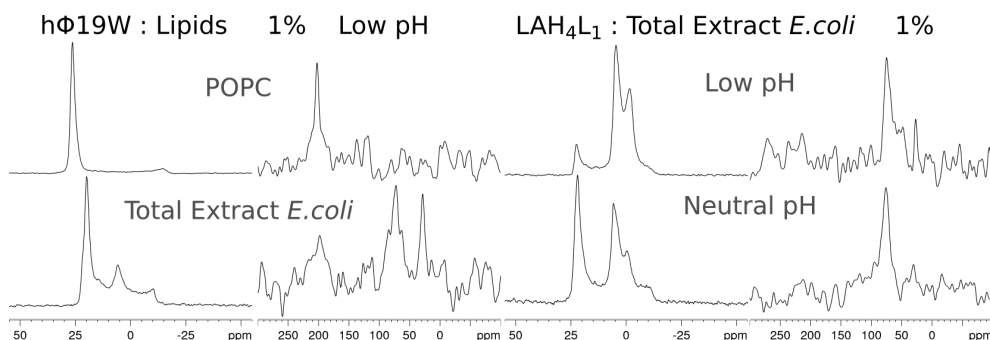
Figure 5.20: Proton-decoupled ^{15}N and the corresponding ^{31}P solid-state NMR (300 MHz spectrometer) spectra of peptides reconstituted in oriented POPC lipids or from a total lipid extract of *E.coli* bilayers: the two first or two last rows are spectra corresponding to the [^{15}N-Leu$_{15}$]-hΦ19W (at low pH) or [^{15}N-Leu$_{14}$]-LAH$_4$L$_1$ (at low and neutral pH), respectively.

Table 5.3: Summary of the chemical shifts of the ^{15}N oriented spectra presented in the figure 5.20 and percentage of IP-TM orientations.

Peptides	hΦ19W		LAH$_4$L$_1$	
Lipids	POPC	Total Extract of *E.coli*		
pH	low			neutral
IP		73.1±1 ppm	74.8±1 ppm	76±1 ppm
LWHH		22 ppm	14 ppm	15 ppm
TM	201.9±0.2 ppm	198.4±2 ppm		
LWHH	5 ppm	33 ppm		
IP-TM	1-99 %	60-40%	72-28%	93-7 %

Concerning the hΦ19W, when reconstituted in POPC membranes, ^{31}P and ^{15}N spectra confirmed the presence of a well oriented membrane with a TM peptide. In total extract, the ^{31}P spectrum presented a main peak corresponding to an intensity of 48% of the total spectrum (integration of the intensity from 30 to 15 ppm). Then 52% remaining should contain mainly

unoriented phospholipids. Howeven, the ^{15}N spectrum was well oriented and exhibited the two orientation, IP and TM. It has to be noticed that the ^{15}N peak presents at 30 ppm, visible also for spectra of the LAH_4L_1 corresponds to the PE lipids.

Concerning the orientation of LAH_4L_1, the quality of the ^{31}P spectra was not so good represented by the intensity of 15 or 38% for the peak of oriented lipids at low or high pH, respectively. Nevertheless, considering the poor quality of the ^{31}P spectra, the ^{15}N peak remains relatively sharp, suggesting a good orientation. The ^{15}N oriented spectra presented at both pH an IP orientation.

In this experiment, it is not surprising to observe the loss of the TM orientation of the LAH_4L_1. On the contrary for the $h\Phi19W$ peptide, the partial TM orientation obtained despite the high hydrophobicity of the peptide, is interesting.

The profile of the ^{31}P spectra of the LAH_4L_1 could be partially induced by the peptide, considering the observed IP orientation. This effect could be confirmed by supplementary samples with diverse peptide concentrations.

Otherwise, it is interesting to notice that orientation of total extract of lipids was possible. It could be useful to quantify the hydration of the sample. And so far, the improvement of the protocol of extraction presented below for the orientation of LAH_4L_1 could be studied in lipids extract from different cells kinds.

5.4 Conclusion

The study of the LAH_4L_1 in membranes model allows to attest the detergent properties of the peptide at low pH, in combination with an increase in concentration of peptide. Interestingly, different orientations of the vesicles were visible at both pH 7.4 and pH 5. The data seemed to indicate different bicelles model depending of the condition, proved by the difference of orientation observed and their temperature/orientation dependencies (illustrated in the figure 5.21).
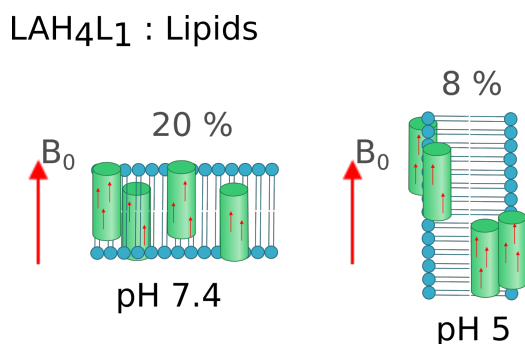
Figure 5.21: Schematisation of the effect observed by solid-state NMR. In blue is represented the lipids bilayer, in green the α-helix of the LAH4-L1 are represented in a cylinder and the red big arrow indicate the orientation of the magnetic field and the small one represented

It could be interesting to prepare ^{15}N labelled LAH_4L_1 oriented samples with different conditions to study the model.

Reproduction of these series of experiments (POPC:POPS 3:1 at pH 7.4 and 5 with increased concentration of peptide until 20%) to other peptide of the LAH_4 family might be useful; in particular for the VF1 peptide which did not present antimicrobial activity. Indeed, antimicrobial activity against *E. coli* was shown for LAH_4 and LAH_4L_1, unlike VF1 which was not able to inhibit bacterial growth of *E. coli* [12,22,23]. In addition to other methods, it can bring information about the propensity to disrupt or fuse membranes.

Furthermore, different experiments have been done in order to have lipids systems closer to biological conditions. Nevertheless, the interpretation was delicate and did not allow to extract precise results.

However, preparation of oriented bilayers with complex mixtures appeared to be feasible. The ^{15}N spectra obtained from preparation with total *E. coli*

lipids extract were well oriented. Hence, additional experiments could bring useful information about the behaviour of the peptide in different cell membranes.

6

Characterization of Peptide-Nucleic Acid Interactions

LAH$_4$ peptides have been shown to be efficient to transfect different nucleic acids, such as DNA or siRNA[17, 26]. Different methods have been used to characterize their interactions, mainly of DNA with LAH$_4$. Quantitative information has been extracted from gel shift assays or ITC experiments[20]. This analysis demonstrated that lowering the pH from neutral to 5.5 resulted in the release of half of the peptide from LAH$_4$:DNA complexes. The concomitant increase in peptide concentration in parallel with the lowering of pH can result in high alteration of the membrane[38]. In the biological context, this condition corresponds to the acidification of the endosome through which the DNA:LAH$_4$ complex passes, during gene delivery into eukaryotic cells. The lowering of the pH allows the delivery of this DNA to the cytoplasm, by dissolving the endosomal membrane by the peptide[21].

Interaction of LAH$_4$ peptide with nucleic acids is mainly driven by electrostatic interactions between the cationic peptides and the negatively charged nucleic acids[20]. This has the advantage to allow reversible interactions, important for the membrane disurptive effects, when lowering the pH. Also, the modulation of the strength of the interaction depends on the hydrophobic angle of the peptide. Nevertheless, estalishing simple correlations is not easy and predictions of the efficiency of the system is still not possible. The numerous effects underlying the interactions of nucleic acids with LAH$_4$ peptide make the interpretation complicated. Indeed, during this complex formation, pep-

tide folding into an α-helix, interaction between peptide and DNA and DNA condensation have to be considered[124]. Hence, supplementary information about structural arrangement between peptide and nucleic acids could help to improve these systems.

Structural characterization of the DNA:LAH$_4$ complex has been performed by solid-state NMR. ^{31}P-^{15}N and ^{31}P-^{13}C NMR spectra allow to determine the implication of the lysine side chains in the complex (figure 6.1).
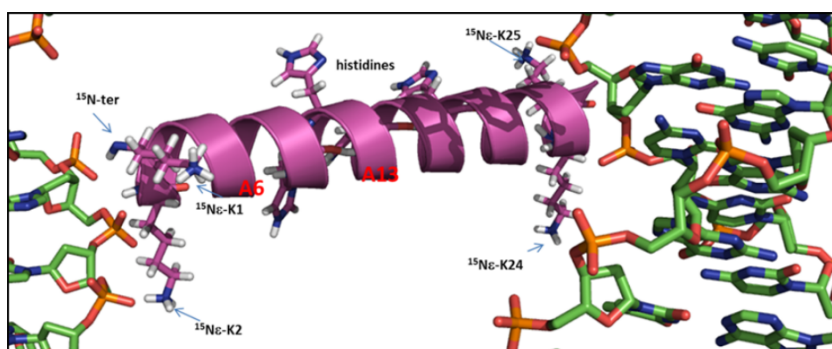
Figure 6.1: Modelization of a possible conformation adopted by the LAH$_4$ peptide between two DNA strands. Lysines residues are close to the phosphate group of the DNA (image provided by Bertani Philippe).

Nevertheless, simulation of the structure of the DNA:LAH$_4$ complex with the available data did not allow to determine a precise unique structure.

Combination of this information with other data could allow to decipher a structural model. Liquid state NMR is also often used for structural determination[138]. However, because of the electrostatic interactions, the fast formation of the complex DNA:peptide is usually not homogeneous and results in big aggregates[124]. In addition, these effects are accentuated by the conditions needed for suitable biophysical analysis. On the contrary, in biological conditions, amount of materials is significantly less concentrated, and studies are performed in complet media. Hence, limited size and homogeneous complex between peptide and nucleic acid can be obtained and are stable over time[34]. Thereupon, condition should be found for liquid state NMR investigation of the complex.

This chapter presents mainly preliminary results and focuses on the characterization of the complex formed by a short DNA 15 mer and the LAH$_4$L$_1$

peptide. In a first part, different titration experiments with LAH_4L_1 and DNA are shown, followed by liquid NMR, in order to find conditions allowing the investigation of the complex. In the second part, complexes have been mixed with lipids to anticipate of further structural investigation. The samples were analysed by ^{31}P and ^2H solid-state NMR (similarly to the previous chapter 5).

6. CHARACTERIZATION OF PEPTIDE-NUCLEIC ACID INTERACTIONS

6.1 Materials

Liquid NMR of DNA:LAH$_4$L$_1$ complex

Sample preparation: Aliquots of the LAH$_4$L$_1$ peptide (MW = 2779 Da) and 15 mer DNA (double strand 5'-GGAGACCAGAGGCCT-3'; MW = 9304,9 Da) were prepared from unique stock solutions, in order to have comparable amounts of material between the different titrations. The peptide LAH$_4$L$_1$ was dissolved in water, and equilibrated at pH 5 by addition of 0.1 or 0.5 M NaOH before aliquoting (equivalent of 0.7 mg per aliquot) and lyophilisation. The DNA was dissolved in water and aliquoted (equivalent of 0.3 mg per aliquot) before lyophilisation.

For measurements, aliquots of peptide were dissolved in different buffers to reach a concentration of 500 μM. In parallel, the DNA aliquots were dissolved in similar buffer in a smaller volume (50 μL) in order to limit the dilution of the sample. Aliquots of DNA corresponds to a DNA:LAH$_4$L$_1$ ratio of 12.5% (mol%).

The peptide was titrated by successive addition of DNA until the desired ratio was reached. Three different conditions were tested:

- Acetate condition: the acetate buffer was prepared at 10 mM pH 5 and contained 10% D$_2$O. The titration was done until a DNA:LAH$_4$L$_1$ ratio of 25% was reached (6 titration points were done).

- DPC condition: 7 mg of deuterated ^{2}H$_{38}$-DPC (dodecylphosphocholine-d$_{38}$, Avanti Polar Lipids, Alabaster, AL) was dissolved in 500 μL H$_2$O (10% D$_2$O) and equilibrated at pH 5. The titration was done until a DNA:LAH$_4$L$_1$ ratio of 25% was reached (7 titration points were done).

- TFE condition: a solution of 50% deuterated TFE (2,2,2-Trifluoroethanol-d$_3$, Sigma-Aldrich, Lyon, France) in H$_2$O was prepared and equilibrated at pH 5. The titration was done until a DNA:LAH$_4$L$_1$ ratio of 31.25% was reached (9 titration points were done).

Liquid state NMR: ^{1}H spectra of the acetate and DPC conditions were acquired on a 400 MHz liquid NMR spectrometer (Bruker Avance III) with an inverse 5 mm ^{1}H-X probe at 25°C. Spectra of the TFE conditions were acquired on a 500 MHz liquid NMR (Bruker Avance II) with a 5 mm ^{13}C-^{1}H cryo-probe at 25°C with 20 Hz spinning. ^{1}H 1D spectra were acquired using a

watergate sequence for water suppression[139]. The 90° and water suppression pulses were optimized on the first spectrum of each condition. Parameters were conserved for the rest of the titration and spectra were acquired with the same number of scans, in order to allow the direct comparison of intensities.

Interpretation of spectra: Spectra were analysed by following the differences of intensities, or by following the change of chemical shifts, as much as possible for sharp peaks (figure 6.2).
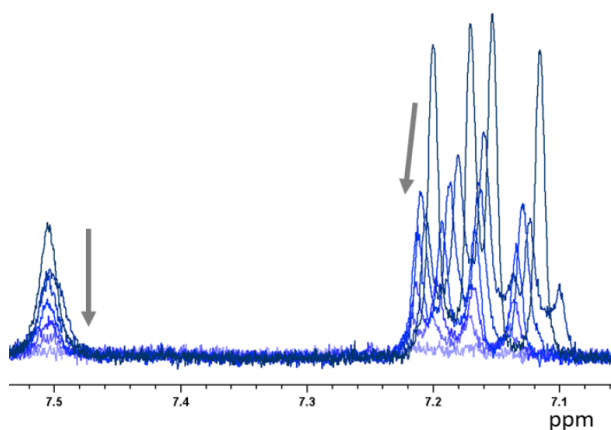
Figure 6.2: Titration of the peptide by DNA followed by liquid NMR (400 MHz spectrometer): arrows indicate the two effects measured; the peak integration to follow the decrease of intensity and the peak picking to follow the modification of chemical shift. The peaks between 6.98 to 7.24 ppm correspond to the imidazole protons of the histidines and the peak around 7.5 ppm to the side chain of the lysine.

In order to follow the decrease of intensity, the dilution of the samples was estimated by integration of a peak specific to the buffer. The plotted intensities were then normalized by the estimated dilution coefficient. The DNA concentration was controlled by a peak identified as corresponding to the DNA solution.

Different spectral regions were determined and followed: Methyl of the alanines (Ala CH_3) from 1 to 2 ppm or the leucines (Leu CH_3) from 0 to 1 ppm, the β and γ proton from 2 to 3 ppm, the α proton from 3 to 4 ppm, the amide proton from 7.5 to 8.5 ppm, two peaks around 7 and 7.5 ppm were estimated to be side chains of lysines, and finally the imidazole rings of the histidines recognizable by sharp peaks between 7 to 7.5 ppm (His) and 8.5 to 9 ppm (His amide side) (figure 6.3).
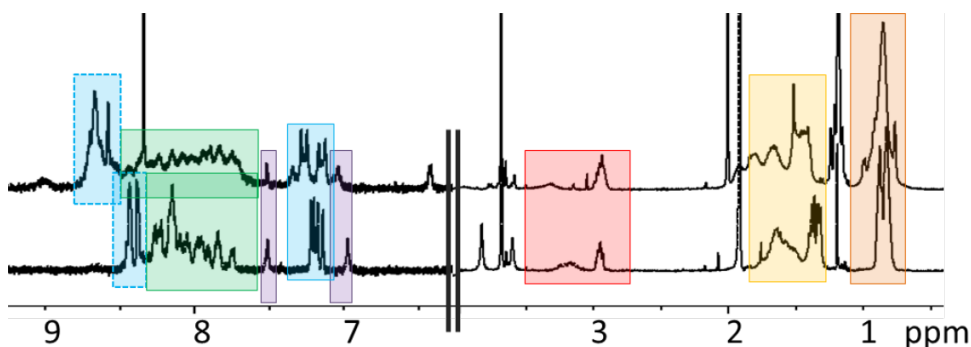
Figure 6.3: 1D ^{1}H NMR spectra of DPC (up) or acetate (bottom) conditions: the different spectral regions are indicated in colours, Leu CH_3 in orange, Ala CH_3 in yellow, α proton in red, lysines in purple, amide proton in green and histidines in blue.

The intensities for there regions were plotted following the titration in a graph for each titration (figure A.5 and A.6).

Monitoring of the chemical shift changes have been compiled by region, similarly to the intensities. The mean values of chemical shift deviation have been summarized in Table A.1.

Solid-state NMR of the MLVs with DNA:LAH$_4$L$_1$ complex

Preparation of MLV MLVs were prepared using the same protocol presented in the lipid chapter 5. Around 13 mg of POPC:POPS 3:1 were prepared and solubilized in $CHCl_3$/MeOH (2:1 v/v). The LAH$_4$L$_1$ (previously solubilized in TFE) was mixed with the DNA 15 mer. The different components were mixed, and the solvent was gently evaporated under a stream of nitrogen, to obtain a lipidic film along the walls of a glass tube. The film was dispersed in MilliQ water and the pH was equilibrated at pH $\approx$ 5 or 7.4 by adding 0.1 or 0.5 M NaOH, and then lyophilized. Samples were lyophilised and stored at -20°C. Just before the experiment, the samples were suspended in either 100 mM Tris buffer (pH 7.4) or in 100 mM acetate (pH 5). Finally, the multilamellar vesicles (MLVs) were equilibrated by three freeze/thaw cycles (10 min at -80°C, 1 min at ambient temperature, and 10 min at 50 ^{o}C, vigorous vortexing). Before acquisition, the samples were stored at 4°C.

Different batches of prepared samples are summarized in the table below. The lipids used were POPC:^{2}H$_{31}$-POPS 3:1 (sample only with lipids were prepared at pH 7.4 and 5):

	DNA	LAH$_4$L$_1$	DNA-LAH$_4$L$_1$	DNA-LAH$_4$L$_1^a$
pH	7.4, 5	7.4, 5	7.4, 5	5
Molar Ratio P/L	1/100, 1/1700			
or in %		2%	2%	8%
Ratio DNA:Peptide			1/34, 1/17^a	1/34

^{a} lipids used were POPC:^{2}H$_{31}$-POPC:POPS 2:1:1

NMR parameters External references were used to reference the spectra and to optimize the parameters: H$_3$PO$_4$ (0 ppm) for ^{31}P NMR spectra and D$_2$O (0 ppm) for ^{2}H NMR spectra.

Proton-decoupled ^{31}P Hahn-echo spectra[67] of MLVs were obtained on a Bruker Avance 300 NMR spectrometer equipped with a 4 mm MAS probe head (Bruker Biospin, Rheinstetten, Germany) without spinning. Temperature was set to 30°C (and 16°C for one of the samples). The following parameters were used: 90° pulse between 2.3 or 3.1 μs; echo delay, 37.1 μs; acquisition time, 10.24 ms; time domain data points, 2048; number of scans, between 5232-10950; recycle delay, 3 s; and continuous wave ^{1}H decoupling around 36 or 40 kHz.

For ^{2}H static solid-state NMR, a solid quadrupolar echo-pulse sequence[75] was used with the following parameters: 90° pulse, 3.4 μs; echo delay, 50 μs; acquisition time, 16.4 ms; dwell time, 0.5 μs; time-domain data points, 32,768; number of scans, between 51,200-145,165; and recycle delay, 0.3 s.

The ^{31}P and ^{2}H spectra were processed with a line broadening of 50 Hz before Fourier transformation.

6.2 Liquid NMR of DNA:LAH$_4$L$_1$ complex

In order to study the interaction between LAH$_4$L$_1$ and DNA, peptide was titrated with DNA in different media, and followed by liquid state NMR spectroscopy. Experiments were performed only at pH 5 to limit the aggregation of the peptide. The ratios have been choosen in the same range of the one determined by gel shift assay for the LAH$_4$ and a plasmidic DNA: at neutral pH, 1 peptide for 1.7 base pairs and at pH 5, 1 peptide for 3.3 base pairs[20]. In our experiment, a short double stranded DNA was used (15 mer) and de facto, titration was done until at least a 25% ratio of DNA:LAH$_4$L$_1$ (mole/mole) to reach an equivalent of 1 peptide for 4 base pairs. Different conditions were tested. The acetate buffer was chosen because it was also used for structural solid-state NMR investigations of DNA:LAH$_4$ complexes[124]. In order to have a folded peptide (in α-helical structure) and to mimic membrane environment, the titrations were also done in DPC or in 50% TFE.

Titration of DNA in LAH$_4$L$_1$ solubilized in acetate buffer appears to result mainly in the precipitation of the complex (figure 6.4).
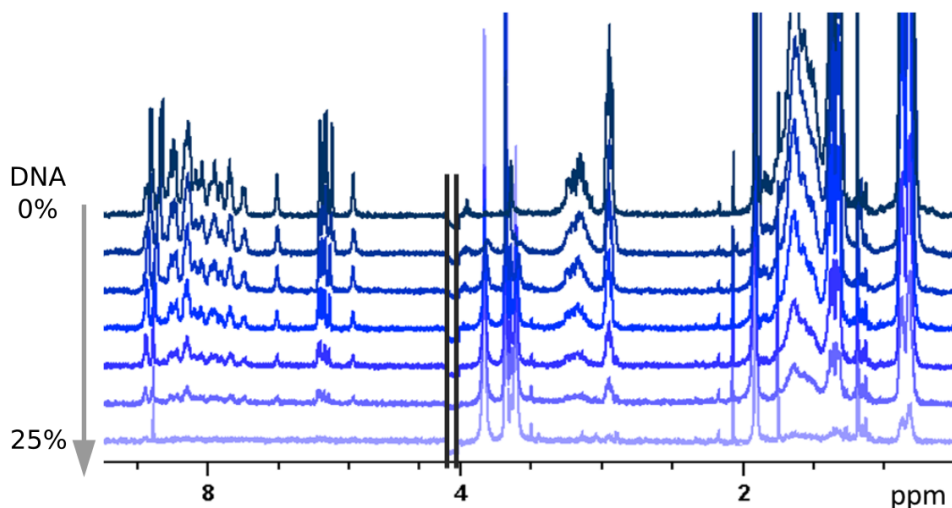
Figure 6.4: Titration in acetate buffer of the peptide by DNA followed by liquid ^{1}H NMR (400 MHz spectrometer): spectra were coloured following the titration from the dark blue to light blue corresponding to a DNA concentration of 0% to 25%, respectively.

After addition of 25 mole% of DNA compared to the peptide concentration, around 70% of the peak intensity was lost (figure A.5). Furthermore,

a successive increase of aggregates sedimentation was observed by eye during the titration. Fluctuation of the chemical shift were negligeable (order of 10^{-3} ppm) but it has to be noted that histidines chemical shifts were deviated at least two times more (Table A.1).

Results obtained with DPC were quite similar to those in the acetate buffer (Figure A.5 and Table A.1). The decrease of the signal is slower, with only around 30% of peak intensity lost in the presence of after 25 mole% DNA. During the titration, sedimentation of big aggregates was also visible. Nevertheless, chemical shift deviation are in the same order of 10^{-3} ppm, but the shift of the histidines were less important.

The titration in the 50% TFE mixture showed the most promising result (figure 6.5).
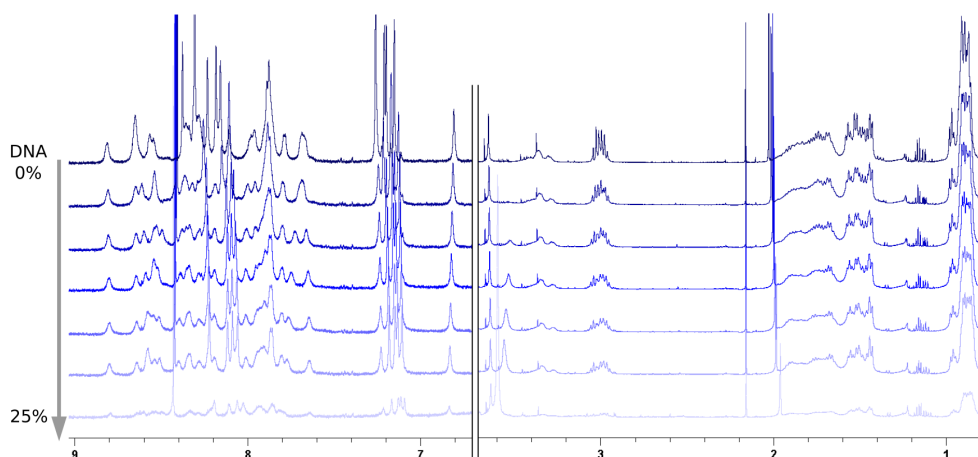
Figure 6.5: Titration in 50% TFE of the peptide by DNA followed by liquid ^{1}H NMR (500 MHz spectrometer): spectra were coloured following the titration from the dark blue to light blue corresponding to a DNA concentration of 0% to 25%, respectively.

Despite a 60% reduction of the signal after addition of 25 mole% DNA and visible aggregates, they were staying in suspension and seemed smaller. Changes in chemical shift were bigger by an order of magnitude (10^{-2} ppm) than under the acetate and DPC conditions.

Hence, decrease of the signal without significant shift of the peak observed for acetate and DPC indicates only sedimentation of nonspecific DNA:LAH$_4$L$_1$ complexes. The interaction in TFE/H$_2$O, potentially represents a more specific DNA:LAH$_4$L$_1$ complex, considering the bigger chemical shift difference

and the lower aggregation of the complex. In TFE/H_2O the peptide adopts mainly an α-helical secondary structure, therefore, the observed shift does not result from the folding of the peptide. Furthermore, it is interesting to note the lower decrease of the signal in presence of DPC detergent. This difference could be explained by the low amount of available peptide, because it is interacting with the lipids.

Further NMR investigations could be done, such as 2D experiments, in order to see if the complex formed in TFE is an homogeneous complex suitable for structural analysis.

6.3 Solid-state investigation of the DNA:LAH$_4$L$_1$ complex in model membranes

In this part, preliminary investigations of the DNA:LAH$_4$L$_1$ complex in the presence of lipids vesicles are presented. These were performed for two purposes. First of all, the objective was to acquire first spectra of the mixture to optimize the conditions for further structural analysis of the complex in membranes. Secondly, the aim was to observe the conservation or not of the lytic effect of the peptide, when complexed with DNA, using similar conditions of the study of the previous chapter (chapter 5).

^{31}P and ^{2}H solid-state NMR spectra were acquired with POPC:POPS 3:1 MLVs formed in presence of the DNA:LAH$_4$L$_1$ complex, at pH 7.4 and 5. In parallel, control of the POPC:POPS 3:1 MLVs with peptide or DNA were recorded (Figures A.7 and A.8). The sample controls with DNA were prepared with two different concentrations: one corresponding to the amount of DNA present in the complex, and another with a higher ratio. For both nuclei, ^{31}P or ^{2}H, no specific effect was observed in presence of DNA. A sharp peak around 0 ppm was observed in the phosphorus spectra. However this peak is probably from the phosphorus of the DNA.

For the complex of DNA:LAH$_4$L$_1$ a ratio of 1/34 has been chosen in order to follow the same ratio peptide/base pair (around 2 peptides per base pair) of nucleic acid used for biological assay[34] (figure 6.6).

Two main effects were observed in these conditions. On the ^{31}P spectrum at pH 5, an important peak was present at 0 ppm. A small peak was also observable in the corresponding spectrum at pH 7.4 (however, it should coincide

Figure 6.6: ^{31}P and ^{2}H solid-state NMR spectra of DNA:LAH$_4$L$_1$: samples were prepared at pH 7.4 and pH 5. Two different concentration of DNA were used 1/34 and 1/17 and colour in black or green, respectively. All spectra were acquired at 30°C.

with the phosphorus present in the DNA). Hence, this peak at 0 ppm at pH 5 would indicate that part of the membrane is highly disturbed by the complex DNA:LAH$_4$L$_1$. It is interesting that this effect is detected with only a ratio of P/L = 2% when the corresponding spectrum without DNA is in accordance with a classical powder pattern spectrum . The second effect observed was on the ^{2}H spectrum of the sample at pH 7.4 (figure A.7). When compared to the spectrum without DNA, the individual resonances defining quadrupolar splittings were broadened.

Similar samples were prepared with twice the amount of DNA (DNA:LAH$_4$L$_1$ 1/17). The ^{31}P spectrum at pH 5 was substantially similar to the one with a DNA:peptide ratio of 1/34. In contrast the ^{2}H spectrum was presenting more pronounced changes than the corresponding sample with less DNA. In contrast, when the peptide alone is added, the stronger effect on the aliphatic chains of lipids is presented at pH 7.4. The increase of the effect with the amount of DNA would indicate than this is the consequence of the DNA.

Hence, it could be interesting to do further investigation of this mixture with the preparation of similar samples with different concentration of peptide and/or DNA. Oriented samples could also be prepared with labelled peptide, to analyse the effect of the DNA in the orientation of the peptide.

6. CHARACTERIZATION OF PEPTIDE-NUCLEIC ACID INTERACTIONS

A complementary sample with the DNA was prepared at 8% of P/L concentration and pH 5, in the condition where LAH_4L_1 was shown to cause large vesicles deformation (chapter 5, figure 6.7).
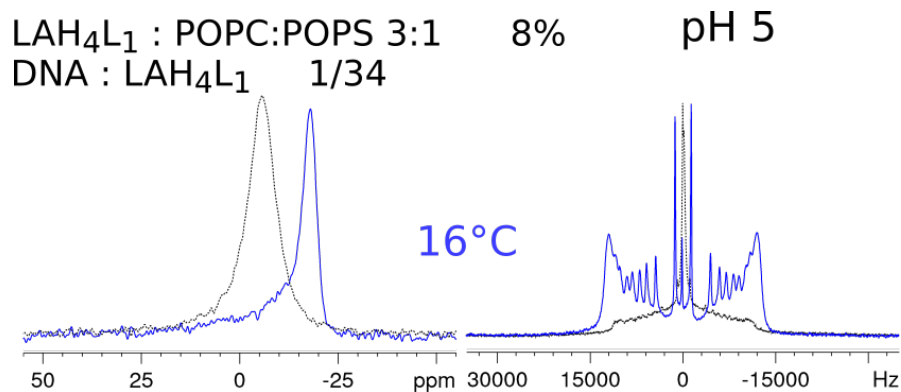
Figure 6.7: ^{31}P and ^{2}H solid-state NMR spectra of DNA:LAH_4L_1: samples were prepared at pH 5 with a P/L = 8%. All spectra were acquired at 30°C and 16°C and coloured in black or blue, respectively.

Similarly to the same condition without DNA, at 30°C, a broad isotropic peak was observed in the ^{31}P spectrum. The ^{2}H spectrum presented also mainly an isotropic peak, but some quadrupolar splitting were still visible, indicating that the sample is not homogeneous. Hence, these spectra result from a mixture of vesicles and assemblies like micelles or isotropic bicelles that tumble fast. Upon lowering the temperature to 16°C, oriented spectra were obtained, indicating that the phospholipids align with their long axis perpendicularly to the magnetic field direction of the NMR spectrometer.

It is interesting to observe that the lytic effect observed for the peptide with vesicles is also present in presence of DNA. Nevertheless, it could be interesting to quantify the amount of peptide bonded to the lipids and to the DNA.

6.4 Conclusion

The preliminary work presented in the chapter showed that it is possible to study the complex formed by DNA and the LAH_4L_1, when solubilized in a mixture of water and TFE. The utilization of TFE can be debatable for structural investigations[51]. TFE induces helical secondary structures, and with LAH_4, an intermediate state of partial α-helical structure is obtained, which is different than in presence of membranes[14]. Nevertheless, considering the fact that interaction with DNA induces α-helical folding of the LAH_4, and comparing with complete media used in biological assays[20], utilization of TFE revealed to be a good compromise to analyse these complexes. Reproduction of these experiments at neutral or intermediate pH could bring valuable information.

2D NMR experiments could be done in order to assign the peptide alone and/or in complex for further structure determination. It has been demonstrated that lysines are interacting with the DNA but not the histidines. Nevertheless, histidines are responsible of the release of peptide from the complex when the pH is lowered[19]. In our case, histidines were quite affected by the different titrations, although those amino acids types are highly sensitive to the environment. Positions of histidines along the peptide is an important determinant for the efficiency of delivery systems[18,23]. Hence, it could be interesting to follow more precisely their interactions with DNA at different pH.

The investigation of the effects of the $DNA:LAH_4L_1$ mixture on membranes presented two main effects. First, the lipids head was highly disturbed at pH 5 when aliphatic chains were most disturbed at neutral pH. Secondly, magnetic orientation of phospholipids observed in similar conditions than without peptide shows that the lytic effect of the peptide is still present, despite the addition of DNA[38]. Screening of conditions with different concentrations of peptide and DNA could be done in order to determine the minimal amount of peptide necessary to observe this effect. Presence of an important isotropic peak at a ratio of 2% indicates that the peptide is more efficient to disturb the membrane when complexed with DNA.

6. CHARACTERIZATION OF PEPTIDE-NUCLEIC ACID INTERACTIONS

7

Conclusion

In this manuscript, the biophysical characterization of LAH_4 peptide family was described. In particular, the focus has been put on peptide-peptide interactions to form fibrillary assemblies, and peptide-lipid/peptide-DNA in order to go further in the characterization of their interactions.

First of all, peptide-peptide interactions were studied with the VF1 peptide. With the aim to determine the molecular structure of fibres of VF1, conditions of fibrillation have been optimized. The utilisation of dialysis to slowly increase the pH allowed the formation of homogeneous fibres. Preliminary solid-state NMR allowed to assess the good quality of the samples, and new experiments will be performed. The protocol was also successfully applied to the LAH_4L_1, which formed elongated fibres. Hence, the application of this protocol could be applied to other LAH_4 peptides, to investigate correlations between peptide-sequences and fibril structures.

Parallely to the investigation of VF1 fibres, this peptide was expressed in bacteria for isotopic labelling. Expression of the pVF1 peptide succeeded however the purification was complicated, by coelution of the fusion protein during reverse phase HPLC. Size exclusion chromatography allowed to recover pure fractions of pVF1. Nonetheless other methods will be tested to optimize the protocol to ensure a maximum yield.

Secondly, the peptide-lipid interactions were probed with the aim to investigate conditions similar to those occurring during endocytosis process. Monitoring the effects of increasing LAH_4L_1 concentration, combined with an acidic pH in model membranes, confirmed the detergent like model[38]. Then,

different mixtures of lipids were used. Nevertheless the results obtained were delicate to interpret. However, encouraging results for investigation of complex conditions were obtained when orientation of the LAH_4L_1 was measurable reconstituted in oriented lipids from total extract of *E. coli*.

Finally, the peptide-DNA interaction was monitored with the LAH_4L_1 and a short DNA sequence. Liquid state NMR allowed to follow the formation of the complex in 50% TFE/H_2O. Noteworthy, experiments with MLVs permitted to observe the effect of the complex LAH_4L_1:DNA on lipids. Further experiments would allow to extract structural information about the complex in solution or in presence of membranes.

References

[1] Inês Rego de Figueiredo, João Miguel Freire, Luìs Flores, Ana Salomé Veiga, and Miguel A.R.B. Castanho. **Cell-penetrating peptides: A tool for effective delivery in gene-targeted therapies: Cell-Penetrating Peptides.** *IUBMB Life*, **66**(3):182–194, March 2014.

[2] Thomas F. Martens, Katrien Remaut, Jo Demeester, Stefaan C. De Smedt, and Kevin Braeckmans. **Intracellular delivery of nanomaterials: How to catch endosomal escape in the act.** *Nano Today*, **9**(3):344–364, June 2014.

[3] Samantha L. Ginn, Ian E. Alexander, Michael L. Edelstein, Mohammad R. Abedi, and Jo Wixon. **Gene therapy clinical trials worldwide to 2012 - an update: Gene therapy clinical trials worldwide to 2012 - an update.** *The Journal of Gene Medicine*, **15**(2):65–77, February 2013.

[4] Nouri Nayerossadat, PalizbanAbas Ali, and Talebi Maedeh. **Viral and nonviral delivery systems for gene delivery.** *Advanced Biomedical Research*, **1**(1):27, 2012.

[5] Hao Yin, Rosemary L. Kanasty, Ahmed A. Eltoukhy, Arturo J. Vegas, J. Robert Dorkin, and Daniel G. Anderson. **Non-viral vectors for gene-based therapy.** *Nature Reviews Genetics*, **15**(8):541–555, August 2014.

[6] May C. Morris, Sebastien Deshayes, Frederic Heitz, and Gilles Divita. **Cell-penetrating peptides: from molecular mechanisms to therapeutics.** *Biology of the Cell*, **100**(4):201–217, April 2008.

[7] Molly E. Martin and Kevin G. Rice. **Peptide-guided gene delivery.** *The AAPS Journal*, **9**(1):E18–E29, March 2007.

[8] Francesca Milletti. **Cell-penetrating peptides: classes, origin, and current landscape.** *Drug Discovery Today*, **17**(15):850–860, August 2012.

[9] Weijun Li, François Nicol, and Francis C Szoka. **GALA: a designed synthetic pH-responsive amphipathic peptide with applications in drug and gene delivery.** *Advanced Drug Delivery Reviews*, **56**(7):967–985, April 2004.

[10] Hilary Brooks, Bernard Lebleu, and Eric Vivès. **Tat peptide-mediated cellular delivery: back to basics.** *Advanced Drug Delivery Reviews*, **57**(4):559–577, February 2005.

[11] Burkhard Bechinger. **Towards membrane protein design: pH-sensitive topology of histidine-containing polypeptides.** *Journal of molecular biology*, **263**(5):768–775, 1996.

[12] Titus C. B. Vogt and Burkhard Bechinger. **The Interactions of Histidine-containing Amphipathic Helical Peptide Antibiotics with Lipid Bilayers THE EFFECTS OF CHARGES AND pH.** *Journal of Biological Chemistry*, **274**(41):29115–29121, August 1999.

[13] Arnaud Marquette, A. James Mason, and Burkhard Bechinger. **Aggregation and membrane permeabilizing properties of designed histidine-containing cationic linear peptide antibiotics.** *Journal of Peptide Science*, **14**(4):488–495, April 2008.

[14] Julia Georgescu, Victor H.O. Munhoz, and Burkhard Bechinger. **NMR Structures of the Histidine-Rich Peptide LAH4 in Micellar Environments: Membrane Insertion, pH-Dependent Mode of Antimicrobial Action, and DNA Transfection.** *Biophysical Journal*, **99**(8):2507–2515, October 2010.

[15] B. Bechinger, J. M. Ruysschaert, and E. Goormaghtigh. **Membrane helix orientation from linear dichroism of infrared attenuated total reflection spectra.** *Biophysical Journal*, **76**(1 Pt 1):552–563, January 1999.

[16] A. James Mason, Amélie Martinez, Clemens Glaubitz, Olivier Danos, Antoine Kichler, and Burkhard Bechinger. **The antibiotic and DNA-transfecting peptide LAH4 selectively associates with, and disorders, anionic lipids in mixed membranes.** *The FASEB Journal*, December 2005.

[17] Antoine Kichler, Christian Leborgne, Josefine März, Olivier Danos, and Burkhard Bechinger. **Histidine-rich amphipathic peptide antibiotics promote efficient delivery of DNA into mammalian cells.** *Proceedings of the National Academy of Sciences of the United States of America*, **100**(4):1564–1568, February 2003.

[18] Antoine Kichler, Christian Leborgne, Olivier Danos, and Burkhard Bechinger. **Characterization of the gene transfer process mediated by histidine-rich peptides.** *Journal of Molecular Medicine*, **85**(2):191–201, February 2007.

[19] Burkhard Bechinger, Verica Vidovic, Philippe Bertani, and Antoine Kichler. **A new family of peptide-nucleic acid nanostructures with potent transfection activities.** *Journal of Peptide Science*, **17**(2):88–93, February 2011.

[20] Lydia Prongidi-Fix, Masae Sugawara, Philippe Bertani, Jesus Raya, Christian Leborgne, Antoine Kichler, and Burkhard Bechinger. **Self-Promoted Cellular Uptake of Peptide/DNA Transfection Complexes.** *Biochemistry*, **46**(40):11253–11262, October 2007.

[21] Antoine Kichler, A. James Mason, and Burkhard Bechinger. **Cationic amphipathic histidine-rich peptides for gene delivery.** *Biochimica et Biophysica Acta (BBA) - Biomembranes*, **1758**(3):301–307, March 2006.

REFERENCES

[22] A. James Mason, Claire Gasnier, Antoine Kichler, Gilles Prévost, Dominique Aunis, Marie-Hélène Metz-Boutigue, and Burkhard Bechinger. **Enhanced Membrane Disruption and Antibiotic Action against Pathogenic Bacteria by Designed Histidine-Rich Peptides at Acidic pH**. *Antimicrobial Agents and Chemotherapy*, **50**(10):3305–3311, January 2006.

[23] Saliha Majdoul, Ababacar K. Seye, Antoine Kichler, Nathalie Holic, Anne Galy, Burkhard Bechinger, and David Fenard. **Molecular Determinants of Vectofusin-1 and Its Derivatives for the Enhancement of Lentivirally Mediated Gene Transfer into Hematopoietic Stem/Progenitor Cells**. *The Journal of Biological Chemistry*, **291**(5):2161–2169, January 2016.

[24] A. James Mason, Wardi Moussaoui, Tamer Abdelrahman, Alyae Boukhari, Philippe Bertani, Arnaud Marquette, Peiman Shooshtarizaheh, Gilles Moulay, Nelly Boehm, Bernard Guerold, Ruairidh J. H. Sawers, Antoine Kichler, Marie-Hélène Metz-Boutigue, Ermanno Candolfi, Gilles Prévost, and Burkhard Bechinger. **Structural Determinants of Antimicrobial and Antiplasmodial Activity and Selectivity in Histidine-rich Amphipathic Cationic Peptides**. *Journal of Biological Chemistry*, **284**(1):119–133, February 2009.

[25] A. James Mason, Christian Leborgne, Gilles Moulay, Amélie Martinez, Olivier Danos, Burkhard Bechinger, and Antoine Kichler. **Optimising histidine rich peptides for efficient DNA delivery in the presence of serum**. *Journal of Controlled Release*, **118**(1):95–104, March 2007.

[26] Bérangère Langlet-Bertin, Christian Leborgne, Daniel Scherman, Burkhard Bechinger, A. James Mason, and Antoine Kichler. **Design and Evaluation of Histidine-Rich Amphipathic Peptides for siRNA Delivery**. *Pharmaceutical Research*, **27**(7):1426–1436, July 2010.

[27] Gilles Moulay, Christian Leborgne, A. James Mason, Christopher Aisenbrey, Antoine Kichler, and Burkhard Bechinger. **Histidine-rich designer peptides of the LAH4 family promote cell delivery of a multitude of cargo**. *Journal of Peptide Science: An Official Publication of the European Peptide Society*, **23**(4):320–328, April 2017.

[28] Yingying Xu, Wanling Liang, Yingshan Qiu, Marco Cespi, Giovanni F. Palmieri, A. James Mason, and Jenny K. W. Lam. **Incorporation of a Nuclear Localization Signal in pH Responsive LAH4-L1 Peptide Enhances Transfection and Nuclear Uptake of Plasmid DNA**. *Molecular Pharmaceutics*, **13**(9):3141–3152, September 2016.

[29] David Fenard, Sandrine Genries, Daniel Scherman, Anne Galy, Samia Martin, and Antoine Kichler. **Infectivity enhancement of different HIV-1-based lentiviral pseudotypes in presence of the cationic amphipathic peptide LAH4-L1**. *Journal of Virological Methods*, **189**(2):375–378, May 2013.

[30] David Fenard, Dina Ingrao, Ababacar Seye, Julien Buisset, Sandrine Genries, Samia Martin, Antoine Kichler, and Anne Galy. **Vectofusin-1, a New Viral Entry Enhancer, Strongly Promotes Lentiviral Transduction of Human Hematopoietic Stem Cells**. *Molecular Therapy-Nucleic Acids*, **2**:e90, May 2013. WOS:000332463700001.

[31] Yarong Liu, Young Joo Kim, Man Ji, Jinxu Fang, Natnaree Siriwon, Li I. Zhang, and Pin Wang. **Enhancing gene delivery of adeno-associated viruses by cell-permeable peptides**. *Molecular Therapy. Methods & Clinical Development*, **1**:12, 2014.

[32] Louic S. Vermeer, Loic Hamon, Alicia Schirer, Michel Schoup, Jérémie Cosette, Saliha Majdoul, David Pastré, Daniel Stockholm, Nathalie Holic, Petra Hellwig, Anne Galy, David Fenard, and Burkhard Bechinger. **Vectofusin-1, a potent peptidic enhancer of viral gene transfer forms pH-dependent α-helical nanofibrils, concentrating viral particles**. *Acta Biomaterialia*, **64**:259–268, December 2017.

[33] Beverly L. Davidson and Xandra O. Breakefield. **Viral vectors for gene delivery to the nervous system**. *Nature Reviews Neuroscience*, **4**(5):353–364, May 2003.

[34] Carl Martin Gotthardt. **Entwicklung und Charakterisierung von LAH4-L1-Peptid-Protamin-siRNA-Partikeln zum siRNA-Transport**, 2017.

[35] Nan Liu, Burkhard Bechinger, and Regine Süss. **The histidine-rich peptide LAH4-L1 strongly promotes PAMAM-mediated transfection at low nitrogen to phosphorus ratios in the presence of serum**. *Scientific Reports*, **7**(1):9585, August 2017.

[36] Christoph Meier, Tanja Weil, Frank Kirchhoff, and Jan Münch. **Peptide nanofibrils as enhancers of retroviral gene transfer**. *Wiley Interdisciplinary Reviews: Nanomedicine and Nanobiotechnology*, **6**(5):438–451, September 2014.

[37] Xibo Tian, Fude Sun, Xi-Rui Zhou, Shi-Zhong Luo, and Long Chen. **Role of peptide self-assembly in antimicrobial peptides**. *Journal of Peptide Science*, **21**(7):530–539, July 2015. WOS:000356813900003.

[38] Justine Wolf, Christopher Aisenbrey, Nicole Harmouche, Jesus Raya, Philippe Bertani, Natalia Voievoda, Regine Süss, and Burkhard Bechinger. **pH-Dependent Membrane Interactions of the Histidine-Rich Cell-Penetrating Peptide LAH4-L1**. *Biophysical Journal*, **113**(6):1290–1300, September 2017.

[39] Stefania Galdiero, Annarita Falanga, Marco Cantisani, Mariateresa Vitiello, Giancarlo Morelli, and Massimiliano Galdiero. **Peptide-Lipid Interactions: Experiments and Applications**. *International Journal of Molecular Sciences*, **14**(9):18758–18789, September 2013.

[40] Puthusserickal A. Hassan, Suman Rana, and Gunjan Verma. **Making Sense of Brownian Motion: Colloid Characterization by Dynamic Light Scattering**. *Langmuir*, **31**(1):3–12, January 2015.

[41] J M Beechem and L Brand. **Time-Resolved Fluorescence of Proteins**. *Annual Review of Biochemistry*, **54**(1):43–71, June 1985.

[42] ALEXANDER P. DEMCHENKO, YVES MÉLY, GUY DU-PORTAIL, AND ANDREY S. KLYMCHENKO. **Monitoring Biophysical Properties of Lipid Membranes by Environment-Sensitive Fluorescent Probes**. *Biophysical Journal*, **96**(9):3461–3470, May 2009.

[43] ANDREA HAWE, MARC SUTTER, AND WIM JISKOOT. **Extrinsic Fluorescent Dyes as Tools for Protein Characterization**. *Pharmaceutical Research*, **25**(7):1487–1499, July 2008.

[44] JOHN H. COOPER. **An evaluation of current methods for the diagnostic histochemistry of amyloid**. *Journal of clinical pathology*, **22**(4):410–413, 1969.

[45] SHARON M. KELLY, THOMAS J. JESS, AND NICHOLAS C. PRICE. **How to study proteins by circular dichroism**. *Biochimica et Biophysica Acta (BBA) - Proteins and Proteomics*, **1751**(2):119–139, August 2005.

[46] A. J. MILES AND B. A. WALLACE. **Circular dichroism spectroscopy of membrane proteins**. *Chemical Society Reviews*, **45**(18):4859–4872, 2016.

[47] LEE WHITMORE AND B. A. WALLACE. **Protein secondary structure analyses from circular dichroism spectroscopy: Methods and reference databases**. *Biopolymers*, **89**(5):392–400, May 2008.

[48] PHINEUS R. L. MARKWICK, THÉRÈSE MALLIAVIN, AND MICHAEL NILGES. **Structural Biology by NMR: Structure, Dynamics, and Interactions**. *PLoS Computational Biology*, **4**(9):e1000168, September 2008.

[49] JOHN CAVANAGH, WAYNE J. FAIRBROTHER, ARTHUR G. PALMER III, NICHOLAS J. SKELTON, AND MARK RANCE. *Protein NMR Spectroscopy: Principles and Practice*. Elsevier, July 2010. Google-Books-ID: h6DNSh02LJcC.

[50] RAFFAELLO VERARDI, NATHANIEL J. TRAASETH, LARRY R. MASTERSON, VITALY V. VOSTRIKOV, AND GIANLUIGI VEGLIA. **Isotope Labeling for Solution and Solid-State NMR Spectroscopy of Membrane Proteins**. In HANUDATTA S. ATREYA, editor, *Isotope labeling in Biomolecular NMR*, **992**, pages 35–62. Springer Netherlands, Dordrecht, 2012.

[51] ERIK STRANDBERG AND ANNE S. ULRICH. **NMR methods for studying membrane-active antimicrobial peptides**. *Concepts in Magnetic Resonance Part A*, **23A**(2):89–120, November 2004.

[52] BURKHARD BECHINGER, RUDOLF KINDER, MICHAEL HELMLE, TITUS C. B. VOGT, ULRIKE HARZER, AND SUSAN SCHINZEL. **Peptide structural analysis by solid-state NMR spectroscopy**. *Peptide Science*, **51**(3):174–190, January 1999.

[53] STEVEN P. BROWN AND HANS WOLFGANG SPIESS. **Advanced Solid-State NMR Methods for the Elucidation of Structure and Dynamics of Molecular, Macromolecular, and Supramolecular Systems**. *Chemical Reviews*, **101**(12):4125–4156, December 2001.

[54] TATYANA POLENOVA, RUPAL GUPTA, AND AMIR GOLD-BOURT. **Magic Angle Spinning NMR Spectroscopy: A Versatile Technique for Structural and Dynamic Analysis of Solid-Phase Systems**. *Analytical chemistry*, **87**(11):5458–5469, June 2015.

[55] ALEXANDRE A. ARNOLD AND ISABELLE MARCOTTE. **Studying natural structural protein fibers by solid-state nuclear magnetic resonance**. *Concepts in Magnetic Resonance Part A*, **34A**(1):24–47, January 2009.

[56] PIETER R. CULLIS AND MICHAEL J. HOPE. **Chapter 1 Physical properties and functional roles of lipids in membranes**. In DENNIS E. VANCE AND JEAN E. VANCE, editors, *New Comprehensive Biochemistry*, **20** of *New Comprehensive Biochemistry*, pages 1–41. Elsevier, January 1991.

[57] ÜNAL COSKUN AND KAI SIMONS. **Cell Membranes: The Lipid Perspective**. *Structure*, **19**(11):1543–1548, November 2011.

[58] KRZYSZTOF MURZYN, TOMASZ RÓG, AND MARTA PASENKIEWICZ-GIERULA. **Phosphatidylethanolamine-Phosphatidylglycerol Bilayer as a Model of the Inner Bacterial Membrane**. *Biophysical Journal*, **88**(2):1091–1103, February 2005.

[59] W. RAWICZ, K.C. OLBRICH, T. MCINTOSH, D. NEEDHAM, AND E. EVANS. **Effect of Chain Length and Unsaturation on Elasticity of Lipid Bilayers**. *Biophysical Journal*, **79**(1):328–339, July 2000.

[60] IMAD YOUNUS HASAN AND ADAM MECHLER. **Analytical approaches to study domain formation in biomimetic membranes**. *Analyst*, **142**(17):3062–3078, 2017.

[61] D. A. KALLICK, M. R. TESSMER, C. R. WATTS, AND C. Y. LI. **The Use of Dodecylphosphocholine Micelles in Solution NMR**. *Journal of Magnetic Resonance, Series B*, **109**(1):60–65, October 1995.

[62] LUKAS FREY, NILS-ALEXANDER LAKOMEK, ROLAND RIEK, AND STEFAN BIBOW. **Micelles, Bicelles, and Nanodiscs: Comparing the Impact of Membrane Mimetics on Membrane Protein Backbone Dynamics**. *Angewandte Chemie International Edition*, **56**(1):380–383, 2017.

[63] ALEKSANDER CZOGALLA, MICHAL GRZYBEK, WALIS JONES, AND ÜNAL COSKUN. **Validity and applicability of membrane model systems for studying interactions of peripheral membrane proteins with lipids**. *Biochimica et Biophysica Acta (BBA) - Molecular and Cell Biology of Lipids*, **1841**(8):1049–1059, August 2014.

[64] PHILIP L. YEAGLE. **Phosphorus NMR of Membranes**. In LAWRENCE J. BERLINER AND JACQUES REUBEN, editors, *Biological Magnetic Resonance*, number 9 in Biological Magnetic Resonance, pages 1–54. Springer US, 1990.

[65] DROR E. WARSCHAWSKI, ALEXANDRE A. ARNOLD, MAÏWENN BEAUGRAND, ANDRÉE GRAVEL, ÉTIENNE CHARTRAND, AND ISABELLE MARCOTTE. **Choosing membrane mimetics for NMR structural studies of transmembrane proteins**. *Biochimica et Biophysica Acta (BBA) - Biomembranes*, **1808**(8):1957–1974, August 2011.

REFERENCES

[66] B Bechinger and S. J Opella. **Flat-coil probe for NMR spectroscopy of oriented membrane samples**. *Journal of Magnetic Resonance (1969)*, **95**(3):585–588, December 1991.

[67] Mark Rance and R. Andrew Byrd. **Obtaining high-fidelity spin-12 powder spectra in anisotropic media: Phase-cycled Hahn echo spectroscopy**. *Journal of Magnetic Resonance (1969)*, **52**(2):221–240, April 1983.

[68] Joachim Seelig. **31P nuclear magnetic resonance and the head group structure of phospholipids in membranes**. *Biochimica et Biophysica Acta (BBA) - Reviews on Biomembranes*, **515**(2):105–140, July 1978.

[69] Michèle Auger. **Structural and Dynamics Studies of Lipids by Solid State NMR**. In *eMagRes*. American Cancer Society, December 2009.

[70] D. L. Worcester. **Structural origins of diamagnetic anisotropy in proteins**. *Proceedings of the National Academy of Sciences*, **75**(11):5475–5477, November 1978.

[71] Cécile Loudet, Anna Diller, Axelle Grélard, Reiko Oda, and Erick J. Dufourc. **Biphenyl phosphatidylcholine: A promoter of liposome deformation and bicelle collective orientation by magnetic fields**. *Progress in Lipid Research*, **49**(3):289–297, July 2010.

[72] Ulrich H.N. Dürr, Ronald Soong, and Ayyalusamy Ramamoorthy. **When detergent meets bilayer: Birth and coming of age of lipid bicelles**. *Progress in nuclear magnetic resonance spectroscopy*, **69**:1–22, February 2013.

[73] F Picard, M J Paquet, J Levesque, A Bélanger, and M Auger. **31P NMR first spectral moment study of the partial magnetic orientation of phospholipid membranes**. *Biophysical Journal*, **77**(2):888–902, August 1999.

[74] Evgeniy S. Salnikov, A. James Mason, and Burkhard Bechinger. **Membrane order perturbation in the presence of antimicrobial peptides by 2H solid-state NMR spectroscopy**. *Biochimie*, **91**(6):734–743, June 2009.

[75] J. H. Davis, K. R. Jeffrey, M. Bloom, M. I. Valic, and T. P. Higgs. **Quadrupolar echo deuteron magnetic resonance spectroscopy in ordered hydrocarbon chains**. *Chemical Physics Letters*, **42**(2):390–394, September 1976.

[76] Burkhard Bechinger and Evgeniy S. Salnikov. **The membrane interactions of antimicrobial peptides revealed by solid-state NMR spectroscopy**. *Chemistry and Physics of Lipids*, **165**(3):282–301, April 2012.

[77] James H. Davis. **The description of membrane lipid conformation, order and dynamics by 2H-NMR**. *Biochimica et Biophysica Acta (BBA) - Reviews on Biomembranes*, **737**(1):117–171, March 1983.

[78] Christopher Aisenbrey, Matthias Michalek, Evgeniy S. Salnikov, and Burkhard Bechinger. **Solid-State NMR Approaches to Study Protein Structure and ProteinâLipid Interactions**. In Jörg H. Kleinschmidt, editor, *Lipid-Protein Interactions*, **974**, pages 357–387. Humana Press, Totowa, NJ, 2013.

[79] Burkhard Bechinger and Christina Sizun. **Alignment and structural analysis of membrane polypeptides by15N and31P solid-state NMR spectroscopy**. *Concepts in Magnetic Resonance*, **18A**(2):130–145, July 2003.

[80] Aimee L. Boyle and Derek N. Woolfson. **De novo designed peptides for biological applications**. *Chemical Society Reviews*, **40**(8):4295, 2011.

[81] R Fairman and K Akerfeldt. **Peptides as novel smart materials**. *Current Opinion in Structural Biology*, **15**(4):453–463, August 2005.

[82] Claudia Piovan, Virna Marin, Cinzia Scavullo, Stefano Corna, Erica Giuliani, Sergio Bossi, Anne Galy, David Fenard, Claudio Bordignon, Gian Paolo Rizzardi, and Chiara Bovolenta. **Vectofusin-1 Promotes RD114-TR-Pseudotyped Lentiviral Vector Transduction of Human HSPCs and T Lymphocytes**. *Molecular Therapy - Methods & Clinical Development*, **5**:22–30, June 2017.

[83] Derek N. Woolfson. **The design of coiled-coil structures and assemblies**. *Advances in protein chemistry*, **70**:79–112, 2005.

[84] David W. H. Frost, Christopher M. Yip, and Avijit Chakrabartty. **Reversible assembly of helical filaments by de novo designed minimalist peptides**. *Biopolymers*, **80**(1):26–33, 2005.

[85] A. Pines, M. G. Gibby, and J. S. Waugh. **Proton-enhanced NMR of dilute spins in solids**. *The Journal of Chemical Physics*, **59**(2):569–590, July 1973.

[86] K. Takegoshi, Shinji Nakamura, and Takehiko Terao. **13C-1H dipolar-assisted rotational resonance in magic-angle spinning NMR**. *Chemical Physics Letters*, **344**(5):631–637, August 2001.

[87] Stephen P. Edgcomb and Kenneth P. Murphy. **Variability in the pKa of histidine side-chains correlates with burial within proteins**. *Proteins: Structure, Function, and Genetics*, **49**(1):1–6, October 2002.

[88] Qingbin Meng, Yingying Kou, Xin Ma, Yuanjun Liang, Lei Guo, Caihua Ni, and Keliang Liu. **Tunable Self-Assembled Peptide Amphiphile Nanostructures**. *Langmuir*, **28**(11):5017–5022, March 2012.

[89] Eleanor F. Banwell, Edgardo S. Abelardo, Dave J. Adams, Martin A. Birchall, Adam Corrigan, Athene M. Donald, Mark Kirkland, Louise C. Serpell, Michael F. Butler, and Derek N. Woolfson. **Rational design and application of responsive α-helical peptide hydrogels**. *Nature Materials*, **8**(7):596–600, July 2009.

[90] Efrosini Moutevelis and Derek N. Woolfson. **A Periodic Table of Coiled-Coil Protein Structures**. *Journal of Molecular Biology*, **385**(3):726–732, January 2009.

[91] S. P. Radko, S. A. Khmeleva, E. V. Suprun, S. A. Kozin, N. V. Bodoev, A. A. Makarov, A. I. Archakov, and V. V. Shumyantseva. **Physico-chemical methods for studying amyloid-β aggregation**. *Biochemistry (Moscow) Supplement Series B: Biomedical Chemistry*, **9**(3):258–274, July 2015.

[92] MINNA GROENNING. **Binding mode of Thioflavin T and other molecular probes in the context of amyloid fibrils-current status**. *Journal of Chemical Biology*, **3**(1):1–18, August 2009.

[93] NADINE D. YOUNAN AND JOHN H. VILES. **A Comparison of Three Fluorophores for the Detection of Amyloid Fibers and Prefibrillar Oligomeric Assemblies. ThT (Thioflavin T); ANS (1-Anilinonaphthalene-8-sulfonic Acid); and bisANS (4,4'-Dianilino-1,1'-binaphthyl-5,5'-disulfonic Acid)**. *Biochemistry*, **54**(28):4297–4306, July 2015.

[94] FIONA T. S. CHAN, GABRIELE S. KAMINSKI SCHIERLE, JANET R. KUMITA, CARLOS W. BERTONCINI, CHRISTOPHER M. DOBSON, AND CLEMENS F. KAMINSKI. **Protein amyloids develop an intrinsic fluorescence signature during aggregation**. *The Analyst*, **138**(7):2156, 2013.

[95] DOROTHEA PINOTSI, LUCA GRISANTI, PIERRE MAHOU, RALPH GEBAUER, CLEMENS F. KAMINSKI, ALI HASSANALI, AND GABRIELE S. KAMINSKI SCHIERLE. **Proton Transfer and Structure-Specific Fluorescence in Hydrogen Bond-Rich Protein Structures**. *Journal of the American Chemical Society*, **138**(9):3046–3057, March 2016.

[96] A. SHUKLA, S. MUKHERJEE, S. SHARMA, V. AGRAWAL, K. V. R. KISHAN, AND P. GUPTASARMA. **A novel UV laser-induced visible blue radiation from protein crystals and aggregates: scattering artifacts or fluorescence transitions of peptide electrons delocalized through hydrogen bonding?** *Archives of Biochemistry and Biophysics*, **428**(2):144–153, August 2004. WOS:000222832200004.

[97] DOROTHEA PINOTSI, ALEXANDER K. BUELL, CHRISTOPHER M. DOBSON, GABRIELE S. KAMINSKI SCHIERLE, AND CLEMENS F. KAMINSKI. **A Label-Free, Quantitative Assay of Amyloid Fibril Growth Based on Intrinsic Fluorescence**. *ChemBioChem*, **14**(7):846–850, May 2013.

[98] ROBERT TYCKO. **Physical and structural basis for polymorphism in amyloid fibrils: Amyloid Polymorphism**. *Protein Science*, **23**(11):1528–1539, November 2014.

[99] CHRISTOPHER AISENBREY AND BURKHARD BECHINGER. **Molecular Packing of Amphipathic Peptides on the Surface of Lipid Membranes**. *Langmuir*, **30**(34):10374–10383, September 2014.

[100] VERICA VIDOVIC, LYDIA PRONGIDI-FIX, BURKHARD BECHINGER, AND SEBASTIAAN WERTEN. **Production and isotope labeling of antimicrobial peptides in Escherichia coli by means of a novel fusion partner that enables high-yield insoluble expression and fast purification**. *Journal of Peptide Science: An Official Publication of the European Peptide Society*, **15**(4):278–284, April 2009.

[101] YIFENG LI. **Carrier proteins for fusion expression of antimicrobial peptides in Escherichia coli**. *Biotechnology and Applied Biochemistry*, **54**(1):1–9, July 2009.

[102] HERMANN SCHÄGGER. **Tricine-SDS-PAGE**. *Nature Protocols*, **1**(1):16–22, June 2006.

[103] EWA IZABELA PODOBAS, ARKADIUSZ BONNA, AGNIESZKA POLKOWSKA-NOWAKOWSKA, AND WOJCIECH BAL. **Dual catalytic role of the metal ion in nickel-assisted peptide bond hydrolysis**. *Journal of Inorganic Biochemistry*, **136**:107–114, July 2014.

[104] NICOLE J. YANG AND MARLON J. HINNER. **Getting Across the Cell Membrane: An Overview for Small Molecules, Peptides, and Proteins**. In ARNAUD GAUTIER AND MARLON J. HINNER, editors, *Site-Specific Protein Labeling*, **1266**, pages 29–53. Springer New York, New York, NY, 2015.

[105] GIULIA GUIDOTTI, LILIANA BRAMBILLA, AND DANIELA ROSSI. **Cell-Penetrating Peptides: From Basic Research to Clinics**. *Trends in Pharmacological Sciences*, **38**(4):406–424, April 2017.

[106] SÓNIA Â TROEIRA HENRIQUES, MANUEL Â NUNO MELO, AND MIGUEL Â A. Â R. Â B. CASTANHO. **Cell-penetrating peptides and antimicrobial peptides: how different are they?** *Biochemical Journal*, **399**(1):1–7, October 2006.

[107] ALFREDO ERAZO-OLIVERAS, NANDHINI MUTHUKRISHNAN, RYAN BAKER, TING-YI WANG, AND JEAN-PHILIPPE PELLOIS. **Improving the Endosomal Escape of Cell-Penetrating Peptides and Their Cargos: Strategies and Challenges**. *Pharmaceuticals*, **5**(11):1177–1209, November 2012.

[108] DAVID ESCORS AND KARINE BRECKPOT. **Lentiviral Vectors in Gene Therapy: Their Current Status and Future Potential**. *Archivum Immunologiae et Therapiae Experimentalis*, **58**(2):107–119, April 2010.

[109] JATTA HUOTARI AND ARI HELENIUS. **Endosome maturation**. *The EMBO Journal*, **30**(17):3481–3500, August 2011.

[110] GERRIT VAN MEER, DENNIS R. VOELKER, AND GERALD W. FEIGENSON. **Membrane lipids: where they are and how they behave**. *Nature Reviews Molecular Cell Biology*, **9**(2):112–124, February 2008.

[111] MATIN ISLAMI, FARAMARZ MEHRNEJAD, FARAHNOOSH DOUSTDAR, MASUMEH ALIMOHAMMADI, MAHMOUD KHADEM-MAAREF, MOHAMMAD MIR-DERIKVAND, AND MAJID TAGHDIR. **Study of Orientation and Penetration of LAH4 into Lipid Bilayer Membranes: pH and Composition Dependence**. *Chemical Biology & Drug Design*, **84**(2):242–252, August 2014.

[112] NATALIIA VOIEVODA, THERESE SCHULTHESS, BURKHARD BECHINGER, AND JOACHIM SEELIG. **Thermodynamic and Biophysical Analysis of the Membrane-Association of a Histidine-Rich Peptide with Efficient Antimicrobial and Transfection Activities**. *The Journal of Physical Chemistry. B*, **119**(30):9678–9687, July 2015.

[113] CHRISTOPHER AISENBREY AND BURKHARD BECHINGER. **Tilt and Rotational Pitch Angle of Membrane-Inserted Polypeptides from Combined ^{15}N and ^{2}H Solid-State NMR Spectroscopy**. *Biochemistry*, **43**(32):10502–10512, August 2004.

[114] PHILIPPE BERTANI, JÉSUS RAYA, AND BURKHARD BECHINGER. **15N chemical shift referencing in solid state NMR**. *Solid State Nuclear Magnetic Resonance*, **61â62**:15–18, July 2014.

REFERENCES

[115] Jésus Raya, Barbara Perrone, and Jérôme Hirschinger. **Chemical shift powder spectra enhanced by multiple-contact cross-polarization under slow magic-angle spinning.** *Journal of Magnetic Resonance*, **227**:93–102, February 2013.

[116] E. G. Bligh and W. J. Dyer. **A Rapid Method of Total Lipid Extraction and Purification.** *Canadian Journal of Biochemistry and Physiology*, **37**(8):911–917, August 1959.

[117] J. Seelig and A. Seelig. **Lipid conformation in model membranes and biological membranes.** *Quarterly Reviews of Biophysics*, **13**(1):19–61, February 1980.

[118] Peter G. Scherer and Joachim Seelig. **Electric charge effects on phospholipid headgroups. Phosphatidylcholine in mixtures with cationic and anionic amphiphiles.** *Biochemistry*, **28**(19):7720–7728, September 1989.

[119] Burkhard Bechinger. **Rationalizing the membrane interactions of cationic amphipathic antimicrobial peptides by their molecular shape.** *Current Opinion in Colloid & Interface Science*, **14**(5):349–355, October 2009.

[120] Burkhard Bechinger. **Detergent-like properties of magainin antibiotic peptides: A 31P solid-state NMR spectroscopy study.** *Biochimica et Biophysica Acta (BBA) - Biomembranes*, **1712**(1):101–108, June 2005.

[121] Piotr Jurkiewicz, Lukasz Cwiklik, Alzbeta Vojtíšková, Pavel Jungwirth, and Martin Hof. **Structure, dynamics, and hydration of POPC/POPS bilayers suspended in NaCl, KCl, and CsCl solutions.** *Biochimica et Biophysica Acta (BBA) - Biomembranes*, **1818**(3):609–616, March 2012.

[122] Gérard Raffard, Siegfried Steinbruckner, Alexandre Arnold, James H. Davis, and Erick J. Dufourc. **TemperatureâComposition Diagram of DimyristoylphosphatidylcholineâDicaproylphosphatidylcholine âBicellesâ Self-Orienting in the Magnetic Field. A Solid State ^{2} H and ^{31} P NMR Study.** *Langmuir*, **16**(20):7655–7662, October 2000.

[123] Erick J. Dufourc, Nicole Harmouche, Cécile Loudet-Courrèges, Reiko Oda, Anna Diller, Benoit Odaert, Axelle Grélard, and Sébastien Buchoux. **CHAPTER 6. Magnetic Liposomes and Bicelles: New Tools for Membrane-Peptide Structural Studies.** In Frances Separovic and Akira Naito, editors, *New Developments in NMR*, pages 98–112. Royal Society of Chemistry, Cambridge, 2014.

[124] Nataliia Voievoda. *Biophysical investigation of the membrane and nucleic acids interactions of the transfection peptide LAH4-L1 : molecular mechanisms of complex formation and cellular entry.* Strasbourg, June 2014.

[125] Ying Li, Aleksandra Z. Kijac, Stephen G. Sligar, and Chad M. Rienstra. **Structural Analysis of Nanoscale Self-Assembled Discoidal Lipid Bilayers by Solid-State NMR Spectroscopy.** *Biophysical Journal*, **91**(10):3819–3828, November 2006.

[126] E. S. Salnikov, G. M. Anantharamaiah, and B. Bechinger. **Supramolecular organization of apolipoprotein A-I - derived peptides within disc-like arrangements,** 2018.

[127] Michael O Eze. **Phase transitions in phospholipid bilayers: Lateral phase separations play vital roles in biomembranes.** *Biochemical Education*, **19**(4):204–208, October 1991.

[128] D L Melchior and J M Steim. **Thermotropic Transitions in Biomembranes.** *Annual Review of Biophysics and Bioengineering*, **5**(1):205–238, June 1976.

[129] T. Pott, J. Dufourcq, and E. J. Dufourc. **Fluid or gel phase lipid bilayers to study peptide-membrane interactions?** *European Biophysics Journal*, **25**(1):55–59, October 1996.

[130] Megumi Shintani and Nobuyuki Matubayasi. **Morphology study of DMPC/DHPC mixtures by solution-state 1H, 31P NMR, and NOE measurements.** *Journal of Molecular Liquids*, **217**:62–69, May 2016.

[131] David I. Fernandez, Marc-Antoine Sani, Andrew J. Miles, B.A. Wallace, and Frances Separovic. **Membrane defects enhance the interaction of antimicrobial peptides, aurein 1.2 versus caerin 1.1.** *Biochimica et Biophysica Acta (BBA) - Biomembranes*, **1828**(8):1863–1872, August 2013.

[132] Barbara Perrone, Andrew J. Miles, Evgeniy S. Salnikov, B. A. Wallace, and Burkhard Bechinger. **Lipid interactions of LAH4, a peptide with antimicrobial and nucleic acid transfection activities.** *European Biophysics Journal*, **43**(10-11):499–507, November 2014.

[133] Evgeniy S. Salnikov and Burkhard Bechinger. **Lipid-Controlled Peptide Topology and Interactions in Bilayers: Structural Insights into the Synergistic Enhancement of the Antimicrobial Activities of PGLa and Magainin 2.** *Biophysical Journal*, **100**(6):1473–1480, March 2011.

[134] Dirk Windisch, Colin Ziegler, Stephan L. Grage, Jochen Bürck, Marcel Zeitler, Peter L. Gor'kov, and Anne S. Ulrich. **Hydrophobic Mismatch Drives the Interaction of E5 with the Transmembrane Segment of PDGF Receptor.** *Biophysical Journal*, **109**(4):737–749, August 2015.

[135] Françoise Hullin-Matsuda, Kiyoshi Kawasaki, Isabelle Delton-Vandenbroucke, Yang Xu, Masahiro Nishijima, Michel Lagarde, Michael Schlame, and Toshihide Kobayashi. **De novo biosynthesis of the late endosome lipid, bis(monoacylglycero)phosphate.** *Journal of Lipid Research*, **48**(9):1997–2008, January 2007.

[136] T. E. Tjelle, A. Brech, L. K. Juvet, G. Griffiths, and T. Berg. **Isolation and characterization of early endosomes, late endosomes and terminal lysosomes: their role in protein degradation.** *Journal of Cell Science*, **109**(12):2905–2914, December 1996.

[137] Edith Sim. *Membrane Biochemistry.* Springer Netherlands, 1982.

[138] Bipasha Dey, Sameer Thukral, Shruti Krishnan, Mainak Chakrobarty, Sahil Gupta, Chanchal Manghani, and Vibha Rani. **DNA-protein interactions: methods for detection and analysis**. *Molecular and Cellular Biochemistry*, **365**(1-2):279–299, June 2012.

[139] M. Piotto, V. Saudek, and V. Sklenár. **Gradient-tailored excitation for single-quantum NMR spectroscopy of aqueous solutions**. *Journal of biomolecular NMR*, **2**(6):661–665, November 1992.

REFERENCES

Appendix A

Appendix

A.1 General Materials

Peptide synthesis:

The peptides LAH_4L_1 (KKALL AHALH LLALL ALHLA HALKK A-$CONH_2$; molecular mass 2778.48 Da); VF1 (KKALL HAALA HLLAL AHHLL ALLKK A-$CONH_2$; molecular mass 2778.48 Da) and [^{15}N-Leu_{15}]-[3,3,3,-$^2H_3$-Ala_{14}]-$h\Phi$19W (KKKAL LALLA LAWAL ALLAL LAKKK-$CONH_2$; molecular mass: 2673 Da) were prepared by standard Fmoc solid-phase peptide chemistry, using a Millipore 9050 automatic peptide synthesizer (Eschborn, Germany). For the LAH_4L_1, a batch was prepared where the ^{15}N-labeled Fmoc-leucine analog was used at the coupling step of the Leu-14 position. After cleavage from the resin, the peptide was purified by reverse-phase high performance liquid chromatography with an acetonitrile/water gradient of increasing hydrophobicity (in the presence of 0.1% trifluoroacetic acid). To exchange the trifluoroacetic acid counterions, the main peak was collected, resolubilized in 4% acetic acid, and lyophilized. The identity and purity of the peptide were controlled by MALDI-TOF mass spectrometry.
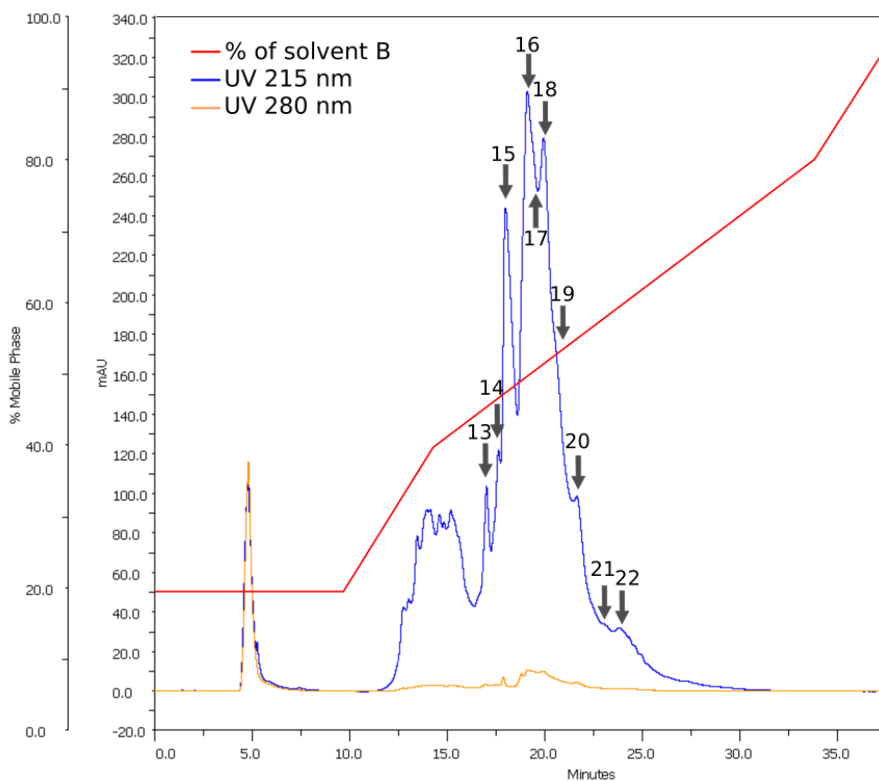
Lipids:

Phospholipids 1,2-dimyristoyl-sn-glycero-3-phosphocholine (DMPC), 1,2-dimyristoyl-d_{54}-sn-glycero-3-phosphocholine ($^2H_{54}$-DMPC), 1-palmitoyl-2-oleoyl-sn-glycero-3-phospho-L-serine (sodium salt) (POPS), 1-palmitoyl-d_{31}-2-oleoyl-sn-glycero-3-phospho-L-serine (sodium salt) ($^2H_{31}$-POPS), 1-palmitoyl-2-oleoyl-sn-glycero-3-phospho-(1'rac-glycerol) (sodium salt) (POPG), Sphingomyelin (Brain, Porcine) and Cholesterol (ovine wool, $> 98\%$) were from Avanti Polar Lipids (Alabaster,

AL) and 1-palmitoyl-2-oleoyl-*sn*-glycero-3-phosphocholine (POPC) was from Sigma-Aldrich (Lyon, France). They were used without further purification.

## A.2 Expression and purification of pVF1 peptide

Figure A.1: HPLC chromatogram of the TAF12-pVF1 cleavage product by reverse phase HPLC: Fractions and their corresponding numbers are indicated on the chromatogram.

A.3 Characterization of Peptide-Lipid Interactions
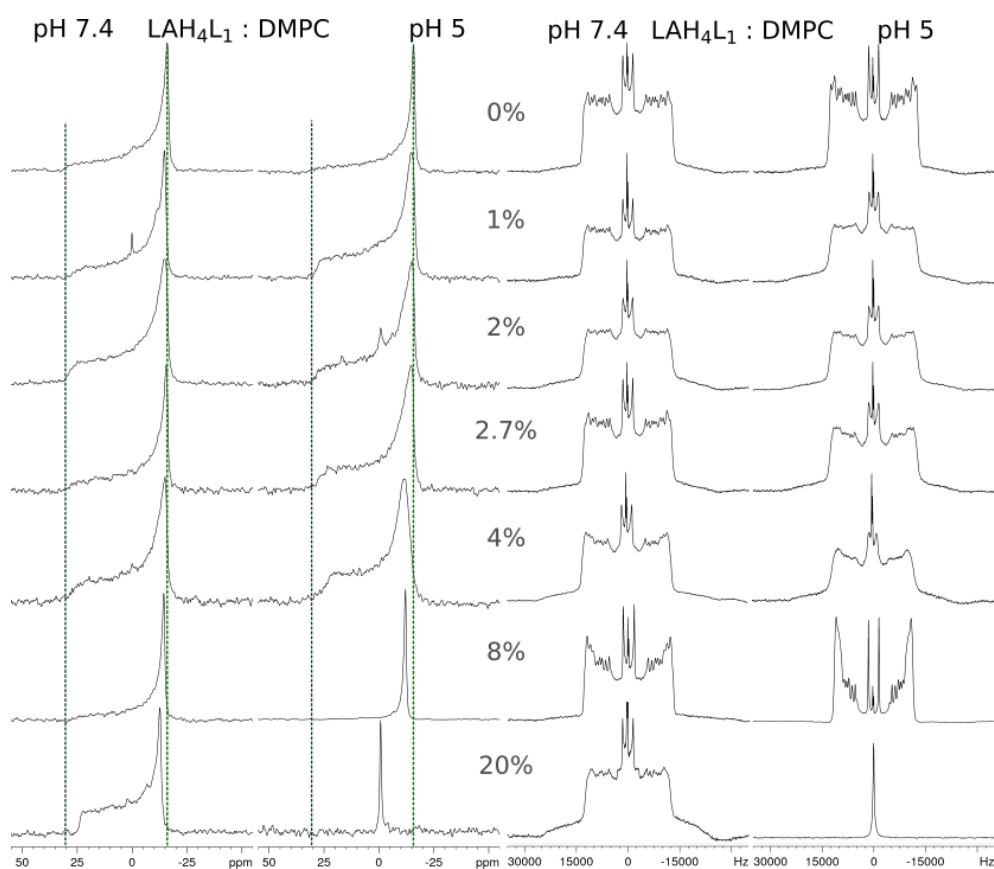
Figure A.2: Increased concentrations of LAH$_4$L$_1$ in MLVs of DMPC studied by ^{31}P and ^{2}H solid-state NMR: Samples were prepared at pH 7.4 (first and third column) and pH 5 (second and fourth column). All spectra were acquired at 37°C. The blue and green dash lines represent the $\delta_{//}$ and $\delta_\perp$ of the reference spectrum (0% P/L) respectively.
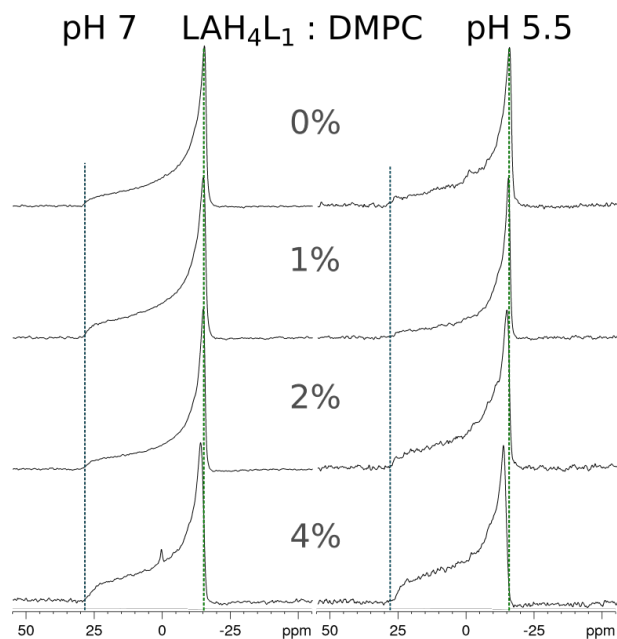
Figure A.3: Increased concentrations of LAH$_4$L$_1$ in MLVs of DMPC studied by ^{31}P solid-state NMR: Samples were prepared at pH 7 and pH 5.5. All spectra were acquired at 37°C. The blue and green dash lines represent the $\delta_{//}$ and $\delta_{\perp}$ of the reference spectrum (0% P/L) respectively.
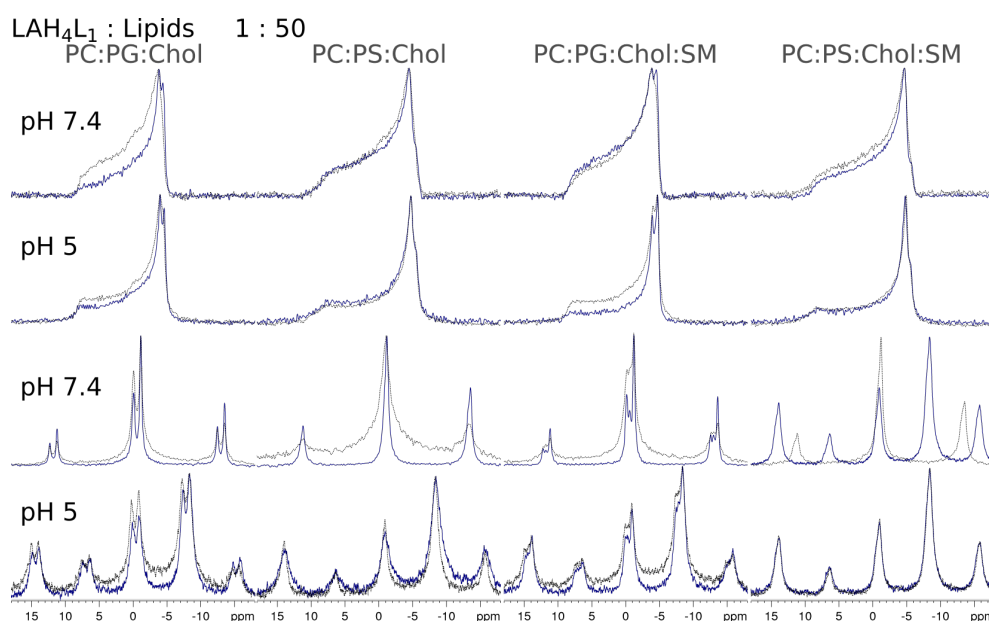

Figure A.4: ^{31}P static and slow MAS spectra (1.5 kHz spinning) of MLV of the different lipids mix at pH 7.4 and pH 5. All the spectra presented were acquired at 15°C. Spectra pH 7.4 except PC:PS:Chol:SM with peptides were acquired on a 300 MHz and all the other on a 500 MHz. The spectra in blue are with LAH4-L1 and the spectra in black dash line are the reference without peptide.

A.4 Characterization of Peptide-Nucleic Acid Interactions
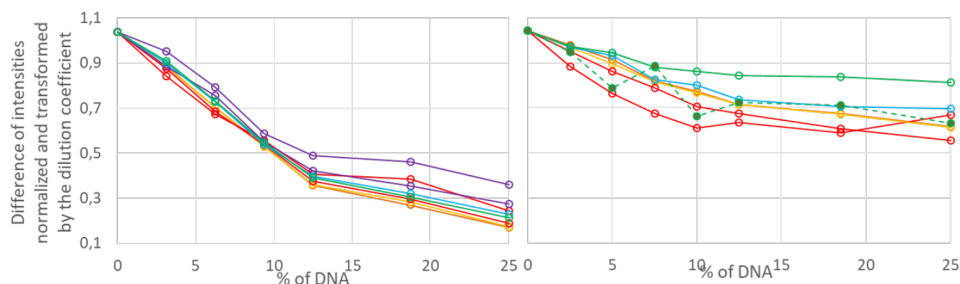
Figure A.5: Graphs representing the intensities of peptide following, the titration of DNA: the graph on the left corresponds to the acetate condition, when the graph on the right represents the result from the titration in presence of DPC. The colours correspond to the different regions of the 1D ^{1}H spectrum, presented in the materials section.
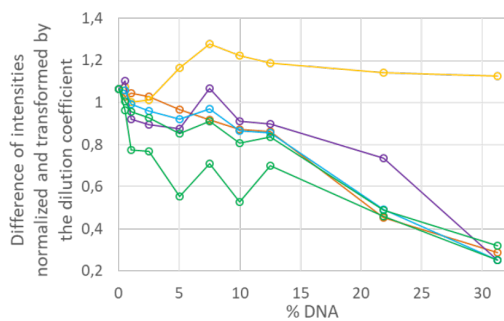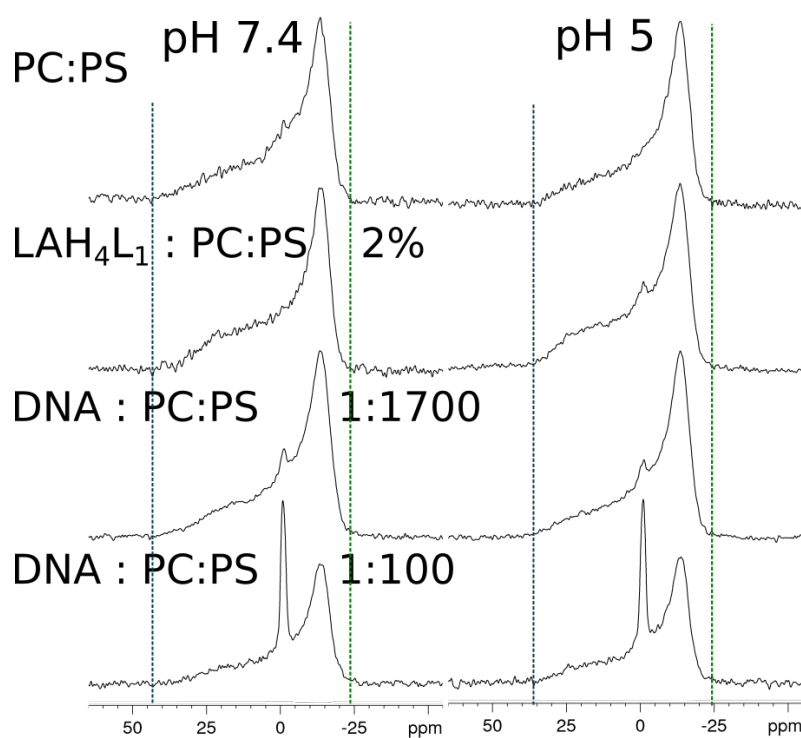

Figure A.6: Graph representing the intensities of peptide following the titration of DNA in TFE 50 %: The colours correspond to the different regions of the 1D ^{1}H spectrum, presented in the materials section.

.

Table A.1: Chemical shift changes, indicated by regions of the spectra. The values have to be multiplied by 10^{-3} and are indicated in ppm.

	Ala CH$_3$	Leu CH$_3$	$\beta\,\gamma$	α ^{1}H	Amide ^{1}H	His	His amide side	Lys side chains
Acetate	1	5		8	5	22	55	5
DPC	5	5		4	2	4	9	5
TFE 50%		25	11	14	36	8	12	36

Figure A.7: ^{31}P solid-state NMR spectra of DNA:LAH$_4$L$_1$: control samples were prepared at pH 7.4 and pH 5 with the different components of the complex: lipids alone or peptide and DNA with different ratio DNA:Lipids 1/1700 and 1/100. The blue and green dash lines represent the $\delta_{//}$ and $\delta_\perp$ of the reference spectrum (0% P/L) respectively. All spectra were acquired at 30°C.
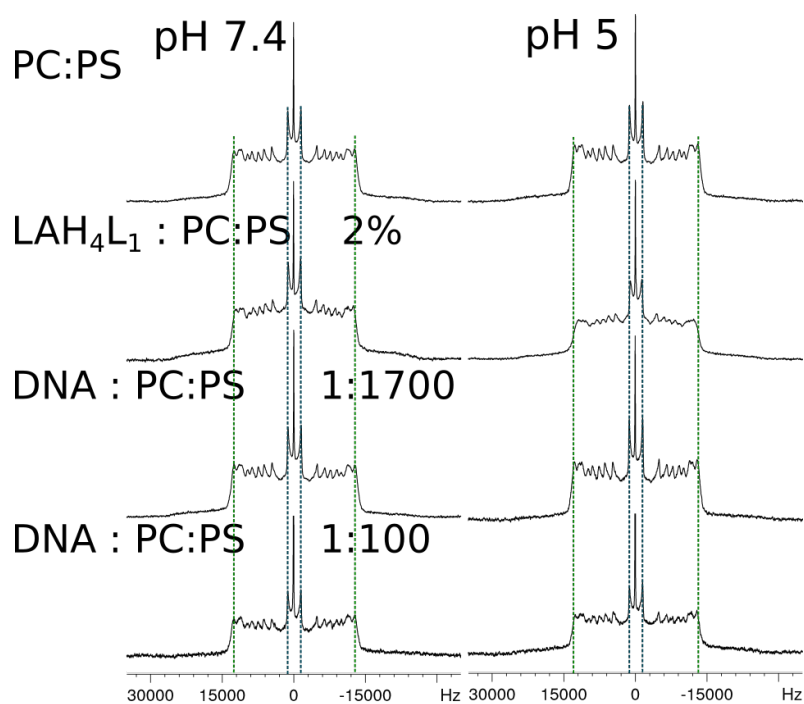
Figure A.8: ^{2}H solid-state NMR spectra of DNA:LAH$_4$L$_1$: control samples were prepared at pH 7.4 and pH 5 with the different components of the complex: lipids alone or peptide and DNA with different ratio DNA:Lipids 1/1700 and 1/100. The blue and green dash lines represent the smaller or bigger quadrupolar splitting of the reference spectrum (0% P/L) respectively. All spectra were acquired at 30°C.

A. APPENDIX

Résumé

1 Introduction

Le peptide LAH4 a dans un premier temps été synthétisé en tant que modèle pour étudier l'interaction peptide-membrane [1]. Le LAH4 est un peptide cationique, hydrophobe capable de se replier en hélice α amphiphile. Long de 26 acides aminés, le LAH4 comporte majoritairement des acides aminés hydrophobes, alanines et leucines, ainsi que deux lysines à chaque extrémité aidant à la solubilité du peptide et quatre histidines qui, lors du repliement du peptide en hélice α, se retrouvent sur la même face lui apportant son amphiphilité. Les histidines de ce peptide ont un état de protonation différent à pH neutre (pH 7) ou pH acide (pH 5), ce qui donne au peptide la capacité de changer son orientation vis-à-vis de la membrane dans une gamme physiologique, de manière dépendante du pH. En effet, à pH neutre les histidines étant déprotonés, le peptide est plus hydrophobe, lui permettant ainsi de s'insérer dans les membranes et d'adopter une orientation transmembranaire. Alors qu'à pH acide, quand les histidines sont protonés, celui-ci reste à la surface de la membrane. Cela a été mis en évidence par RMN du solide sur des bicouches orientées mécaniquement [1] ainsi que par FT-IR, qui a permis également de confirmer que ce basculement s'opère à un pH de 6,1 ±0,2 [2].

Dans un premier temps, l'activité antimicrobienne du LAH4 a été mise en évidence [3]. Puis, il a été utilisé pour aider et améliorer l'entrée d'ADN plasmidique capable de modifier l'expression d'un gène utile à une application thérapeutique [4]. Les peptides de la famille du LAH4 se sont montrés efficaces pour ce type d'activité avec de nombreux systèmes de modification des gènes - habituellement séparé en systèmes utilisant ou non des virus (transduction ou transfection) - tels que du siARN [5] ou des virus [6], et cela même dans des cellules connues pour être difficiles à transfecter [7]. Le LAH4 a également était utilisé avec des systèmes divers tel que des quantum dots [8] ou pour des vaccins [9].

Depuis la synthèse du LAH4, de nombreux dérivés ont été désignés mais certains
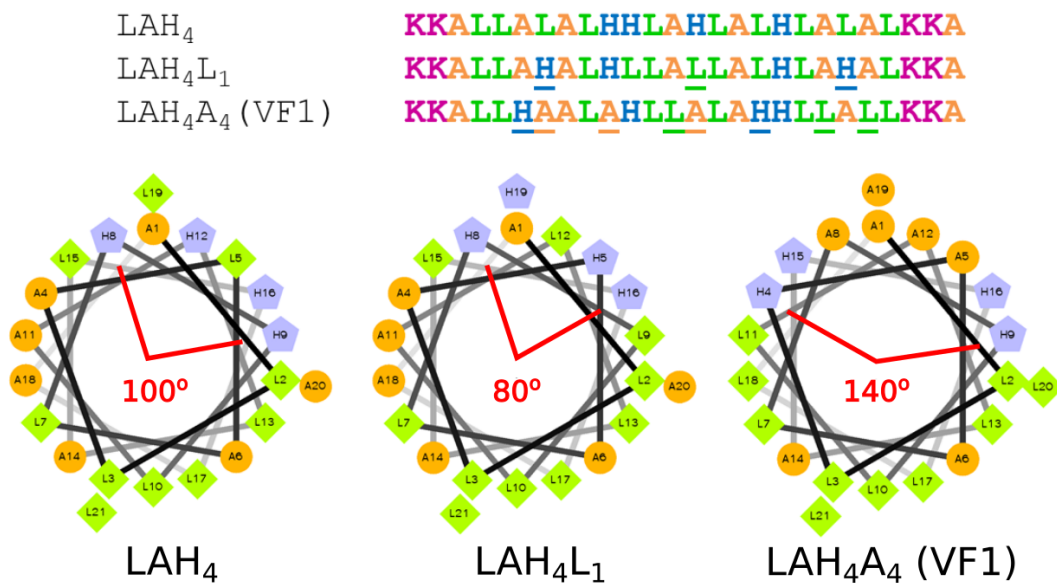
1

FIGURE 1 – Représentation en hélice des trois principaux peptides étudiés, le LAH4, LAH4L1 et la VF1. Les hélices ne comportent pas les lysines car elles ne sont généralement pas incluses dans la structure secondaire en hélice α. Les alanines sont représentées en orange, les leucines en vert et les histidines en bleu. (Représentation en hélices faite à partir de http ://rzlab.ucr.edu/scripts/wheel/wheel.cgi)

critères sont déterminants pour garder une activité biologique tels que : la longueur de 26 acides aminés, les 4 lysines aux extrémités (2 en N-terminal et 2 en C-terminal) [10]. Les 4 histidines positionnées sur la même face considérant le peptide en hélice α [11]. L'angle entre ces histidines, aussi appelé angle hydrophobe, peut varier de 60° à 140°. Deux peptides présentent une efficacité de transfection et transduction plus importante : le LAH4L1 et le LAH4A4 (VF1) (Figure 1).
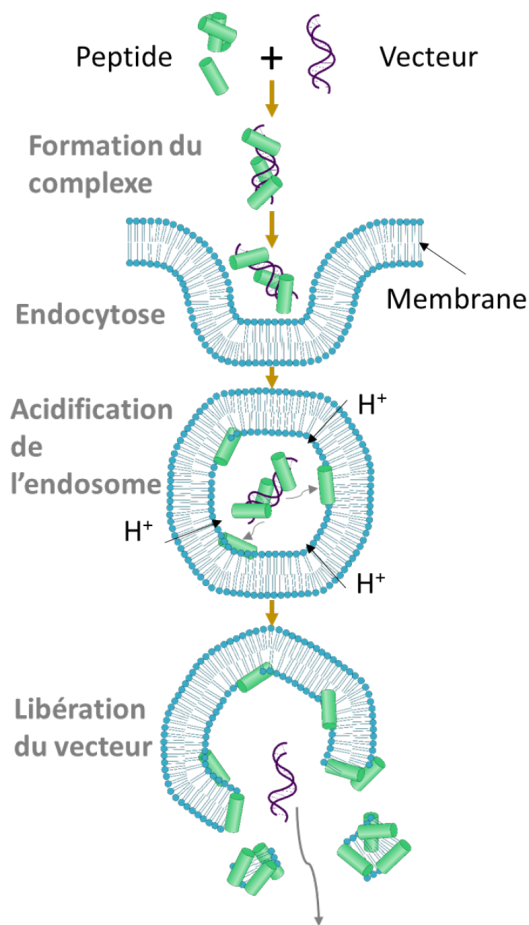
Dans ce manuscript, l'étude de peptides de la famille du LAH4 a été conduit avec en perspective le développement de transport de gènes. Avec les capacités de ces peptides à pénétrer dans les cellules (CPP, cell penetrating peptide), le LAH4, LAH4L1 and VF1 ont montrés leurs capacités à améliorer l'efficacité un grande variété de système de transport de gène. Néanmoins, d'un cargo à l'autre, les peptides ne présentent pas la même efficacité, rendant l'optimisation de ce genre de système complexe. En effet, les systèmes de transport de gènes sont capables de modifier l'expression de gènes avec efficacité, mais le facteur limitant est l'entrée dans la cellule. De ce fait, des molécules sont ajoutées au système, pour d'une part interagir avec

le cargo pour former un complexe avec celui-ci, puis permettre l'interaction avec la membrane de la cellule, et finalement échapper à l'endosome formé autour du complexe avant dégradation de celui-ci par le lysosome de la cellule. De ce fait, des connaissances plus approfondies concernant l'interaction des différents composants de ce genre de système pourrait permettre une amélioration et une optimisation plus facile.

L'étude s'est faite principalement sur le LAH4L1 étant très efficace pour la transfection de différents acides nucleiques (par exemple : DNA, siRNA). Et avec le LAH4A4 (VF1) qui a présenté de très bonne capacité pour aider à la transduction de virus (lentivirus). Habituellement divisé en deux catégories : transduction et transfection ; dans notre cas, le peptide étant principalement ajouté pour permettre la déstabilisation de la membrane, on différentiera deux mécanismes suivant le vecteur utilisé (Figure 2) : la libérateur du vecteur par destruction de la membrane pour les acides nucléiques et les virus non enveloppés (nus) et la libération par fusion membranaire pour les virus enveloppés.

Le travail de cette thèse est divisé en trois parties dans le but de caractériser de manière biophysique les différentes interactions ayant lieux lors de la livraison du système de transport de gènes à l'intérieur d'une cellule. L'interaction peptide-peptide : avec l'étude de l'agrégation en fibrilles de la Vectofusin-1 ; l'interaction peptide-membrane : avec le LAH4L1 et différents types de membranes ; et l'interaction peptide-ADN : avec le suivi de l'interaction entre le LAH4L1 et un ADN de peptide taille (15 mer).
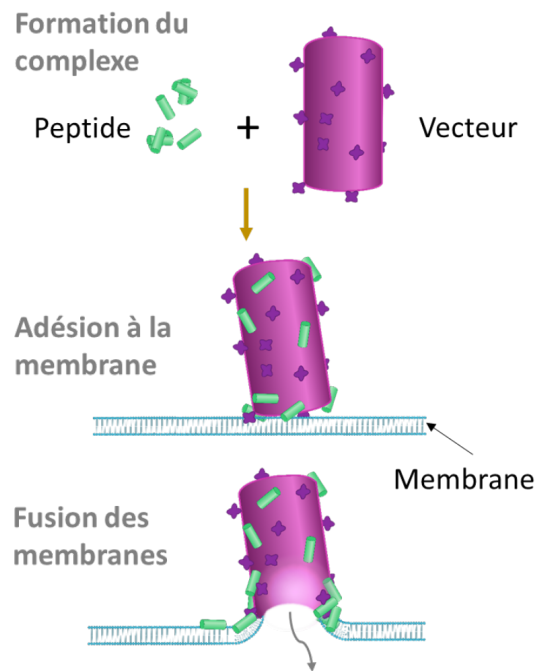
3

FIGURE 2 – Schématisation des mécanismes de transport de vecteurs avec les peptides de la famille du LAH4.

2 Résultats et discussions

2.1 Interaction peptide-peptide

L'auto-assemblage de peptide a été mis en évidence pour de nombreux peptides antimicrobiens, et cela pourrait être en lien avec l'activité et le mode d'action de ceux-ci [12]. Récemment, il a été mis en évidence que la VF1 était capable de s'auto-assembler en nano-fibrilles permettant ainsi d'améliorer l'efficacité de transduction d'un vecteur viral [13]. La formation de ces nano-fibrilles permettrait d'optimiser l'interaction cellules-virus par la concentration des particules virales, facilitée grâce à leur interaction avec les fibrilles. En comparaison avec les autres membres de la famille du LAH4, et ce malgré la similarité de séquence, la VF1 présente la meilleure efficacité d'amélioration de la transduction de ce virus [14]. C'est pour cela que l'étude structurale de ces fibrilles pourrait permettre de mieux comprendre d'une part le mécanisme de formation d'auto-assemblage de celle-ci mais également le lien entre structure et fonction.

Dans un milieu riche et à pH physiologique comme ceux utilisés en biologie cellulaire, la VF1 s'assemble en fibrilles comportant de multiples particules sphériques d'un diamètre aux alentours de 10 nm [13]. Néanmoins, ce type de milieux trop riches n'est pas compatible avec des analyses biophysiques. Aussi, la spontanéité de formation de ces fibrilles aboutit généralement à un assemblage hétérogène n'étant pas compatible avec des études structurales. Pour cela, les conditions de fibrillation du peptide ont dues être optimisées. L'agrégation des peptides de la famille du LAH4 dépend majoritairement du pH [15]. De ce fait, lors d'une augmentation trop rapide ou à un pH trop haut, il a été observé que la VF1 présentait de grosses particules agrégées et non des fibrilles comme attendues.

Par l'augmentation progressive du pH via dialyse et à un pH juste au-dessus du pKa des histidines, des fibrilles homogènes ont pu être obtenues. L'analyse de la qualité des échantillons a été faite par microscopie électronique à transmission (TEM). En effet, l'augmentation de la taille des particules a pu être attestée par diffusion dynamique de la lumière (DLS) ainsi que la structure secondaire en hélice α par dichroïsme circulaire (CD) mais cela ne permet pas de confirmer la formation
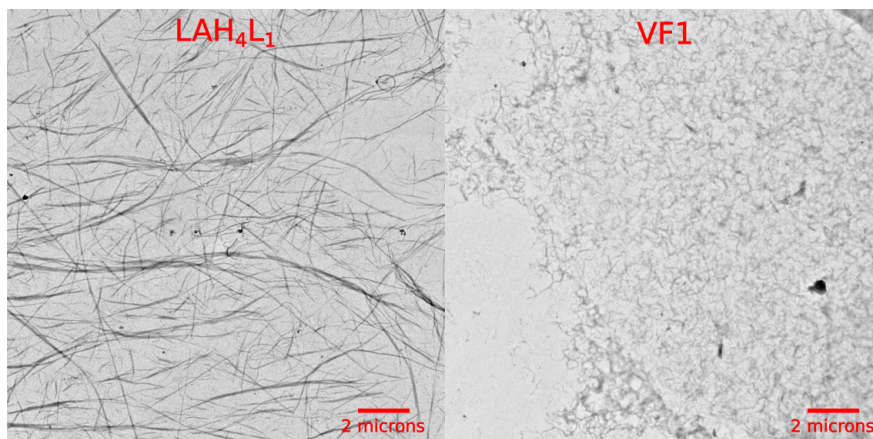
FIGURE 3 – Images de microscopie électronique à transmission de VF1 et LAH4L1 après application du même protocole de fibrillation.

de fibres. L'homogénéité structurale a été confirmée par RMN ^{13}C du solide avec l'observation de pics fins. Ce même protocole a été appliqué au peptide LAH4L1 aboutissant à l'observation de fibres allongées (Figure 3).

L'étude de la structure au niveau atomique de fibres devant être faite par RMN du solide, il est nécessaire d'enrichir le peptide en isotopes ^{13}C et/ou ^{15}N. Pour cela, l'expression et la purification en milieu bactérien de la pVF1 a été faite à partir du protocole mis au point pour la synthèse du pLAH4 [16]. Néanmoins, dû à la coélution du peptide et de la protéine de fusion (TAF12) nécessaire à son expression, des étapes supplémentaires de purification ont été ajoutées.

Des spectres 2D de corrélation ^{13}C-^{13}C de RMN du solide des fibrilles de pVF1 uniformément marqué ^{13}C-^{15}N ont été acquis (Figure 4). Par attribution des différents groupements des leucines et alanines, la structure en hélice α des fibrilles de pVF1 a pu être confirmé.

Cependant, du fait de la redondance d'acides aminés dans la séquence du peptide, les spectres n'ont pas pu être attribués. Toutefois, dans le but d'attribuer entièrement le peptide, différents peptides VF1 partiellement marqués seront synthétisés et analysés de la même manière.
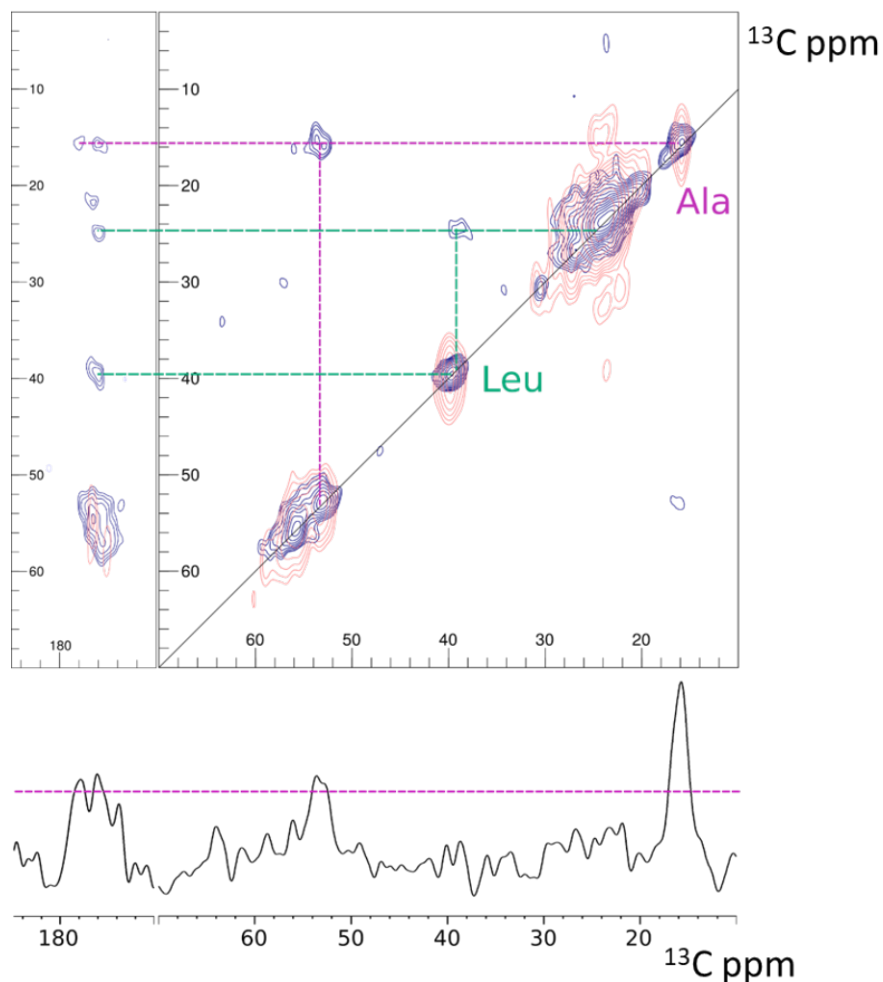
FIGURE 4 – Spectres 2D ^{13}C-^{13}C de rotation à l'angle magique de RMN à l'état solide de fibres de pVF1. Le spectre violet et le spectre rose possèdent deux temps de contact différents de 75 et 25 ms, respectivement. En les lignes hachurées violettes et vertes son présenter les corrélations entre les différents atomes des alanines et leucines, respectivement. En dessous est présenté la tranche correspondant au groupement méthyl de l'alanine.

2.2 Interaction peptide-membrane

Lors de l'endocytose du complexe de transport de gènes, plusieurs paramètres modifient l'environnement de celui-ci. La modification du pH au cours de la maturation de l'endosome conduit à un effet important au niveau du complexe [17]. En effet, par exemple, lorsque le peptide est complexé avec de l'ADN, l'acidification du milieu conduit à la libération de la moitié du peptide depuis le complexe [16]. Cela conduit à une concentration élevée de peptides interagissant potentiellement avec la membrane. Pour étudier cet effet, des vésicules avec des quantités croissantes de peptides ont été formées à pH physiologique et acide [18]. L'étude par RMN du solide ^{31}P et ^{2}H a permis de montrer qu'à pH acide, le peptide présente des propriétés détergentes. En effet, à haut ratio de peptide, une déformation très importante des vésicules est présente avec l'observation de la formation de bicelles capables de s'orienter vis-à-vis du champ magnétique. De plus, à très haut ratio de peptide, la présence de petites vésicules indique la lyse de la membrane. Au contraire, à pH physiologique, même au plus haut ratio de peptide, l'intégrité de la membrane est toujours visible. Les spectres ^{31}P sont présentés dans la figure ci-dessous (Figure 5).

Au cours de la maturation de l'endosome, la membrane subit également une modification de sa composition avec la diminution de lipides chargés tels que la phosphatidylsérine (POPS) ou la sphyngomyéline (SM) et d'autre part, l'augmentation de la phosphatidylcholine (POPC) ou du bis(monoacylglycero)phosphate (BMP) [19]. Les peptides de la famille du LAH4 présentent une affinité plus importante aux lipides anioniques tels que le phosphatidylglycerol (POPG) ou POPS, du fait de leurs charges [3][20]. Différents mélanges de lipides ont été ainsi préparés pour trouver des conditions plus semblables à la composition des membranes. La formation de vésicules a été possible, néanmoins, l'étude par RMN du solide des vésicules formées s'est trouvée trop complexe pour extraire des paramètres précis pour l'interprétation.
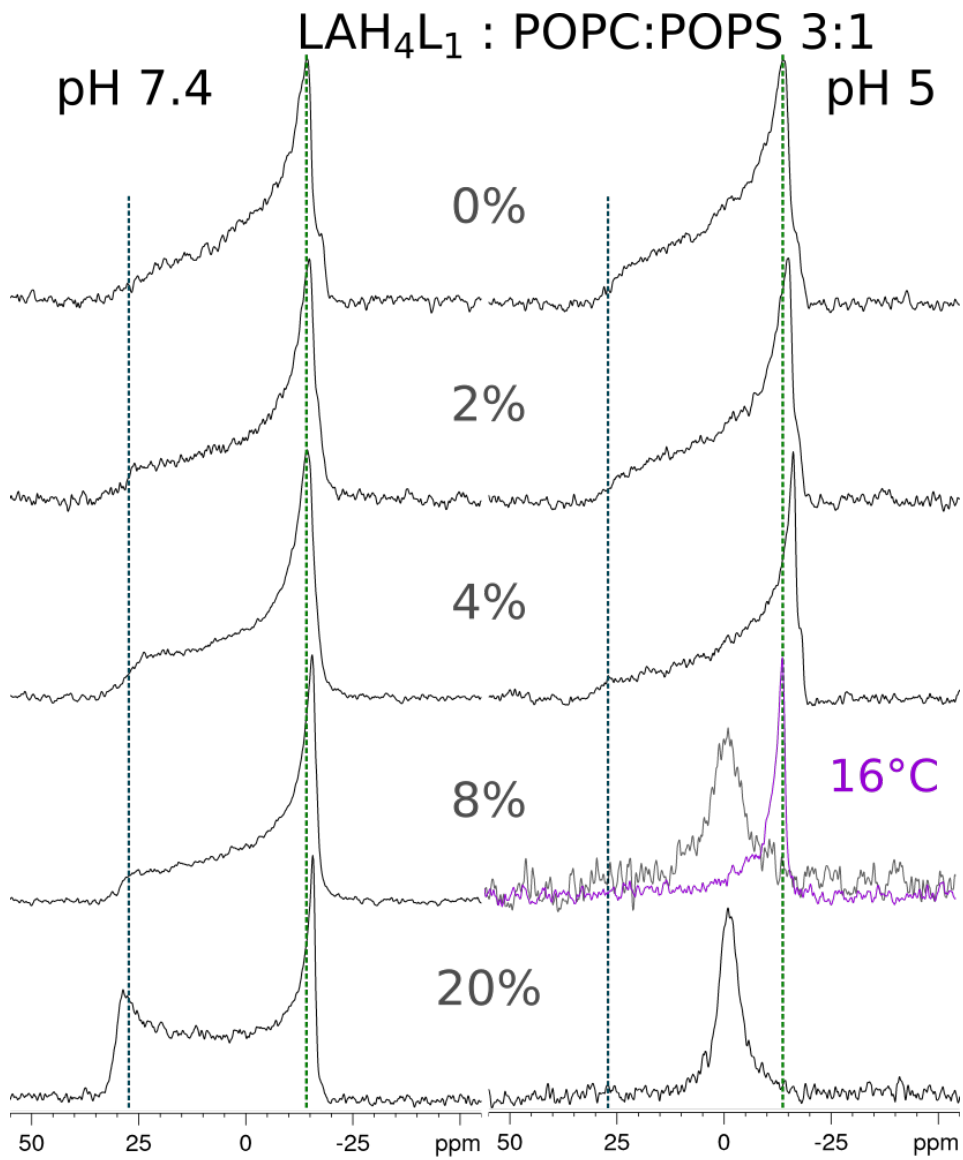
FIGURE 5 – Spectres de vésicules de POPC :POPS ^{31}P statique de RMN à l'état solide. Les échantillons ont été préparer avec un concentration croissante en peptide LAH4L1 à deux pH : 7,4 et 5.

2.3 Interaction Peptide-ADN

L'ADN est un des vecteurs utilisés comme modificateur de gènes. L'interaction ADN-LAH4 a été caractérisée par différentes méthodes, tels que par retard sur gel ou titrage calorimétrique isotherme, permettant ainsi de déterminer le nombre de peptides associés par paire de bases d'ADN suivant le pH, ou que l'interaction électrostatique était l'interaction la plus importante lors de la formation du complexe [21]. Par RMN du solide, des spectres de REDOR ^{31}P-^{15}N ont permis de mettre en évidence la proximité des chaines latérales des lysines ainsi que phosphore de l'ADN [22]. Néanmoins, les informations de distance n'ont pas donné lieux à l'élucidation d'une structure du complexe, du fait des différentes conformations possibles, compte tenu des informations de distance.

Dans le but d'extraire de nouvelles données, et afin de résoudre la structure, l'étude de l'interaction s'est faite avec le peptide LAH4-L1 et un ADN 15mer par RMN du liquide. Du faite de l'interaction électrostatique, lors du mélange des deux composés, l'interaction spontanée en agrégats insolubles empêche toutes observations. Différentes titrations ont été faites afin d'obtenir des conditions où le complexe était visible. Pour les titrations dans un tampon acétate ou en présence de micelles de DPC, la formation du complexe a donné lieu à la formation d'agrégats. Au cours de la titration la perte du signal a été proportionnelle à l'ajout d'ADN sans observer de modifications significatives du signal du peptide toujours visible en solution.

En revanche, lors de la titration dans un mélange H$_2$O/TFE 50%, il a été possible d'observer des différences de déplacements chimiques du peptide avec une formation d'agrégats plus limitée. Ainsi, dans ces conditions l'étude du complexe semble possible et pourra donner lieux à de nouvelles expériences afin d'élucider la structure du complexe.

Les conditions de formation du complexe ont ensuite été appliquées pour la préparation de vésicules membranaires pour l'étude ^{31}P et ^{2}H par RMN du solide. Dans les conditions testées, en présence du complexe LAH4-L1-ADN, une perturbation des têtes lipidiques à pH 5 visible par l'apparition d'un pic isotrope sur les spectres ^{31}P. D'autre part à pH 7,4, une perturbation des chaines aliphatiques des lipides a
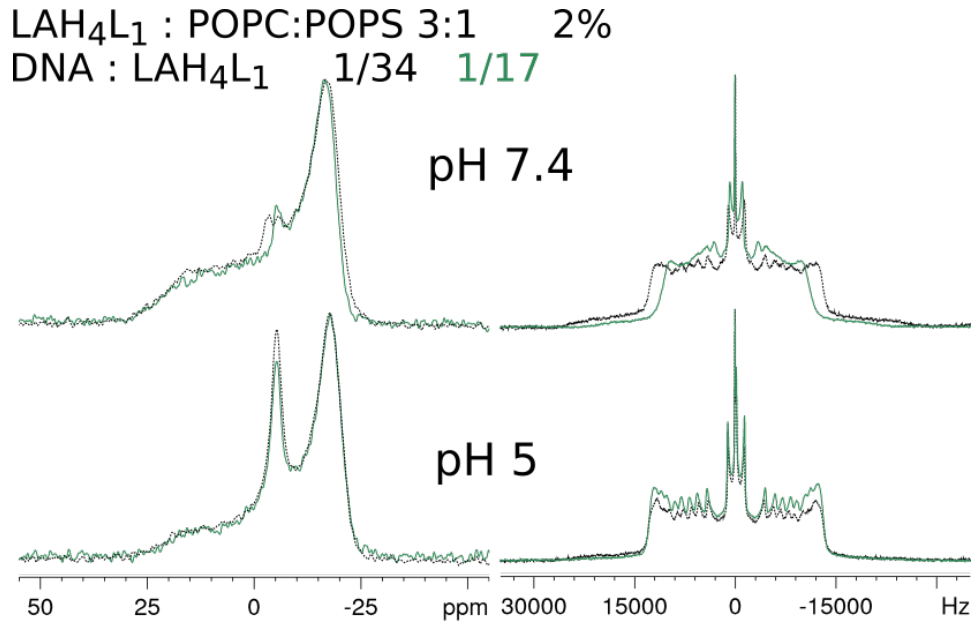
FIGURE 6 – Spectres de vésicules de POPC :POPS ^{31}P et ^{2}H statique de RMN à l'état solide. Les échantillons ont été préparer avec un mélange de peptide LAH4-L1 et d'un ADN 15mer à deux concentration différentes et à deux pH : 7,4 et 5.

été constatée sur les spectres ^{2}H. Il est intéressant de voir que ces effets sont accentués avec l'augmentation de la quantité d'ADN (Figure 6).

Dans un second temps, afin de voir si l'effet détergent du peptide LAH4-L1 était conservé également en présence d'ADN, un échantillon dans des conditions similaires à celle présentées dans la partie interaction peptide-membrane a été préparé. A pH 5 et avec un concentration en peptide de 8% et en conservant la ratio en ADN des échantillons précédents, l'effet détergent a été constaté (Figure 7).

La présence d'ADN pourrait aider à la stabilisation du peptide sur la membrane. Des expériences supplémentaires pourraient confirmer cet effet avec par exemple la préparation d'échantillon de bicouche lipidique orientées pour voir si le peptide s'oriente plus facilement dans la membrane en présence d'ADN.
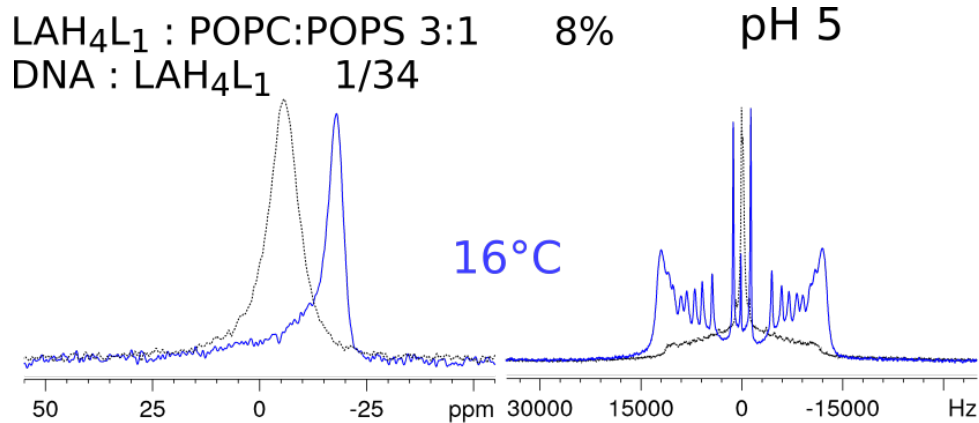
FIGURE 7 – Spectres de vésicules de POPC :POPS ^{31}P et ^{2}H statique de RMN à l'état solide. Les échantillons ont été préparer avec un mélange de peptide LAH4-L1 (à 8%) et d'un ADN 15mer (ratio 1/34 de ADN/peptide) à pH 5.

3   Conclusion générale

L'utilisation de peptide comme amplificateur de système de transport de gènes présente de nombreux avantages tels que la biocompatibilité, la faible toxicité (biodégradabilité) ou la simplicité de production [13]. Les peptides de la famille du LAH4 permettent ainsi de pallier à l'un des facteurs les plus limitants de ce type de vecteur qui est l'échappement de l'endosome. Toutefois, la spécificité d'interaction du complexe avec un type de cellules reste encore à améliorer. Cela peut être envisagé par la modification du peptide lui-même en ajoutant de nouvelles fonctions ou par l'addition d'autres molécules aux complexes. Néanmoins, pour ce faire, une meilleure connaissance du mécanisme d'action au niveau moléculaire est nécessaire.

Dans cette thèse, l'étude de l'interaction peptide-membrane par RMN du solide a permis de valider l'hypothèse d'effet détergent du peptide, montrant que l'effet coordonné du pH et de la concentration élevée en peptide est nécessaire pour obtenir la dissolution des membranes. La formation de complexe stable en solution de peptide et d'ADN permet d'envisager l'élucidation de la structure du complexe. Finalement, la mise au point d'un protocole de formation des fibrilles pour la VF1 s'est montré également efficace pour la formation de fibre du LAH4-L1. Le LAH4-L1 étant moins efficace pour la transduction de certains virus en comparaison à la VF1, tous deux étant capable de s'auto-assembler en fibres, la structure même de

ces dernières pourrait avoir une influence, d'où l'intérêt de leurs études. En effet, la formation de ces fibres pourrait aider d'avantage qu'à la concentration à la surface cellulaire des particules virales et aider à la fusion membranaire. Contrairement au LAH4, la VF1 n'est pas un aussi bon antimicrobien [14]. Ainsi ce protocole pourrait être appliqué au LAH4 pour attester de la présence ou non de fibres.

De par la similarité de séquence de ces peptides et de leurs diversités de fonctions biologiques, cette famille de peptide est un modèle d'étude intéressant pour élucider le lien entre l'auto-assemblage de peptides et de leurs fonctions.

4   Références

[1] Bechinger, B., 1996. Towards membrane protein design : pH-sensitive topology of histidine-containing polypeptides. Journal of molecular biology 263, 768–775.

[2] Bechinger, B., Ruysschaert, J.M., Goormaghtigh, E., 1999. Membrane helix orientation from linear dichroism of infrared attenuated total reflection spectra. Biophys. J. 76, 552–563.

[3] Vogt, T.C.B., Bechinger, B., 1999. The Interactions of Histidine-containing Amphipathic Helical Peptide Antibiotics with Lipid Bilayers THE EFFECTS OF CHARGES AND pH. J. Biol. Chem. 274, 29115–29121.

[4] Kichler, A., Mason, A.J., Bechinger, B., 2006. Cationic amphipathic histidine-rich peptides for gene delivery. Biochimica et Biophysica Acta (BBA) - Biomembranes 1758, 301–307.

|5] Langlet-Bertin, B., Leborgne, C., Scherman, D., Bechinger, B., Mason, A.J., Kichler, A., 2010. Design and Evaluation of Histidine-Rich Amphipathic Peptides for siRNA Delivery. Pharmaceutical Research 27, 1426–1436.

[6] Liu, Y., Kim, Y.J., Ji, M., Fang, J., Siriwon, N., Zhang, L.I., Wang, P., 2014. Enhancing gene delivery of adeno-associated viruses by cell-permeable peptides. Mol Ther

Methods Clin Dev 1, 12.

[7] Liu, N., Bechinger, B., Süss, R., 2017. The histidine-rich peptide LAH4-L1 strongly promotes PAMAM-mediated transfection at low nitrogen to phosphorus ratios in the presence of serum. Scientific Reports 7, 9585.

[8] Gemmill, K., Muttenthaler, M., Delehanty, J., Stewart, M., Susumu, K., Dawson, P., Medintz, I., 2013. Evaluation of diverse peptidyl motifs for cellular delivery of semiconductor quantum dots. Anal Bioanal Chem, 405(19) :6145-6154.

[9] Zhang, T., Kang, T., Ma, B., Xu, Y., Hung, C., Wu. T., 2012. LAH4 enhances CD8+ T cell immunity of protein/peptide-based vaccines. Vaccine, 30(4) :784-793.

[10] Kichler, A., Leborgne, C., Danos, O., Bechinger, B., 2007. Characterization of the gene transfer process mediated by histidine-rich peptides. J Mol Med 85, 191–201.

[11] Mason, A.J., Martinez, A., Glaubitz, C., Danos, O., Kichler, A., Bechinger, B., 2005. The antibiotic and DNA-transfecting peptide LAH4 selectively associates with, and disorders, anionic lipids in mixed membranes. FASEB J. 20, 320-322.

[12] Tian, X., Sun, F., Zhou, X.-R., Luo, S.-Z., Chen, L., 2015. Role of peptide self-assembly in antimicrobial peptides. J. Pept. Sci. 21, 530–539.

[13] Vermeer, L.S., Hamon, L., Schirer, A., Schoup, M., Cosette, J., Majdoul, S., Pastre, D., Stockholm, D., Holic, N., Hellwig, P., Galy, A., Fenard, D., Bechinger, B., 2017. Vectofusin-1, a potent peptidic enhancer of viral gene transfer forms pH-dependent alpha-helical nanofibrils, concentrating viral particles. Acta Biomater. 64, 259–268.

[14] Majdoul, S., Seye, A.K., Kichler, A., Holic, N., Galy, A., Bechinger, B., Fenard, D., 2015. Molecular determinants of Vectofusin-1 and its derivatives for the enhancement of lentiviral-mediated gene transfer into hematopoietic stem/progenitor cells. Journal of Biological Chemistry jbc.M115.675033.

[15] Marquette, A., Mason, A.J., Bechinger, B., 2008. Aggregation and membrane permeabilizing properties of designed histidine-containing cationic linear peptide antibiotics. J. Peptide Sci. 14, 488–495.

[16] Vidovic, V., Prongidi-Fix, L., Bechinger, B., Werten, S., 2009. Production and isotope labeling of antimicrobial peptides in Escherichia coli by means of a novel fusion partner that enables high-yield insoluble expression and fast purification. J. Pept. Sci. 15, 278–284.

[17] Huotari, J., Helenius, A., 2011. Endosome maturation. EMBO J, 30(17) :3481-3500.

[18] Wolf, J., Aisenbrey, C., Harmouche, N., Raya, J., Bertani, P., Voievoda, N., Süss, R., Bechinger, B., 2017. pH-Dependent Membrane Interactions of the Histidine-Rich Cell-Penetrating Peptide LAH4-L1. Biophys. J. 113, 1290–1300.

[19] van Meer, G., Voelker, D.R., Feigenson, G.W., 2008. Membrane lipids : where they are and how they behave. Nature Reviews Molecular Cell Biology 9, 112–124.

[20] Islami, M., Mehrnejad, F., Doustdar, F., Alimohammadi, M., Khadem-Maaref, M., Mir-Derikvand, M., Taghdir, M., 2014. Study of Orientation and Penetration of LAH4 into Lipid Bilayer Membranes : pH and Composition Dependence. Chem Biol Drug Des, 84(2) :242-252.

[21] Prongidi-Fix, L., Sugawara, M., Bertani, P., Raya, J., Leborgne, C., Kichler, A., Bechinger, B., 2007. Self-Promoted Cellular Uptake of Peptide/DNA Transfection Complexes. Biochemistry 46, 11253–11262.

[22] Bechinger, B., Vidovic, V., Bertani, P., Kichler, A., 2011. A new family of peptide-nucleic acid nanostructures with potent transfection activities. Journal of Peptide Science 17, 88–93.

Justine WOLF
Etude biophysique de peptides de la famille du LAH₄

Résumé

Les peptides de la famille du LAH₄ sont des peptides cationiques capables de se replier en hélice α amphiphile. Ils comportent notamment des histidines qui permettent de moduler les interactions dans une gamme de pH physiologique. En présence de membranes, à pH neutre le peptide adopte une conformation transmembranaire alors qu'à pH acide, la protonation des histidines favorise la conformation à la surface de la membrane. Dans cette conformation, le peptide est capable de perturber davantage les membranes.

Dans le domaine des systèmes de modification de gènes, les peptides tels que le LAH₄ sont utilisée, pour interagir avec des molécules cargo afin de former un complexe avec celles-ci, puis permettre l'interaction avec la membrane de la cellule, et finalement, échapper à l'endosome. Néanmoins, d'une molécule cargo à l'autre, les peptides ne présentent pas la même efficacité rendant l'optimisation de ce genre de système complexe d'où l'intérêt de comprendre davantage les mécanismes moléculaires sous-jacents.

Le travail de cette thèse a été divisé en trois parties dans le but de caractériser de manière biophysique les différentes interactions ayant lieu lors de la livraison du système de transport de gènes à l'intérieur d'une cellule. L'interaction peptide-peptide : avec l'étude de l'agrégation en fibrilles de la Vectofusin-1 ; l'interaction peptide-membrane : avec l'effet du LAH4L1 en présence de différents types de membranes ; et l'interaction peptide-ADN : avec le suivit de l'interaction entre le LAH4L1 et un ADN de petite taille (15 mer).

Mots clés : peptide membranaire, RMN du solide, interaction peptide-peptide, fibres, interaction peptide-lipides, interaction peptide-acides nucléiques, système de transport de gènes

Summary

The LAH₄ family consists of cationic amphiphilic peptides with propensity to fold in α-helical secondary structures. They contain histidines allowing the modulation of their interactions in a pH dependent manner in the physiological range. In membranes, at neutral pH the peptide assumes a transmembrane orientation, while at acidic pH protonation of the histidines favour an in planar configuration. In this state, the peptide is also able to disrupt membranes.

In the field of gene delivery systems, peptides like LAH₄ are used. They are able to firstly interact with different cargoes in order to form stable complexes, then interact with the cell membrane, and finally, promote to escape from the endosome. Depending on the cargo, the peptides' efficiencies vary making their optimisation difficult. Hence, better knowledge about the mechanisms underlying these systems, and their interactions would be useful.

This PhD has been divided into three parts in order to characterize, with biophysical methods, the interactions occurring during the delivery of these gene systems: peptide-peptide interactions with a focus on the study of VF1 fibre formation; peptide-membrane interactions: with the investigation of the effect of LAH₄L₁ in different membranes; and peptide-DNA interactions, where the interactions of LAH₄L₁ with a small DNA fragment (15 mer) were measured.

Key words : cell-penetrating peptide, solid-state NMR, peptide-peptide interaction, peptide-lipid interaction, peptide-nucleic acid interaction, gene delivery systems